

Katja Fiehler: Temporospacial Characteristics of Error Correction.
Leipzig: Max Planck Institute for Human Cognitive and Brain Sciences,
2004 (MPI Series in Human Cognitive and Brain Sciences; 54)



Temporospatial characteristics of error correction

Von der Fakultät für Biowissenschaften, Pharmazie und Psychologie
der Universität Leipzig genehmigte

DISSERTATION

zur Erlangung des akademischen Grades

doctor rerum naturalium

Dr. rer. nat.,

vorgelegt von

Diplom-Psychologin Katja Fiehler

geboren am 14. November 1977 in Dresden

Dekan:

Prof. Dr. Kurt Eger

Gutachter:

Prof. Dr. D. Yves von Cramon

Prof. Dr. Erich Schröger

Prof. Dr. Axel Mecklinger

Tag der Verteidigung: 25. November 2004

Acknowledgements

I would like to express my gratitude to all those who have helped me in accomplishing this work.

My greatest thanks go to Dr. Markus Ullsperger who introduced me to the very interesting research topic on the neural mechanisms of error processing. Dr. Markus Ullsperger continuously provided support in every stage of my work and encouraged me to get acquainted with new research methods and analysis procedures. He capably taught me in fMRI analysis as well as task programming and assisted me in any perl matters. Dr. Markus Ullsperger made an undeniably significant contribution to this work. My special thanks also go to Prof. D. Yves von Cramon who opened up to me new ways of thinking by constructive and fruitful discussions and provided me excellent working conditions at his department of Neurology.

I sincerely acknowledge the support of the following people: the exec group and former exec.doc group for their interest in data discussion and their useful comments on trial talks, Kristiane Werrmann, Cornelia Schmidt, Anke Mempel and Mandy Naumann for their qualified assistance in data collection, and Maren Grigutsch for the development of the heart rate analysis software used in the present work. Especially, I want to thank Dr. Stefan Debener who aroused my interest in experimental research and provided me with the opportunity to work at the Max Planck Institut for Human Cognitive and Brain Sciences in Leipzig in the context of my diploma thesis.

For funding, I would like to express my gratitude to the German Research Foundation which supported the present work (SPP 1107).

Last but not least, I would like to thank my parents who believed in my skills and gave me emotional support during all stages of my dissertation. Particularly, I would like to thank Nils for his tireless support in mastering the English language and for keeping me grounded over the past two years.

Contents

1	Introduction	1
2	Theoretical Background	5
2.1	Behavioral Findings of Error Processing	6
2.2	Electrophysiological Correlates of Error Processing	8
2.2.1	The Error-related Negativity (ERN)	8
2.2.2	The ERN and Error Correction	10
2.2.3	The Error Positivity (Pe)	11
2.3	Models of Performance Monitoring	12
2.3.1	The Mismatch Hypothesis	12
2.3.2	The Response Conflict Hypothesis	16
2.3.3	Evaluative Monitoring	19
2.4	Psychophysiological Correlates of Error Processing	21
2.5	Hemodynamic Correlates of Error Processing	23
2.5.1	Neuroanatomy of the Frontomedian Wall	23
2.5.2	The Frontomedian Wall and Error Detection	28
2.5.3	The Frontomedian Wall and Error Correction	32
2.6	Aims of the Present Studies	32
3	Methods in Cognitive Neuroscience	35
3.1	Electrophysiological Method: Event-related Potentials	36
3.1.1	The Electroencephalography	36
3.1.2	Derivation of the ERPs	39

3.1.3	The Generation of ERPs	40
3.1.4	Lateralized Readiness Potentials	41
3.2	Psychophysiological Method: Heart Rate	44
3.2.1	The Electrocardiogram	45
3.2.2	Measures of Cardiac Activity	47
3.2.3	Modulation of HR Activity	47
3.3	Functional Magnetic Resonance Imaging	52
3.3.1	Magnetic Resonance Imaging	52
3.3.2	Functional Magnetic Resonance Imaging	56
3.3.3	Experimental Design in fMRI	58
3.3.4	Analysis of fMRI Data	59
3.4	Concluding Remarks	63
4	Experiment 1a (ERP)	65
4.1	Introduction	65
4.2	Method	67
4.2.1	Participants	67
4.2.2	Experimental Procedure	68
4.2.3	Data Recording	69
4.2.4	Data Analysis	70
4.3	Behavioral Data	74
4.3.1	Results	74
4.3.2	Discussion	78
4.3.3	Derivation of ERP Hypotheses	81
4.4	Electrophysiological Data	82
4.4.1	ERP Results	82
4.4.2	LRP Results	92
4.4.3	Discussion	94
4.5	Conclusion	100
5	Experiment 1b (HR)	101
5.1	Introduction	101

<i>CONTENTS</i>	ix
5.2 Method	102
5.2.1 Participants	102
5.2.2 Data Recording	102
5.2.3 Data Analysis	102
5.3 Results	103
5.4 Discussion	104
5.5 Conclusion	105
6 Experiment 2 (fMRI)	107
6.1 Introduction	107
6.2 Method	108
6.2.1 Participants	108
6.2.2 Experimental Procedure	109
6.2.3 fMRI Procedure	109
6.2.4 Statistical Analysis	110
6.3 Results	111
6.3.1 Behavioral Data	111
6.3.2 FMRI Data	112
6.4 Discussion	115
6.4.1 Error Detection	117
6.4.2 Error Correction	118
6.5 Conclusion	121
7 General discussion and future perspectives	123
Bibliography	131
List of figures	153
List of tables	155
Abbreviations	160
Curriculum Vitae	161

Chapter 1

Introduction

*Having made a mistake,
not to correct it
is a mistake indeed.
(Confucius 551-479 B.C.,
Chapter 15, Verse 29)*

Thinking about human errors, tragic accidents come often to mind at first, such as the Chernobyl disaster of 1986 or the Piper Alpha oil platform explosion in 1988. The *Swiss Cheese Model* by Reason (2000) provides one possible explanation how human errors can emerge. In an ideal safe system, there are many intact defensive layers, e.g., alarms, automatic shutdowns or control room operators. In reality, however, the defensive layers rather resemble a swiss cheese. The holes in the cheese represent weak spots in the defensive layers. Weak spots in any one layer do not normally cause a bad outcome. Generally, tragic accidents happen when weak spots in many defensive layers momentarily line up to permit a trajectory of accident opportunity. These holes arise for two reasons: active failures and latent conditions. Active failures are the unsafe acts committed by people who are in direct contact with the system. At Chernobyl, for example, the operators wrongly violated plant procedures and switched off successive safety systems, thus creating the immediate trigger for the catastrophic explosion. But, human errors are primarily consequences rather than causes, having their origins

in the system itself. Such latent conditions are caused by decisions made by designers, builders or managers, which can lead to error provoking conditions (e.g., time pressure, inexperience) and long-lasting weaknesses in the defenses (e.g., unworkable procedures, construction deficiencies). Applied research has focused on the issue of how the incidence of dangerous errors can be limited by creating systems that are better able to tolerate the occurrence of errors.

From the mid-1970s onwards, human error has become a proper research topic in experimental psychology. Empirical studies focused on an adequate description of cognitive control processes to predict correct performance as well as varieties of human fallibility. Following the psychological definition by Reason (1990, p. 9), human errors

” ... encompass all those occasions in which a planned sequence of mental or physical activities fails to achieve its intended outcome, and when these failures cannot be attributed to the intervention of some chance agency.”

A taxonomy of different error types was proposed by Reason (1990). He distinguished three primary types of errors according to the cognitive stages at which they occur. Errors arising during planning an action are classified as *mistakes* and refer to a failure in identifying the goal of an action and/or in deciding upon the means to achieve it. Thus, they involve a mismatch between the prior intention and the intended consequences. Mistakes, for example, refer to failures in expertise, where some preestablished problem solution is applied inappropriately. Failures in the storage phase, the phase between formulating the intended action and running it off, are denominated *lapses*. A third error type emerging during the actual implementation of the stored plan is termed *action slips*. Action slips occur, if the correct response is known, but the individual failed in its execution, regardless of whether or not the plan which guided him was adequate to achieve its objectives. Action slips are easy to detect and frequently corrected by the individ-

ual. Familiar examples are slips of the tongue or slips of the pen. The distinction between mistakes and action slips can be summarized as follows:

”If the intention is not appropriate, this is a mistake. If the action is not what was intended, this is a slip.” (Reason, 1990, p. 8)

In consequence of the ease in error detection, experimental psychology has primarily focused on action slips. Different paradigms causing execution errors have been designed. A frequency manipulation provides one alternative, which results in a largely automatic performance of highly frequent stimuli, whereas action slips emerge on less frequent stimuli. Second, dual task situations demand a spread in attention so that actions slips are likely to occur. Additionally, tasks in which a prepotent response needs to be overcome represent a prevalent paradigm to provoke action slips, e.g., the Eriksen flanker task (Eriksen, & Eriksen, 1974). A common feature of these tasks is their performance under time pressure that causes premature responses.

In the 1990s of the last century, experimental research into the field of human errors has received new impulses by psychophysiological investigations using electroencephalography. This work was pioneered by the research groups around Falkenstein and Gehring. With a short delay, both groups reported an electrical potential in the electroencephalogram related to erroneous responses, denominated error negativity (Ne; Falkenstein, Hohnsbein, Hoormann, & Blanke, 1990) or error-related negativity (ERN; Gehring, Goss, Coles, & Meyer, 1993). The discovery of the Ne/ERN has initiated an extensive interest in this field that has been further enhanced by the usage of imaging techniques. Fewer studies, however, have focused on the consequences of errors. While in the end-1960s to 1970s, a wide variety of behavioral experiments investigated error correction (e.g., Rabbitt, 1966a,b; Rabbitt, & Rodgers, 1977), studies using electrophysiological or imaging techniques have rarely concentrated on this topic.

Outline of the present work The aim of the present work is a comprehensive multi-methodological investigation of *error correction*. In addition to behavioral

data, electrophysiological and imaging techniques are applied to examine the temporal and spatial characteristics of error correction. Moreover, cardiac activity as a psychophysiological measure is used to investigate changes of the autonomic nervous system related to error correction.

Chapter 2 will give the theoretical background of the experiments. In this chapter, the electrophysiological, psychophysiological and neural correlates of error detection and error correction will be reviewed and the current theories of error processing will be outlined. *Chapter 3* will describe the applied methods, including event-related potentials (Chapter 3.1), heart rate (Chapter 3.2), and functional magnetic resonance imaging (Chapter 3.3). The empirical part of the present work is addressed in the subsequent Chapters 4 to 6. *Chapter 4* will report the electrophysiological results, *Chapter 5* the psychophysiological results and *Chapter 6* the imaging results. Each of these chapters will end with a discussion of the obtained results within the framework of the current theories of error processing. *Chapter 7* will summarize the main findings of the present work and provide an integrative discussion of these findings.

Chapter 2

Theoretical Background

Different paradigms, such as the Eriksen flankers task (e.g., Gehring et al., 1993), the Stroop task (e.g., Kerns, Cohen, Macdonald, Cho, Stenger, & Carter, 2004), the GoNogo task (e.g., Falkenstein, Hohnsbein, & Hoormann, 1996) or the Stop-Signal task (e.g., Christ, Falkenstein, Heuer, & Hohnsbein, 2000) have been used to investigate error-related processes. A common feature of these tasks is the need to overcome a prepotent response under time pressure, in which participants often fail and produce errors. Referring to the classification by Reason (1990), committed errors can be defined as action slips, which are easy to detect by the person (cf., page 2). A substantial portion of these errors are immediately followed by corrections.

In the following chapter, empirical findings about error processing will be reviewed. First, behavioral studies will be described. This will be followed by an introduction to electrophysiological studies investigating error-related components by means of the electroencephalogram (EEG). The resultant theoretical concepts underlying error processing will be explained afterwards. Recently, changes in psychophysiological measures, such as cardiac or electrodermal activity, have been related to error processing. Studies investigating heart rate changes associated with error processing will be surveyed in this chapter. Finally, the status quo of error-related fMRI findings will be reviewed.

2.1 Behavioral Findings of Error Processing

In simple serial choice reaction time tasks participants can detect and correct their errors very efficiently without being given an external signal that an error had occurred (Cooke, & Diggle, 1984; Rabbitt, 1968, 1966a,b). Error corrections are also made involuntarily when prohibited by experimental instruction (Reason, 1990; Rabbitt, & Rodgers, 1977). In a study by Rabbitt (1968), young adults signaled their errors by pressing a key which was not applied in the task. The data showed that participants were able to detect 71% of their errors, taking an average of 676 milliseconds [ms] to do so. Error corrections were more accurate and much faster than "error signaling responses" when participants made the response which should have been made. Depending on the task and the method of measurement, error corrections can be completed within 30 to 120 ms after the error that they follow (Angel, 1976; Higgins, & Angel, 1970; Angel, & Higgins, 1969; Rabbitt, 1968, 1966a,b). Cooke and Diggle (1984) showed that 50 ms before any overt sign of limb movement the electromyographic (EMG) activity of the muscle producing the error movement was suppressed, while the EMG activity of the muscle moving the fingers to the correct direction was enhanced. Because error correction is one of the fastest cognitive processes, an internal monitoring of a motor copy of the generated response has been proposed that is termed *efference copy*. This internal monitoring process is assumed to allow correcting errors more quickly than responding to an external signal.

Error corrections can be explained in terms of a continuous flow of information into the response selection process leading to an accumulation of information over time. If a response is delivered prematurely, little information can be accumulated and the response will be selected upon the basis of incomplete information making an erroneous response likely. While an error is being committed, stimulus processing continues resulting in the correct response, the error correction (Rabbitt, & Vyas, 1981; Rabbitt, Cumming, & Vyas, 1978; Rabbitt, 1966b). Figure 2.1 depicts a simplified diagram of the *Information Processing Model*. The model details the different stages of information processing and internal representations engaged when an error is committed and corrected. In this diagram, a feedback

loop is proposed that receives as input the efference copy of the motor outflow. The internal representation of the generated response is compared with the internal representation of the predicted correct response arising from motor selection. If a mismatch occurred, an error signal is elicited, which triggers a modulation of the motor command resulting in a corrective response as fast as possible.

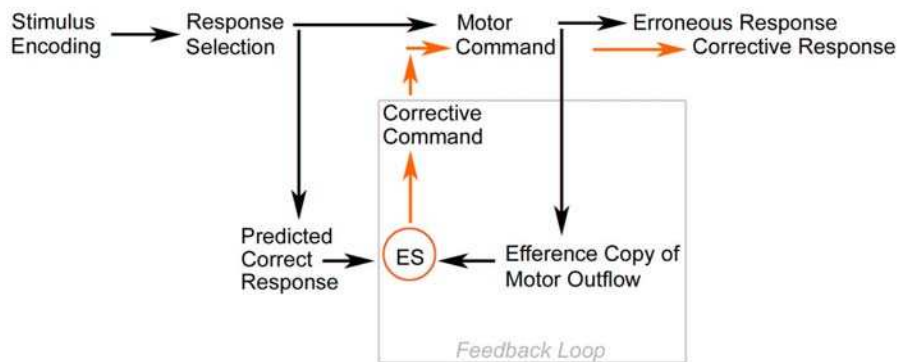


Figure 2.1: *Simplified diagram of the Information Processing Model detailing different stages of information processing and internal representations engaged in error production and correction (adapted from Desmurget and Grafton, 2000). The large grey square delineates the feedback loop used to correct the erroneous response. When a motor command is selected, an efference copy is generated and compared with the predicted correct response resulting from motor selection. If a mismatch occurred, an error signal (ES) is elicited, which triggers the corrective motor command as fast as possible.*

In addition to immediate error corrections, participants adjust their behavior in subsequent trials following an error. Rabbitt (1968) reported *post-error slowing (PES)* meaning that reaction times are slower for correct responses following an erroneous response than for other correct responses. The PES effect was also observed for errors that had not been overtly signaled when error-signaling instructions had been given. The PES effect, however, is inconsistently reported in the literature. While some studies found reaction time slowing after errors (Ullsperger, & Szymanski, 2004; Rabbitt, 2002; Gehring, & Fencsik, 2001; Rabbitt, & Vyas, 1970; Rabbitt, 1968), other studies did not observe a PES effect (Ullsperger, & von Cramon, 2001) or did not mention it. Stemmer and colleagues (2004)

showed a large variability of the PES effect across individuals suggesting that post-error slowing reflects an effect of low robustness. In a later study, Rabbitt and Rodgers (1977) demonstrated that responses following errors are not only slow, but also inaccurate. The authors suggest that participants have to suppress the tendency to correct their errors, if they are required to make any other response resulting in longer reaction times and more errors on subsequent trials. In addition, confusion in the choice of responses after committing an error might have increased erroneous responses after errors.

2.2 Electrophysiological Correlates of Error Processing

The investigation of error processing by means of electrophysiological measures was inspired primarily by the discovery of an event-related potential (ERP) associated with errors. Thus, a considerable series of ERP studies were conducted to examine the characteristics and functional significance of this component, which will be reviewed in the following.

2.2.1 The Error-related Negativity (ERN)

ERP studies revealed a negative voltage component associated with errors, the error negativity (Ne; Falkenstein et al., 1990), or error-related negativity (ERN; Gehring et al., 1993). In the following, the term ERN will be used. The ERN starts at the onset of the EMG activity preceding the overt error response and peaks about 50 to 100 ms after key press (Kopp, & Rist, 1999; Gehring et al., 1993). It shows an amplitude in the range of 10 microvolt (μV) or larger and is fronto-centrally distributed over the scalp (see Figure 2.2). Source localization studies suggest that the ERN is generated in the dorsal part of the anterior cingulate cortex (ACC), particularly in the rostral cingulate zone (RCZ) (cf., chapter 2.5.1, page 25; Luu, & Tucker, 2001; Dehaene, Posner, & Tucker, 1994).

The ERN occurs when errors of choice (erroneous response in choice-reaction time task), errors of action (uninhibited response on NoGo trials) (Scheffers, Coles, Bernstein, Gehring, & Donchin, 1996), or late responses (Luu, Flaisch,

2.2. ELECTROPHYSIOLOGICAL CORRELATES OF ERROR PROCESSING⁹

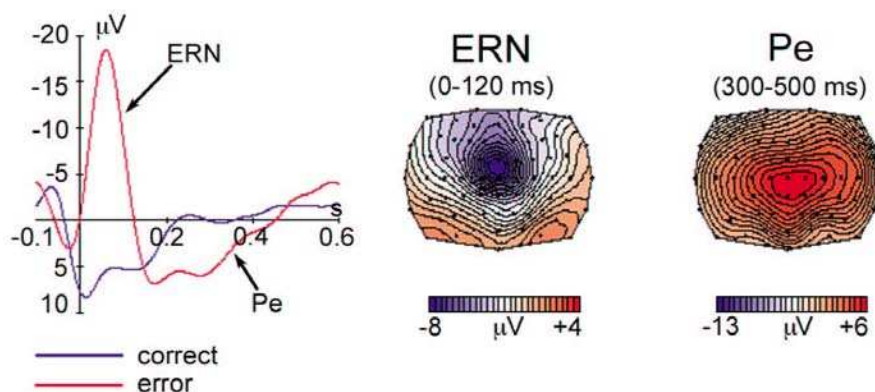


Figure 2.2: *Left: Response-locked ERPs on correct trials and error trials at FCz. Error trials show a prominent error-related negativity (ERN) followed by an error positivity (Pe). Right: Isopotential maps of error trials in the time window of the ERN (0-120 ms) and the Pe (300-500 ms).*

& Tucker, 2000b) are committed. The appearance of the ERN is independent of the fact whether errors were corrected or not suggesting that this component is not simply a reflection of error correction. Moreover, the ERN is unaffected by perceptual properties of the stimuli (Bernstein, Scheffers, & Coles, 1995) as well as stimulus (Falkenstein, Hohnsbein, Hoormann, & Blanke, 1991) and response modality (Nieuwenhuis, Ridderinkhof, Blom, Band, & Kok, 2001; Gehring, & Fencsik, 2001; Masaki, Tanaka, Takasawa, & Yamazaki, 2001; Falkenstein, Hoormann, Christ, & Hohnsbein, 2000; Van 't Ent, & Apkarian, 1999; Holroyd, Dien, & Coles, 1998). Its amplitude, however, can be modulated by several factors, such as error detectability (Falkenstein et al., 2000; Bernstein et al., 1995), time pressure (Falkenstein et al., 2000; Falkenstein, Hohnsbein, & Hoormann, 1994; Falkenstein et al., 1990), error force (Scheffers et al., 1996; Kopp, Rist, & Mattler, 1996), individual error salience (Ullsperger, & von Cramon, in press; Pailing, Segalowitz, Dywan, & Davies, 2002; Dikman, & Allen, 2000; Luu, Collins, & Tucker, 2000; Bernstein et al., 1995), or age (Nieuwenhuis et al., 2002; Falkenstein et al., 2000).

In general, the ERN is elicited after action slips (cf., page 2), e.g., due to premature responding, but not in experimental settings, in which participants have too little information for detecting the error without external feedback (Holroyd, & Coles, 2002; Coles, Scheffers, & Holroyd, 2001; Scheffers, & Coles, 2000). In such underdetermined conditions, an ERN-like wave can be elicited by external error feedback, denominated feedback-ERN (Holroyd, & Coles, 2002; Badgaiyan, & Posner, 1998; Miltner, Braun, & Coles, 1997) or medial frontal negativity (MFN; Gehring, & Willoughby, 2002). Due to the fact that error feedback is presented externally by using sensory stimuli, the ERN seems to be at least partially independent of the motor system. In addition to self-generated errors, latest findings demonstrated that the ERN is also elicited by observed errors (van Schie, Rogier, Coles, & Bekkering, 2004).

2.2.2 The ERN and Error Correction

Few psychophysiological studies have systematically investigated the relationship between the ERN and error correction. These studies revealed inconsistent findings about whether ERN amplitude and latency vary as a function of whether errors are corrected or not. Gehring and colleagues (1993) related the ERN amplitude to three measures of compensatory behavior by using the Eriksen flanker task (Eriksen, & Eriksen, 1974). They found a modulation of the ERN amplitude by the probability of error correction. The data showed that the larger the ERN, the greater the probability that an error would be corrected on the same trial. Second, the ERN amplitude was modulated by error response force showing a larger ERN for a small response force than for a large response force. Third, they found that the larger the ERN, the slower the response in the immediately following correct trial. The authors suggested that the tendency to adopt a more conservative strategy following an error is related to the size of the ERN on error trials.

Consistent with the results by Gehring et al. (1993), Falkenstein and colleagues (1994) reported a larger ERN amplitude for corrected compared to uncorrected errors in a two-choice reaction time task. However, this effect was only found after auditory but not after visual stimuli. Thus, the authors assumed that

2.2. ELECTROPHYSIOLOGICAL CORRELATES OF ERROR PROCESSING 11

the ERN is not associated with error correction. In a later study of the same group, however, an enhanced ERN amplitude for corrected compared to uncorrected errors was observed after both auditory and visual stimuli (Falkenstein et al., 1996). Falkenstein and colleagues (1996) argued that errors may have been detected less clearly or later for uncorrected errors resulting in a decreased amplitude of the ERN. This finding was strengthened by recently published data showing a larger ERN for corrected than uncorrected errors (Rodriguez-Fornells, Kurzbuch, & Münte, 2002). Comparison of the onset and time course of the ERN and LRP components showed that corrective activity precedes the ERN indicating parallel processing of the erroneous and correct response tendencies. This result is inconsistent with the assumption that the process underlying the ERN triggers error correction. The authors further found a modulation of ERN amplitude by correction speed exhibiting a larger ERN for quickly compared to slowly corrected errors. They assumed that the temporal overlap of the response tendencies for error and corrective responses is greater for fast than for slow corrections reflected in a larger ERN.

Inconsistent findings were also reported with regard to ERN latency. Falkenstein and colleagues (1994) observed no latency differences of the ERN between corrected and uncorrected errors neither after auditory nor after visual stimuli. In a later experiment of the same group, a modulation of ERN latency between corrected and uncorrected errors was discovered revealing a later peak for uncorrected compared to corrected errors after both auditory and visual stimuli (Falkenstein et al., 1996). In contrast, a study by Rodriguez-Fornells et al. (2002) did not find latency differences of the ERN between corrected and uncorrected errors nor between slow and fast error corrections.

2.2.3 The Error Positivity (Pe)

The ERN is frequently followed by a second ERP component, the error positivity (Pe; Falkenstein et al., 2000, 1990). The Pe occurs about 300 ms to 500 ms after the onset of an erroneous response and is maximal at centro-parietal electrode sites (see, Figure 2.2). Some studies also reported a more midline central distribution

(Ullsperger, & von Cramon, 2001; Falkenstein et al., 2000). The Pe does not seem to be related to error correction, whereas it varies with error rate, error detectability and age (Falkenstein et al., 2000).

The functional significance of the Pe is less understood. It seems to vary independently of the ERN and shows a high variance across subjects and tasks (Falkenstein et al., 2000; Falkenstein, 2004). In their review, Falkenstein et al. (2000) suggested that the Pe reflects further error or post-error processing, such as: first, conscious error recognition (Hajcak, McDonald, & Simons, 2003; Nieuwenhuis et al. 2001; Falkenstein et al., 2000; Leuthold, & Sommer, 1999), second, an adaptation of response strategy after a perceived error (Hajcak et al., 2003; Nieuwenhuis et al., 2001; Leuthold, & Sommer, 1999; but see Ullsperger, & Szymanowski, 2004, for conflicting findings), and third, subjective emotional error processing, which is modulated by the motivational significance of an error (van Veen, & Carter, 2002; Falkenstein et al., 2000) .

2.3 Models of Performance Monitoring

Several models of performance monitoring have been proposed to explain the ERN phenomenon and its modulations. The first conceptualization was the *Mismatch Hypothesis* put forward by Falkenstein and colleagues in 1990, which will be described first. Eight years later, an alternative account was presented by Carter and colleagues. This *Response Conflict Hypothesis* will be reviewed afterwards. Moreover, recent studies suggest an *evaluative monitoring* function of the ERN, which will be discussed at the end.

2.3.1 The Mismatch Hypothesis

The Mismatch Hypothesis interprets the ERN as an error detection signal resulting from a mismatch between the internal representation of the intended correct response and the internal representation of the actually performed erroneous response (Gehring et al., 1993; Falkenstein et al., 1990). A schematic illustration of the Mismatch Hypothesis is depicted in Figure 2.3. The error-processing system

is comprised of two main components: a monitoring system that detects errors and a remedial action system. The basic feature of the monitoring system is the comparator which compares the representations of the intended correct response with the actually performed erroneous response.

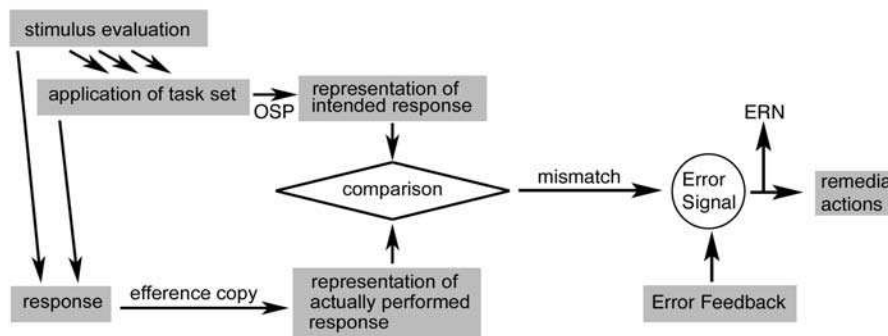


Figure 2.3: Schematic illustration of the Mismatch Hypothesis showing an erroneous response. ERN: error-related negativity, OSP: ongoing stimulus processing.

The Mismatch Hypothesis assumes that if a stimulus is fully evaluated and the task set is applied appropriately, then this yields a correct response. While the correct response is being performed, stimulus processing continues resulting in an internal representation of the actually performed response. Consistent with the Information Processing Model described above (see, Figure 2.1), the Mismatch Hypothesis assumes a comparison between the internal representation of the intended correct response arising from ongoing stimulus processing and the internal representation of the actually performed response resulting from the efference copy of the motor outflow. If a correct response is performed, the comparison process will yield a match. In contrast, if the stimuli are evaluated insufficiently, an inappropriate task set might be chosen leading to an error or a premature abortion of stimulus processing, which results directly in an erroneous response. The comparison between the two internal representations will lead to a mismatch eliciting an ERN and initiating remedial actions, e.g., error correction or compensational processes. Falkenstein and colleagues (2000) showed that the larger the difference

between the representations/the mismatch, the easier the error will be detected, and the larger and/or earlier the ERN will be.

Different variants of the Mismatch Hypothesis have been debated. Falkenstein and colleagues (1991, p.453) assumed that the ERN is "elicited at the moment of the completion of the response selection process", i.e., after completion of stimulus processing, when both response representations are fully available. The authors later refined their argument suggesting that the ERN reflects a comparison process rather than the outcome itself, i.e., error detection (Falkenstein et al., 2000). Thus, an ERN-like wave could occur after correct responses as a reflection of the comparison process, while the ERN on error trials would reflect this process and the superimposed error signal. Coles and colleagues (2001) further assumed that the correct response negativity (CRN; Coles et al., 2001; Vidal, Hasbroucq, Grapperon, & Bonnet, 2000; Falkenstein et al., 2000; Gehring, & Knight, 2000; Scheffers, & Coles, 2000), an ERN-like wave following correct responses, reflects the compromised comparison process, when one of the response representations is disturbed.

Behavioral observations and ERP results have challenged the Mismatch Hypothesis. The rapidness of the error detection process (c.f., Chapter 2.1) and the early onset of the ERN suggest that the representation of the correct response results from an efference copy rather than from proprioceptive feedback. Starting from these findings, Coles and colleagues (2001) proposed an *alternative version of the Mismatch Hypothesis* which assumes that the comparison process takes place, when the efference copy of the actual performed response arrives and does not wait "until all possible information about the appropriate response is available. Rather it uses whatever information is available at the time of the response." (Coles et al., 2001, p.175). The representation of the appropriate or correct response is assumed to be derived from further, continued stimulus processing.

Computational modeling further refined the Mismatch Hypothesis. Holroyd and Coles (2002) introduced a reinforcement-learning theory of the ERN based on an evaluative monitoring system. Figure 2.4 depicts a schematic illustration of the *Holroyd Model*. The model proposes a motor control system located in the ACC,

which generates behavior appropriate to the current external context. Simultaneously, a monitoring system involving the basal ganglia predicts the outcome of the response (good vs. bad). This prediction is based on information from the external environment and an efference copy of the motor outflow. If the monitoring system classifies that event as better than expected, then a "good" error signal is produced. In contrast, if the event is classified as worse than expected, then a "bad" error signal is generated. These error signals are coded as phasic increases of the tonic activity of the mesencephalic dopamine system in case of a "good" error signal and as phasic decreases in case of a "bad" error signal. The mesencephalic dopamine system sends the error signals to the ACC, where they reinforce performance on the present task. From there, the error signals are carried back to the basal ganglia, where they are used to improve the predictions of the monitoring system. Thus, the ERN is elicited by a phasic decrease of the tonic activity of the mesencephalic dopamine system depolarizing large proportions of apical dendrites of Layer V neurons in the ACC and summing up to a measurable EEG signal. Following the Holroyd Model, the ERN reflects an error in reward prediction.

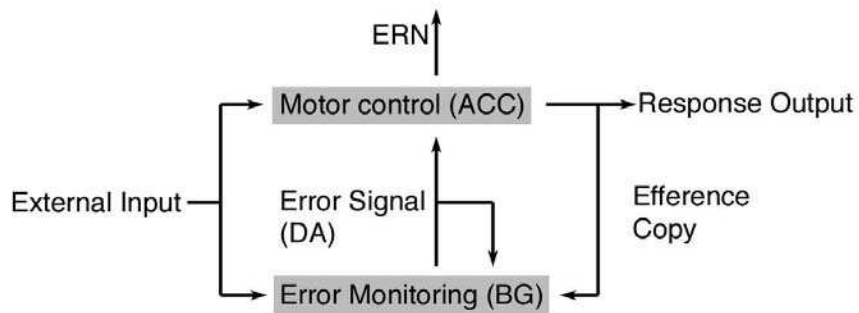


Figure 2.4: Schematic illustration of the Holroyd Model. ERN: error-related negativity; ACC: anterior cingulate cortex; BG: basal ganglia; DA: dopamine.

A recently published study tested this theory in an experiment, in which the frequency of reward occurrence varied between conditions (Holroyd, Nieuwenhuis, Yeung, & Cohen, 2003). In a reward condition, participants received positive

feedback on about 75% of the trials, and in a non-reward condition, participants received negative feedback on about 75% of the trials. On each trial the type of feedback stimulus was selected at random. Consistent with the Holroyd Model, a larger ERN was elicited by unexpected absence of reward.

2.3.2 The Response Conflict Hypothesis

Studies using computational modeling revealed evidence that the ERN can be explained in terms of the *Response Conflict Hypothesis* (Yeung, Botvinick, & Cohen, in press; Botvinick, Braver, Barch, Carter, & Cohen, 2001; Carter, Braver, Barch, Botvinick, Noll, & Cohen, 1998). This hypothesis proposes that the ERN reflects response conflict rather than errors per se. A response conflict arises, when multiple response tendencies compete in order to reach the same goal. The presence of response conflict indicates situations, where errors are likely to occur. Following this view, error detection does not reflect an independent process but is based on the presence of response conflict.

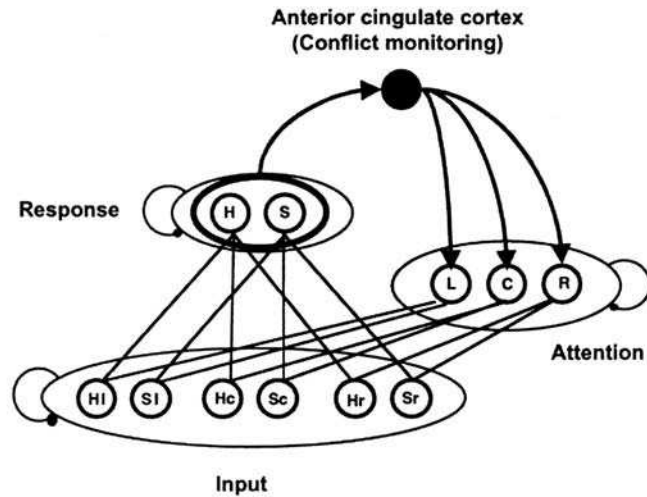
The Response Conflict Hypothesis was primarily tested in the connectionist model by Botvinick and colleagues (2001). Consistent with this hypothesis, they observed a larger response conflict on error trials than on correct trials, particularly in the period following the response. Yeung et al. (in press) further refined these results. Their basic connectionist model of the Eriksen flanker task (Eriksen, & Eriksen, 1974) is illustrated in Figure 2.5 A. This model comprises three layers of units: an input layer consisting of an array of six position-specific letter units; a response layer consisting of a unit for each response; and an attentional layer with units corresponding to each location in the letter array. The information flow is realized by bi-directional excitatory weights between layers. Competition is elicited by inhibitory links between all of the units within each layer. A conflict monitoring feedback loop simulates the role of the ACC in performance monitoring and adjustments of attentional control. When an input pattern is applied to the letter units, activations flow through their connections to the response units. According to the task, a biasing input from the attention layer favors the letter in the center of the array and the corresponding response is activated in the response

layer. The measured response conflict depends on the relative activation levels of the competing response units and is computed by a multiplication of the response unit activations. When one response unit is active and the other inhibited, conflict is low or zero. When both response units are active, however, the product of their activations is large and hence the degree of response conflict is large. If a response unit crosses an arbitrary response threshold, the corresponding response will be produced.

The model by Yeung et al. (in press) replicated previous findings showing a larger response conflict on error trials than on trials with correct responses. The model produces an *error* when noise causes the incorrect response unit to exceed threshold before the stimulus has been adequately processed (see, Figure 2.5 B, lower row). Following the incorrect response, stimulus processing continues resulting in an activation of the correct response unit (see, Figure 2.5 B, middle row). Then, a brief period follows the incorrect response, where both response units are simultaneously activated, leading to a large response conflict (see, Figure 2.5 B, upper row). This type of conflict that is arising from a competition between multiple activated response units is termed *post-response conflict* and has been associated with the ERN. According to the Response Conflict Hypothesis, the ERN should peak at the time of maximal post-response conflict. When the correct response unit is sufficiently activated to exceed threshold after the incorrect response has been produced, an error correcting response will be issued. This assumption is in line with recently published data suggesting that fast error corrections are *delayed correct responses* that have been initiated before the erroneous response has been completed and executed briefly after them (Rabbitt, 2002).

On *correct trials*, the activated correct response unit exceeds threshold and the continuous stimulus processing following the correct response reinforces the response decision made. Thus, the correct response unit is increasingly activated, while the incorrect response unit is further inhibited, leading to no response conflict after the correct response (see, Figure 2.5 B, upper row). Conflict due to competing input units, however, should occur on incorrect trials as well as on cor-

A



B

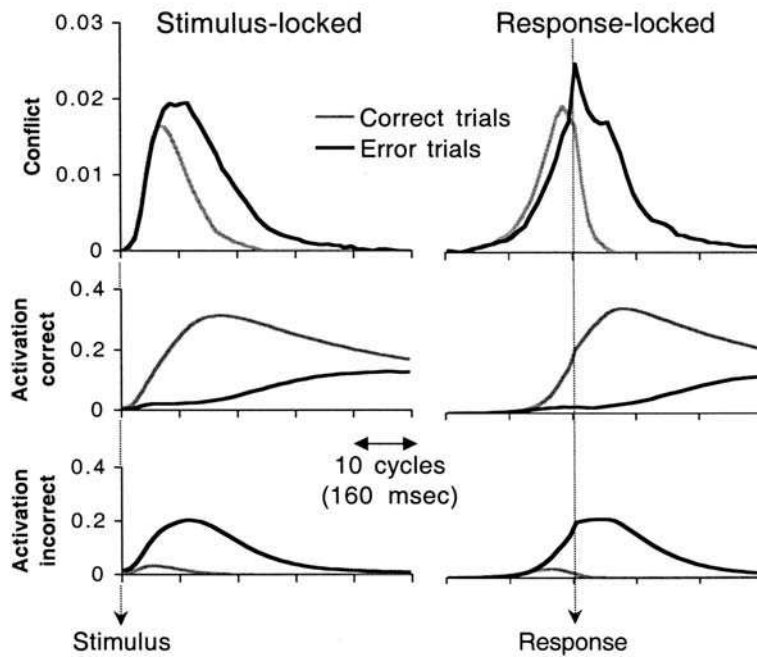


Figure 2.5: A: Illustration of the basic connectionist model of the Eriksen flanker task. The letters H and S designate the stimulus input, which can occur on the left (l/L), in the center (c/C) or on the right (r/R) side of the computer screen. The black lines indicate bi-directional excitatory weights between input, attention and response layers. The arrows represent the conflict monitoring feedback loop. B: Simulated activity on stimulus-locked and response-locked averages of correct and error trials. Response conflict (upper row) is the scaled product of the activity in the correct response unit (middle row) and the incorrect response unit (lower row). (source: Yeung et al., in press)

rect trials involving high response conflict, termed *pre-response conflict*. Yeung et al. (in press) proposed that a negative ERP component, denominated *N2*, is related to pre-response conflict. Kopp and colleagues (1996) already suggested a stimulus-locked ERP component related to conflict monitoring, the so called *N2c*. Later studies revealed supportive results showing a higher amplitude of the *N2* in conditions involving high conflict on the stimulus level compared to low conflict conditions (Nieuwenhuis, Yeung, & Cohen, 2004; van Veen, & Carter, 2002).

2.3.3 Evaluative Monitoring

Additional accounts suggest that the ERN reflects the activity of a general evaluative system concerned with the motivational significance of errors and emotional reactions to errors. Evidence of motivational effects for the ERN was first provided by an experiment of Gehring and colleagues (1993). In one condition, accuracy was emphasized by associating errors with financial penalties. In a second condition, speed was emphasized by offering bonuses for quick responses. In addition, a neutral condition was introduced, where values were altered to produce an intermediate speed-accuracy level. The results showed a larger ERN when accuracy was emphasized relative to the neutral condition and a diminished ERN when instructions emphasized speed. These findings were replicated recently by Ullsperger and Szymanowski (2004). A study by Gehring and Willoughby (2002) suggests that the motivational impact of an event (gain vs. loss) is more important than relative differences in monetary outcomes (low gain/loss vs. high gain/loss). Using a monetary gambling task, they discovered that the MFN was enhanced for loss compared to gain trials, whereas the relative differences in monetary outcomes were not reflected in the MFN. Some debate, however, remains whether both components, the MFN and the ERN, are the same.

Further evidence for the evaluative monitoring account comes from investigations of individual differences. The ERN amplitude has been shown to vary with neuropsychiatric conditions, such as obsessive compulsive disorder (OCD) (Hajcak, & Simons, 2002; Gehring, Himle, & Nisenson, 2000), general anxiety disorder (Hajcak, McDonald, & Simons, 2003), negative affect and negative

emotionality (Luu et al., 2000a), or impulsivity (Pailing et al., 2002). Luu and colleagues (2000a) related the ERN to questionnaire scores using the Positive Affect Negative Affect Scale (PANAS; Watson, Clark, & Tellegen, 1988) and the Multidimensional Personality Questionnaire (MPQ; Tellegen, & Waller, 1996). In the initial block of the experiment, individuals who scored high on the negative affect scale (NA) of the PANAS and the negative emotionality scale (NEM) of the MPQ showed larger ERN amplitudes than individuals scoring low on these dimensions. In later stages of the experiment, the ERN amplitude decreased for individuals with high NA and NEM scores. Based on behavioral data and individuals' self reports, the authors ascribed the initial increase of ERN amplitude to an overengagement in the task and the following decrease of ERN amplitude to a disengagement from that task. Results from patient studies investigating OCD confirm this view (Hajcak, & Simons, 2002; Gehring et al., 2000). OCD patients showed a larger ERN amplitude than controls presumably due to their difficulty in disengaging from extremely distressing behaviors and thoughts. Patients with OCD continually doubt and check their action, regardless of whether or not an error has actually been made. In a later study, Hajcak et al. (2003) generalized the findings beyond OCD within the anxiety spectrum disorders. The authors reported an enhanced ERN for individuals who scored high on a measure of general anxiety and worry relative to phobic individuals and controls. According to Luu et al. (2000), the results were interpreted in terms of high NA associated with anxiety.

A recently published study examined changes in the ERN in relation to motivational incentives and personality traits (Pailing, & Segalowitz, 2004). Monetary incentives for finger and hand accuracy were altered across motivational conditions to either be equal or to favor one type of accuracy over the other. A personality questionnaire (International Personality Item Pool, IPIP, Pool, 2001) and a socialization scale (Gough's Socialization scale, CPI, Gough, 1957) were used to measure different personality domains. A modulation of the ERN related to motivational error significance was only observed for some personality types. Individuals who scored high on conscientiousness displayed smaller motivation-related

2.4. PSYCHOPHYSIOLOGICAL CORRELATES OF ERROR PROCESSING²¹

changes to increasing incentives in the ERN than individuals scoring low on this dimension. These data suggest that the ability to selectively invest in error monitoring is modulated by the underlying personality. Findings from Dikman and Allen (2000) also demonstrate that motivational error significance is affected by personality. Individuals with low scores on the CPI socialization scale produced smaller ERNs during a punishment task than during a reward task. In contrast, individuals scoring high on the CPI socialization scale produced similar ERNs in both conditions.

2.4 Psychophysiological Correlates of Error Processing

Error processing has been hardly investigated by means of autonomic measures, such as electrodermal activity or heart rate (HR). These measures of somatic states provide useful information about changes of the autonomic nervous system associated with cognitive, motivational and emotional processes. An implicit linkage between factual knowledge and somatic states implemented in the ventromedian prefrontal cortex has been proposed by the *Somatic Marker Hypothesis* (for an overview see, Bechara, Tranel, & Damasio, 2002). According to this hypothesis, the re-occurrence of a certain situation leads to the recall of pertinently associated facts as well as to a re-activation of the somatic state that in past experience has been associated with that situation. The result of the combined activation is the approximate reconstruction of a previously learned factual-somatic set used to act successfully in similar future situations. Patients lesioned in the ventromedian prefrontal cortex often showed a weakened ability to generate somatic states in anticipation of future events, e.g., reflected by an inability to anticipate errors and/or to learn from previous mistakes.

Several studies relating *heart rate* changes to error processing have been reported recently. Some experiments examined the effects of external feedback on HR. Using a computerized Wisconsin Card Sorting Task, Somsen et al. (2000) revealed a cardiac deceleration on positive and negative feedback suggesting that HR is sensitive to performance feedback. The strength, however, of the HR de-

celeration depended on the nature of the feedback. Negative feedback elicited a greater HR slowing than positive feedback. The authors reasoned that the increased cardiac deceleration on negative feedback is caused by a detected *mismatch* between the expected and the received feedback. Beside the valence of the feedback stimulus (positive vs. negative), the *information value* of the feedback also influenced the amount of cardiac slowing. The HR deceleration to negative feedback was more pronounced when the sorting rule was changed, so that feedback provided useful information to successfully perform the task relative to the repeated rule application.

A study by van der Veen and colleagues (2004, 2000) further examined the effects of information value and the relation to remedial action by using a time-production task (Miltner et al., 1997). Participants were instructed to push a button whenever they thought that a 1-s interval had passed starting after the onset of a cue. Each trial was followed by a feedback of monetary gain (positive feedback) or monetary loss (negative feedback) depending on task performance. Only the negative feedback was informative to successfully perform the task. In addition, a yoked-control condition was introduced, in which feedback was unrelated to performance and could not be used to generate more precise intervals. Consistent with the findings by Somsen et al. (2000), positive and negative feedback elicited a cardiac deceleration. Exclusively on negative feedback, cardiac deceleration was related to the performance on subsequent trials. The data showed a smaller cardiac deceleration when performance was adjusted successfully on subsequent trials. This result indicates that cardiac slowing following response errors is related to *remedial actions*. HR deceleration on negative feedback, however, did not discriminate between the experimental condition and the yoked-control condition. Participants seemed to continue feedback processing regardless of whether it was informative or not. Van der Veen et al. (2004, 2000) reasoned that neither the mismatch between expected and actual feedback nor the information value provided by the feedback plays a crucial role in the modulation of the cardiac response. Rather, the cardiac response seems to be sensitive to the *valence* of the feedback

stimulus (positive vs. negative), especially to its affective evaluation reflected in a more pronounced deceleration for negative feedback.

Crone and colleagues (2003) tested the different hypotheses proposed by Somsen et al. (2000) and by van der Veen et al. (2004, 2000) using a probabilistic learning task (Holroyd, & Coles, 2002). In this task, the degree to which a response is predictive of the feedback value differed as follows: in the "100% condition" the feedback was 100% valid, in the "50% condition" feedback was in 50% positive and in 50% negative and in the "always condition" feedback was always positive or always negative independent of the actual response. Confirming previous results, HR slowing was observed for negative feedback in the "100% condition" suggesting that cardiac slowing following errors is associated with response monitoring. In the "50% condition", however, both positive and negative feedback elicited a cardiac deceleration, but only when the feedback alternated between successive trials. In accordance with Somsen et al. (2000), the authors assumed that HR slowing to feedback is due to a *violation* in the predictions of the outcome, either positively or negatively. This interpretation was strengthened by the finding that HR did not change between positive and negative feedback in the "always condition".

A recently published study by Hajcak and colleagues (2003) examined the relationship among the ERN, the Pe, behavioral responses and two autonomic measures, namely skin conductance and HR. Regarding the HR data, they found a greater HR deceleration for errors compared to correct responses. Extending the results by Somsen et al. (2000), the authors suggested that the cardiac deceleration indicates external feedback to response errors as well as internal processes associated with *error monitoring*.

2.5 Hemodynamic Correlates of Error Processing

2.5.1 Neuroanatomy of the Frontomedian Wall

This chapter presents the neuroanatomical findings about the frontomedian wall, which covers 22% to 26% of the frontal lobes. A number of regional specifica-

tions have been proposed. The frontomedian wall can be distinguished into the orbitofrontal cortex (OFC), the frontomedian cortex (FMC) and the ACC. The OFC is located above the eye socket (orbita) and includes the mesial orbital gyrus as well as the anterior, lateral, and posterior orbital gyri. The FMC can be further differentiated into the posterodorsal frontomedian cortex (pdFMC) comprising mesial parts of Brodmann Area (BA, for a definition see below) 6 and BA8, the anterodorsal frontomedian cortex (adFMC) comprising mesial parts of BA9 and BA10 and the ventral frontomedian cortex (vFMC) comprising pre- and subgenual parts of BA10 and BA32. Anatomical studies in nonhuman primates and functional imaging studies in humans support a dorsal-ventral functional distinction within the FMC (Gusnard, Akbudak, Shulman, & Raichle, 2001; Bush, Luu, & Posner, 2000; Ongur, & Price, 2000; Morris, Pandya, & Petrides, 1999; Petrides, & Pandya, 1999).

The identification and classification of different regions on the frontomedian wall are based on the appearance of surface landmarks and the microscopic analysis of the constituent neurons. The frontomedian wall is demarcated by the central sulcus posteriorly with regions being parcellated based on the laminar distribution and packing density of neurons (cf., Amunts, & Zilles, 2001; Amunts, Malikovic, Mohlberg, Schormann, & Zilles, 2000). Following the nomenclature by Mesulam (1996), cortical regions are divided into four types: limbic areas (corticoid areas, allocortex), paralimbic areas (periallocortex, proisocortex), homotypical association isocortex and idiotypic cortex. There is a progressive laminar differentiation from the allocortex showing one or two cell layers to the isocortex defined by six distinct cell layers. This laminar differentiation goes along with an increase in myelin content, an emergent granular layer IV, increased pyramidal cell size and increased cellular density (Kaufer, & Lewis, 1999). The paralimbic areas represent a transition from the allocortex to the isocortex. Parts of the paralimbic areas that border the allocortex are termed as periallocortex, whereas parts closest to the isocortex are called proisocortex.

At the microscopic level, a number of different cytoarchitectonic maps of the cortex have been constructed. One of the most widely used human cytoarchitec-

tonic maps was developed by Korbinian Brodmann (1909), which delineates 43 cortical regions, denominated Brodmann Areas (BAs). In combination with the BA classification, the Talairach stereotactic atlas (Talairach, & Tournoux, 1988) derived from one particular brain is also used to identify brain regions. The coordinate system is aligned to the anterior commissure (AC) and the posterior commissure (PC). In the following, the neuroanatomy of the BAs related to error processing are described in more detail, namely BA24, BA32, BA6 and BA8.

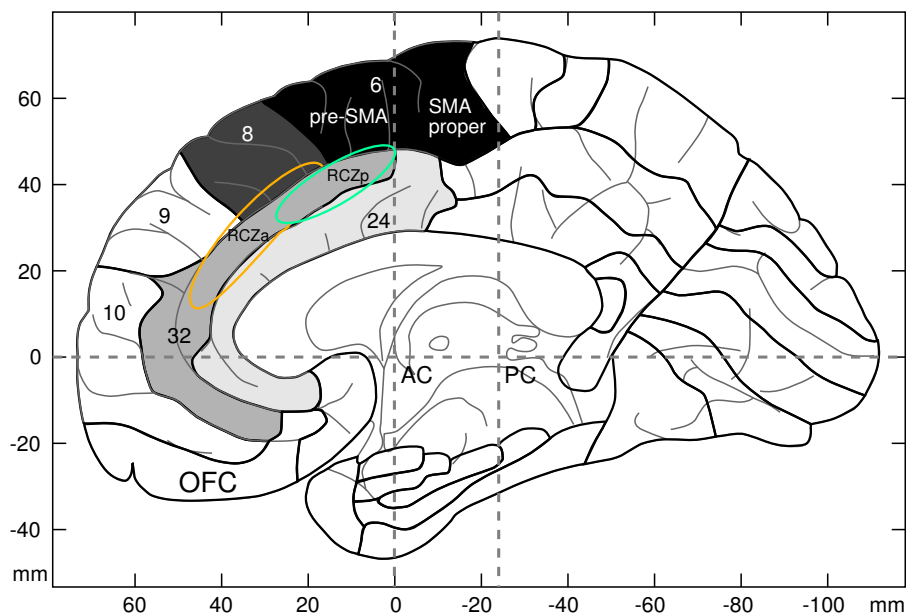


Figure 2.6: The frontomedian wall of the right hemisphere integrated into the coordinate system by Talairach and Tournoux (1988), which is aligned to the anterior commissure (AC) and the posterior commissure (PC). Brodmann areas of interest (BA24, BA32, BA8, BA6) are color-coded. The location of the anterior rostral cingulate zone (RCZa) and the posterior rostral cingulate zone (RCZp) are schematically drawn in.

Neuroanatomy of the Cingulate Cortex

The cingulate cortex can be subdivided into the ACC and the posterior cingulate cortex on the basis of cytoarchitecture, patterns of projections and function. The ACC is located in the median wall of the frontal lobes in each hemisphere and

includes area BA24. It surrounds the anterior part of the corpus callosum on the mesial surface and lies in the cingulate gyrus. The boundaries of the ACC are demarcated by the sulcus cinguli superiorly and the sulcus corporis callosi inferiorly. This area extends posteriorly as far as area BA6 and continues anteriorly around the genu and rostrum of the corpus callosum. Regarding cytoarchitecture, the BA24 belongs to the proisocortex defined by a lack of the inner granule cell layer IV (agranular cortex). In its posterior portion, BA24 is characterized by large, deeply stained spindle cells in layer V, which resemble in appearance large motor neurons. This area is surrounded by area BA32, the so called paracingulate cortex, with a small inner granule cell layer IV (dysgranular cortex). It can be considered a transitional type of cortex between the proisocortex and the isocortex. The BA32 is located between the cingulate sulcus and, when present, the paracingulate sulcus (cf., Bush et al., 2000; Petrides, & Pandya, 1999) .

Several subdivisions of the ACC have been proposed. Based on convergent data from cytoarchitectural, lesion, electrophysiological and imaging studies, a dorsal cognitive division composed of the areas BA 24b'-c' and BA 32' has been differentiated from a rostral-ventral affective division composed of the areas BA 24a-c, BA 32, BA 25 and BA 33 (Bush et al., 2000; Vogt, Nimchinsky, Vogt, & Hof, 1995) . The location of these areas is visualized in Figure 2.7. The dorsal cognitive division includes cortex on the dorsal and ventral banks of the cingulate sulcus and maintains strong reciprocal interconnections with the lateral prefrontal cortex, the parietal cortex and premotor and supplementary motor areas. In contrast, the affective subdivision has connections to the amygdala, the periaqueductal gray, nucleus accumbens, hypothalamus, anterior insula, hippocampus and orbitofrontal cortex (Devinsky, Morrell, & Vogt, 1995).

Data from primate studies revealed a more fine-grained subdivision of the dorsal ACC into the caudal cingulate motor area (CMA) (BA6c, BA23c, BA24c) and the rostral CMA (BA24c, BA32'). An imagined perpendicular line through the AC (VCA) separates the two regions. The rostral CMA covers the region anteriorly to the VCA, the caudal CMA is located posteriorly to the VCA (Picard, & Strick, 2001, 1996). The CMA is connected to the primary motor cortex and the

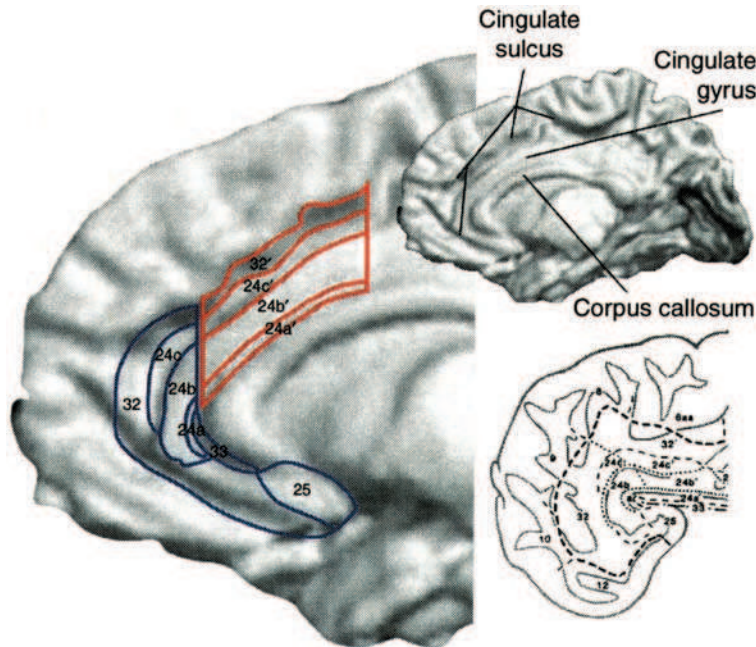


Figure 2.7: *Left: Schematic representation of cytoarchitectural areas of the anterior cingulate cortex (ACC) is shown on the enlarged section of the medial surface of the right hemisphere. Cognitive division areas are outlined in red and affective division areas are outlined in blue. Right: Reconstructed MRI of the medial surface of the right hemisphere (upper row). Schematized flat map of the anterior cingulate cortical areas (lower row). (source: Bush et al., 2002, page 216.)*

spinal cord (Dum, & Strick, 1991). The two portions of the CMA, however, differ with respect to their density of corticospinal neurons. While the caudal CMA exerts a strong influence on the spinal cord, the rostral CMA exerts a comparatively weak influence (Picard, & Strick, 2001, 1996). Corresponding areas in humans have been proposed: a caudal cingulate zone (CCZ) and a rostral cingulate zone (RCZ) with two subdivisions, anterior RCZ and posterior RCZ. While the CCZ and the posterior RCZ are likely to be connected with the spinal cord, a connection between the anterior RCZ and the spinal cord is still unclear (Bush, Vogt, Holmes, Dale, Greve, Jenike, & Rosen, 2002; Picard, & Strick, 2001; Picard, & Strick, 1996). The location of the RCZ is schematically illustrated in Figure 2.6.

Neuroanatomy of the pdFMC

The mesial BA8 adjoins the BA32 inferiorly. It occupies the posterior part of the superior and middle frontal gyri and extends as far as the paracingulate sulcus. It belongs to the six cell layer prefrontal isocortex characterized by a well developed inner granule cell layer IV (Petrides, & Pandya, 1999). Posteriorly adjacent to BA8, the BA6 is located. Because no anatomical landmarks are available, this border is not clearly defined. Based on cyto- and chemoarchitectonic differences, two regions of BA6 can be distinguished: the pre-supplementary motor area (pre-SMA), located anteriorly to the VCA, and the supplementary motor area (SMA) proper, located posteriorly to the VCA (Picard, & Strick, 2001). Given cytoarchitectonic similarities within the SMA proper, this area also differs in some cytoarchitectonic features, e.g., number of large pyramidal cells or degree of lamination of cell layer V. Starting from this finding, the SMA proper can be further subdivided into the caudal SMA (SMAc) and the rostral SMA (SMAr) (Vorobiev, Govoni, Rizzolatti, Matelli, & Luppino, 1998).

In contrast to the pre-SMA, the SMA proper projects directly to the spinal cord and the primary motor cortex (BA4), which borders anteriorly on the SMA (Dum, & Strick, 1991). The pre-SMA is interconnected with regions of the prefrontal cortex and other non-primary motor areas (Bates, & Goldman-Rakic, 1993). Thus, the SMA proper is related more to motor functions, such as motor execution, while the pre-SMA is involved in cognitive functions, e.g., selection and preparation of movements (Picard, & Strick, 2001, 1996).

2.5.2 The Frontomedian Wall and Error Detection

It has been proposed that the ACC, specifically the RCZ, plays a crucial role in the processing of erroneous responses using different methodological approaches, such as functional magnetic resonance imaging (fMRI) (Rubia, Smith, Brammer, & Taylor, 2003; Garavan, Ross, Kaufman, & Stein, 2003; Ullsperger, & von Cramon, 2003; Garavan, Ross, Murphy, Roche, & Stein, 2002; Ullsperger, & von Cramon, 2001; Kiehl, Liddle, & Hopfinger, 2000; Carter et al., 1998), lesion studies (Husain, Parton, Hodgson, Mort, & Rees, 2003; Swick, & Turken, 2002),

intracerebral ERP recordings (Brazdil, Roman, Falkenstein, Daniel, Jurak, & Rektor, 2002) or dipole source modeling of the ERN (Luu, & Tucker, 2001; Dehaene et al., 1994). In these studies, the error-related increase in hemodynamic activity in the vicinity of the ACC belonged most often to the RCZ. An activation in this area can be elicited by self-produced errors (e.g., Ullsperger, & von Cramon, 2001), observed errors (van Schie et al., 2004) as well as external error feedback (Holroyd, Nieuwenhuis, Yeung, Nystrom, Mars, Coles, & Cohen, 2004). In addition to the ACC, brain regions in the pdFMC and in the dorsolateral prefrontal cortex have been related to error processing (Ullsperger, & von Cramon, 2003; Garavan et al., 2003, 2002; Ullsperger, & von Cramon, 2001; Milham, Banich, Webb, Barad, Cohen, Wszalek, & Kramer, 2001; Kiehl et al., 2000; Carter et al., 1998).

It is still an open question, whether the activation in the RCZ is elicited by the error per se or by response conflict. Findings by Carter and colleagues (1998) support the latter view. The authors reported an increased activation in the dorsal ACC during errors as well as during correct responses under conditions of increased response conflict. They argued that the RCZ detects conditions, under which errors are likely to occur rather than errors per se. Following this view, the RCZ is assumed to perform an evaluative function reflecting the degree of response conflict (Kerns et al., 2004; Durston, Davidson, Thomas, Worden, Tottenham, Martinez, Watts, Ulug, & Casey, 2003; Milham et al., 2001; Carter, Macdonald, Botvinick, Ross, Stenger, Noll, & Cohen, 2000; Macdonald, Cohen, Stenger, & Carter, 2000; Barch, Braver, Sabb, & Noll, 2000; Botvinick, Nystrom, Fissell, Carter, & Cohen, 1999). Van Veen and colleagues (2001) showed that conflict-related activity in the ACC varies with the degree of conflict at the response level but not with the degree of conflict at the level of stimulus identification. Thus, higher activation in the RCZ in conditions, where stimuli are hard to detect, reflect rather uncertainty than response conflict. Using a prediction task, a recently published study reported activations in the pdFMC that vary with the amount of uncertainty (Volz, Schubotz, & von Cramon, 2003).

Alternative findings have been revealed by fMRI studies, which aimed to disentangle processes related to error detection and response conflict. Based on the results of a Go/Nogo task, Kiehl and colleagues (2000) showed that the rostral and caudal portion of the ACC is engaged in error detection while response conflict activated the pFMC. These results were confirmed by a recent fMRI study using the same paradigm (Mathalon, Whitfield, & Ford, 2003). A similar activation pattern was reported by Ullsperger and von Cramon (2001) using a speeded modified flanker task. The authors found an activation related to error detection in the RCZ, whereas response conflict activated the pre-SMA and the mesial BA8. Activation in the pre-SMA (BA6) was observed during both, error detection and response conflict. The findings by Garavan and colleagues (2002, 2003) support the central role of the RCZ in error detection. The activation focus associated with response conflict was located posteriorly adjacent to the BA8, in the pre-SMA (BA6) (Garavan et al., 2003). Figure 2.8 depicts activation foci associated with error detection colored in red (Ullsperger & von Cramon, in press; Kerns et al., 2004; Rubia et al., 2003; Garavan et al., 2003, 2002; Ullsperger & von Cramon, 2001; Kiehl et al., 2000) and response conflict colored in green (Kerns et al., 2004; Garavan et al., 2003; Durston et al., 2003; van Veen, Cohen, Botvinick, Stenger, & Carter, 2001; Milham et al., 2001; Ullsperger & von Cramon, 2001; Barch et al., 2000; Macdonald et al., 2000; Carter et al., 2000; Botvinick et al., 1999; Carter et al., 1998) reported in 16 fMRI studies. Hemodynamic activations associated with error processing seem to cluster in the RCZ, while response conflict related activations are located in the mesial BA8, mesial BA6 and the BA32.

Lesion studies provide further evidence for a regional dissociation of error detection and response conflict. A single-case ERP study reported that a patient lesioned in the dorsal ACC showed a diminished ERN, whereas the conflict-related N2 component was enhanced (Swick, & Turken, 2002). The authors conclude that the dorsal ACC is related rather to error detection than to response conflict. This finding was supported by a study using single-cell recording in the monkeys' ACC, which exhibited that neurons were active during committing of an error,

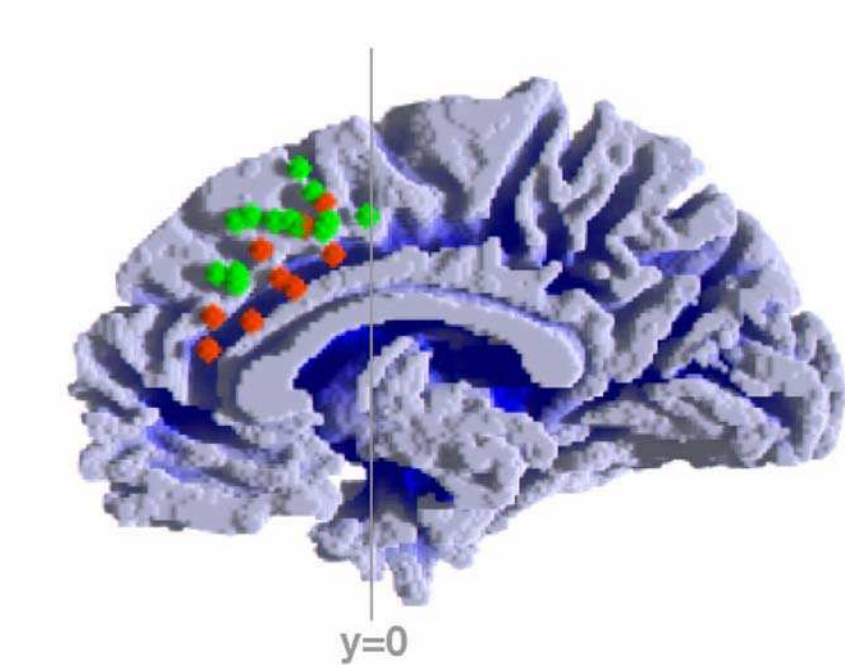


Figure 2.8: *Metaanalysis of frontomedian activations of 16 fMRI studies investigating error-related processes. The right frontomedian wall of a white matter segmented individual brain is shown from the midline. The vertical line marks $y=0$ in the Talairach space. Activation foci associated with error detection are colored in red; activations related to response conflict are colored in green.*

whereas no neurons responded to the conflict condition (Ito, Stuphorn, Brown, & Schall, 2003). Regarding the lesion study by Husain and colleagues (2003), the pre-SMA seems to be more engaged in response conflict. In this study, a patient with a highly selective lesion in the pre-SMA showed an impaired control of eye movements during response conflict, error detection, however, was not affected. The authors suggest that the pre-SMA plays a critical role in the motoric implementation of control during response conflict rather than in error detection.

2.5.3 The Frontomedian Wall and Error Correction

Imaging studies have focused little on the consequences of errors. A system located in the dorsal ACC and/or pre-SMA has been proposed, which monitors performance on-line and comes into play, when an error is detected in time for a correction to be attempted (Dehaene et al., 1994).

Studies using single-cell recording in monkeys revealed evidence that the monkey homologue of the RCZ, the rostral CMA, is related to an alternation in behavior after detecting an error (Shima, & Tanji, 1998) and monitors behavioral consequences (Ito et al., 2003). Swick and Turken (2002) reported reduced error corrections in a patient with a lesion in the RCZ. An engagement of the RCZ in long-term adjustments following errors was supported by fMRI studies in humans. Garavan and colleagues (2002) investigated the neural correlates of the PES effect (cf., page 7) revealing activation in the RCZ bilaterally, the pre-SMA bilaterally, the left inferior frontal and precentral gyri and the right putamen. A patient study showed a diminished rostral ACC activation and a reduced PES effect in a group of schizophrenic patients compared to a control group (Carter, Macdonald, Ross, & Stenger, 2001). Latest findings also reported a relation of increased ACC activation on error trials and PES on the subsequent trial (Kerns et al., 2004).

2.6 Aims of the Present Studies

The present work focuses on the temporospatial characteristics of error correction by applying electrophysiological, psychophysiological, and imaging techniques. To achieve comparability to a variety of reported studies, a modified version of the Eriksen flanker task was used known to elicit a high number of error trials (for a task description see page 68, Ullsperger, & von Cramon, 2001).

The first experiment examines the electrophysiological correlates of error correction and its time course by means of behavioral data, event-related potentials, and lateralized readiness potentials. Given the inconsistent findings about the re-

relationship of the ERN and error correction, the experiment further investigates whether the ERN is modulated by error correction and/or correction speed when slowly and quickly corrected errors are compared.

The functional implementation of error correction is studied in the second experiment using fMRI. The issue is addressed whether error detection and error correction rely on a common neuroanatomical substrate or whether both processes are implemented by different cortical areas. For this purpose, brain regions related to error detection and error correction should be identified and compared with respect to their localization. Based on these results, the functional role of the underlying brain regions should be specified and discussed in the framework of the current models of performance monitoring.

To further elaborate the electrophysiological and imaging results, cardiovascular changes associated with error detection and error correction are examined.

Chapter 3

Methods in Cognitive Neuroscience

In the last century, electrophysiology has attracted wide attention in psychological research. Scalp-recorded brain potentials have been used to record the temporal course of information processing in the human brain. The successive deflections of the electroencephalogram (EEG) have been successfully linked to many psychological processes involved in perception, attention, emotion, memory, language or motor function. At the beginning of the nineties, the usage of imaging techniques, such as functional magnetic resonance imaging (fMRI) or positron emission tomography (PET), has increased significantly. Imaging techniques provide information about the implementation of cognitive processes within regions of the human brain. The ability to localize the neural circuitry underlying specific mental processes helps to understand brain functions. While electrophysiological methods have an excellent temporal resolution of a few milliseconds [ms], but poor spatial resolution of several centimeters [cm], imaging methods have a high spatial resolution of a few millimeters [mm], but a moderate temporal resolution of several seconds [s] (Cabeza, & Nyberg, 2000). A combination of electrophysiological and imaging techniques can conflate the advantages of both methods and provide information about the time course of putative generators underlying cognitive functions.

The following chapter will give an introduction to the methods used in the present work. First, two electrophysiological measures, event-related potentials and lateralized readiness potentials, will be reviewed. Further on, heart rate as a psychophysiological measure extending electrophysiological methodology will be introduced. Finally, the fMRI method will be described in detail.

3.1 Electrophysiological Method: Event-related Potentials

Performance measures reflect the end product of cognitive processes. Interpreting overt performance as evidence for or against a hypothesis about the properties of covert cognitive processes thus requires inferential processes (see, Coles, 1989). Event-related brain potentials (ERPs) derived from the EEG signal provide a more direct access to cognitive activity. In contrast to behavioral data, ERPs can be recorded online and continuously while cognitive processes are operating. They provide precise information about the time course of brain activity and thus are a valuable method to investigate the temporal dynamics of cognitive mechanisms. Moreover, the high temporal resolution of ERPs is very suitable to distinguish subprocesses underlying different cognitive functions. ERP research aims to describe the relationships between ERP components and specific cognitive processes, such as stimulus discrimination or response selection (see also, Coles, Gratton, & Fabiani, 1990).

3.1.1 The Electroencephalography

Electrophysiological research in humans was initiated by Hans Berger in 1929, who first published recorded electrical brain wave activity in humans. He identified different patterns of brain waves in the human EEG. A regular wave pattern occurring with a frequency of about 8 to 12 Hertz [Hz] was termed *alpha* waves. A second pattern of brain waves was characterized by a smaller amplitude and a higher frequency of about 12 to 30 Hz compared to the alpha waves. Following the Greek alphabet, Berger denominated this wave pattern *beta* waves. Based on these findings, electrophysiological research in humans has been continued

3.1. ELECTROPHYSIOLOGICAL METHOD: EVENT-RELATED POTENTIALS 37

leading to an identification of further brain wave patterns, which differ in their amplitude and frequency (see Table 3.1). These brain wave patterns have been functionally related to different cognitive processes.

Table 3.1: *Most prominent frequency ranges of oscillatory activity.*

<i>Oscillatory Activity</i>	<i>Frequency Range</i>
delta	≤ 4 Hz
theta	4 - 7 Hz
alpha	8 - 12 Hz
beta	12 - 30 Hz
gamma	30 - 80 Hz

Measurement of the EEG

The EEG measures electrical activity from the scalp, which is caused by a summation of various electrical processes within the brain. These voltage differences are recorded between two electrode sites. Two types of recording can be distinguished: monopolar and bipolar recordings. In monopolar recordings, one active electrode is placed at the scalp over a cortical area of interest, whereas a second reference electrode is attached to an electrically inactive region, e.g., the mastoid or the nose. In bipolar recordings, such as the vertical (EOGV) or horizontal (EOGH) electrooculogram, the voltage difference between two active electrodes is measured.

The number of electrode sites recorded in an experiment depends on the spatial distribution of the cognitive function of interest. Usually, several active electrodes are placed over different brain regions and are referenced to the same reference electrode. Electrode locations are generally described with regard to the international standardized 10-20 system, which is illustrated in Figure 3.1 (Jasper, 1958, for an extended version see, Pivik, Broughton, Coppola, Davidson, Fox, & Nuwer, 1993). The original 10-20 system contains 21 electrode sites placed

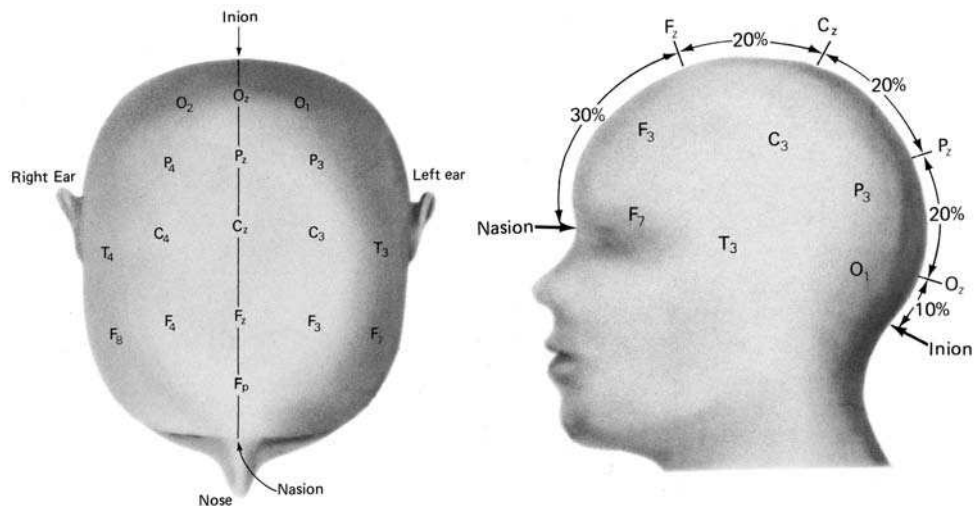


Figure 3.1: *International EEG 10-20 system for electrode placement. Left: Top view of scalp locations. Right: Left side view of scalp locations. The percentages indicate the distance between each electrode. The nasion, the bridge of the nose, and the inion, the occipital protuberance, serve as standard points. F: frontal, T: temporal, C: central, P: parietal, O: occipital z: midline.*

at relative distance (10% or 20% steps) to standard points on the scalp, e.g., the nasion, the inion and the preauricular points. The electrode labelling is specified in terms of their proximity to particular regions of the brain. Frontal placements are labeled with *F*, temporal ones with *T*, central ones with *C*, parietal ones with *P* and occipital ones with *O*. The label *z* is used for electrodes placed at the midline. *Even numbers* indicate that electrodes are placed at the right hemisphere, *odd numbers* indicate left electrode placement. In order to improve spatial resolution of the EEG, 64 or 128 electrode channels are recorded in cognitive experiments in compliance with the American EEG Society (1991).

The recorded EEG signal can be affected by artifacts caused by sources other than the brain. Filtering procedures provide one possibility to attenuate artifactual electrical activity. Low-pass filtering can be used to decrease the influence of high-frequent muscle activity, whereas high-pass filters attenuate low-frequent activity, such as direct-current (DC) shifts. Movements of the eyes and eyelids are

frequently appearing artifacts, which strongly distort the original signal. Filtering procedure cannot be applied, because the frequencies of interest are part of the frequencies within the range of the eye movement artifacts. Therefore, the EEG epochs distorted by the frequencies of eye movement artifacts have to be discarded from statistical analysis or a correction procedure has to be applied (e.g., Pfeifer, 1993).

3.1.2 Derivation of the ERPs

ERPs are voltage differences, which can be measured in the EEG before, during or after a sensory, motor or psychological event. The occurrence of an event evokes a time locking of a specific part of electric brain activity in the EEG. Thus, ERPs reflect electrical activity of the brain time-locked to ongoing information processes of a particular event, for instance the presentation of a stimulus or a response to a stimulus (Hillyard, & Kutas, 1983). Because the voltage differences of the ERPs are small (μV) in relation to the background EEG (tens of μV), an arithmetical averaging technique has to be applied. In order to extract event-related activity from the background EEG, a number of EEG epochs, time-locked to repetitions of the same event, are averaged. This averaging technique is based on the assumption that event-related activity is time-locked to the event of interest, whereas the background EEG fluctuates randomly and should not correlate with the event. Thus, arithmetical averaging of these EEG epochs will lead to an elimination of the randomly varying background EEG and the isolation of the event-related activity, which is called *event-related potential* (ERP) (e.g., Coles, Gratton, Kramer, & Miller, 1986). Consequently, the ERP is the more stable the more EEG epochs are averaged. To yield a reliable signal-to-noise ratio (SNR), 20 to 30 repetitions of the same event have to be averaged. A schematic illustration of the derivation of the ERP from the EEG signal is depicted in Figure 3.2.

The resulting ERP waveform is characterized by a sequence of temporally consecutive negative and positive deflections of voltage (see Figure 3.2). These deflections are described in terms of their polarity relative to a baseline (positive [P] versus negative [N]), their amplitude relative to a baseline or relative to the

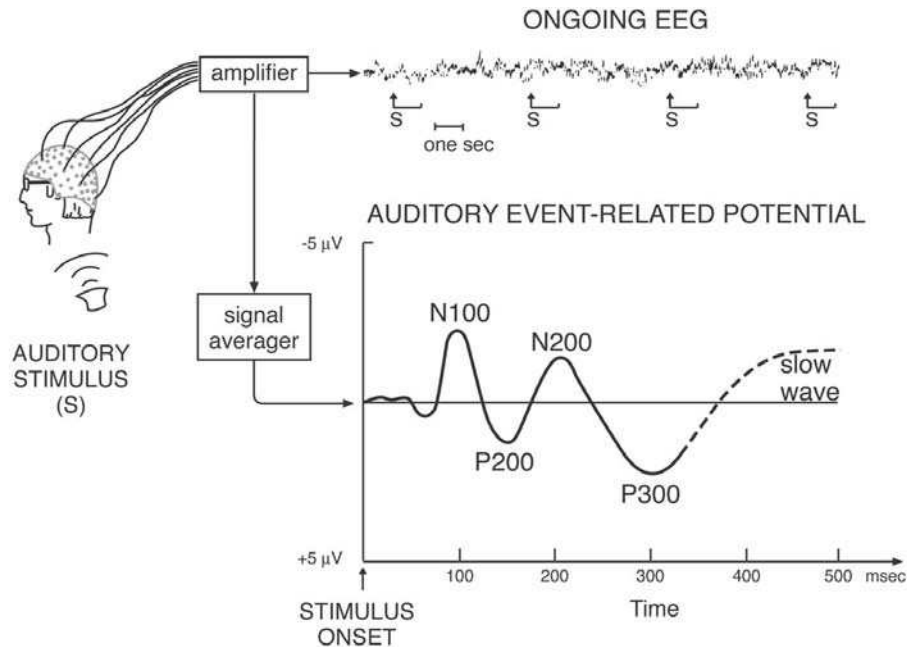


Figure 3.2: *Idealized auditory event-related potential. Following an auditory stimulus, a series of voltage deflections can be observed from scalp recordings. Event-related activity phase-locked to the stimulus onset (S) is mostly too small to be distinguished from the background EEG (upper panel). By averaging a number of EEG epochs, time-locked to repetitions of the same event, event-related activity can be extracted (lower panel). (source: Hillyard, & Kutas, 1983, p.35)*

preceding peak (in μV), their latency relative to an event of interest (in ms), and their characteristic scalp distribution. The baseline is usually defined as the mean voltage level for a specified time period, which is measured immediately prior to the stimulus or event of interest.

3.1.3 The Generation of ERPs

It is generally accepted that ERPs mirror cortical activity originating within the brain. The relationship, however, between the neurophysiological processes taking place in the brain and the voltage changes observed at the scalp is not fully understood (for a detailed discussion see, Norman, 1981; Wood, 1987).

3.1. ELECTROPHYSIOLOGICAL METHOD: EVENT-RELATED POTENTIALS 41

Scalp-recorded ERPs reflect primarily summed dendritic inhibitory (IPSP) and excitatory (EPSP) post-synaptic potentials of simultaneously activated pyramidal cells in the neocortex. ERPs represent electrical fields associated with the synchronized activity of sizeable populations of neurons (about 1 million). The neurons must be configured in a certain geometry such that their individual electrical fields summate to yield a dipolar field. This configuration is termed *open field*. In such a configuration, neurons are usually aligned in a parallel orientation, perpendicular to the scalp surface. Much neural activity, however, is never apparent at the scalp. This can be caused by an insufficient synchronisation of neural activity, even in an open field configuration, or an insufficient summation of electrical fields due to a certain geometric arrangement of the neurons. While the neural geometry facilitates the summation and propagation of electrical activity in the cerebral cortex, it is limiting in other structures, such as the thalamus (cf., Norman, 1981; Rugg, & Coles, 1995).

The resultant selectivity of the ERP method has to be taken into account when interpreting ERP data. First, the neural activity of numerous functionally important neural processes cannot be detected. Second, the neural source of the measured signal cannot be located exactly. Third, the neural source of the measured signal waveform at the scalp can result from the summation of neural activity that may be generated by several different sources in the brain.

3.1.4 Lateralized Readiness Potentials

Slow potentials that precede and accompany movements are a particular form of the ERP. The EEG recorded from an electrode placed over the central areas of the cortex shows a gradually increasing negative shift, which is terminated simultaneously with the beginning of a voluntary movement. This increase in surface negativity is referred to as the Bereitschaftspotential (Kornhuber, & Deecke, 1965) (readiness potential, RP, De Jong, Wierda, Mulder, & Mulder, 1988; Gratton, Coles, Sirevaag, Eriksen, & Donchin, 1988). The beginning of the move-

ment is accompanied by a large positive deflection and a recovery to the baseline, the so called movement-related potential (MRP; Vaughan, Costa, & Ritter, 1968; Shibasaki, Barrett, Halliday, & Halliday, 1980).

The RP is initially equally large over both hemispheres but begins to lateralize before the onset of the motor response. The lateralization is maximal for recording sites above the motor cortex and more pronounced over the hemisphere contralateral to the response side. The beginning of the lateralization reflects the point in time at which the response side (left vs. right) is determined (Kutas, & Donchin, 1980). Kutas and Donchin (1980) argued that the lateralization of the RP indicates the differential engagement of the left and right motor cortices in the preparation and initiation of unimanual motor responses. The information contained in the RP, however, is not related only to motor function, because the two hemispheres are differentially engaged in a variety of cognitive functions. Consequently, it is necessary to isolate the asymmetrical brain activity that can be attributed solely to movement, which is called the *lateralized readiness potential* (LRP).

Derivation of the LRP

The LRP is derived from the electrical activity recorded from two electrodes placed over the left and right central areas of the cortex. Frequently chosen recording site pairs are C3' and C4', located 1 cm anterior of the left central C3 and right central C4 sites specified by the 10-20 system (Jasper, 1958; cf., Figure 3.1, page 38).

As mentioned before, movement-related asymmetrical brain activity has to be isolated from brain activity related to other cognitive functions. This can be accomplished by a double *subtraction-averaging procedure* proposed by Coles (1989). First, the asymmetrical activity is computed separately for the left and

3.1. ELECTROPHYSIOLOGICAL METHOD: EVENT-RELATED POTENTIALS 43

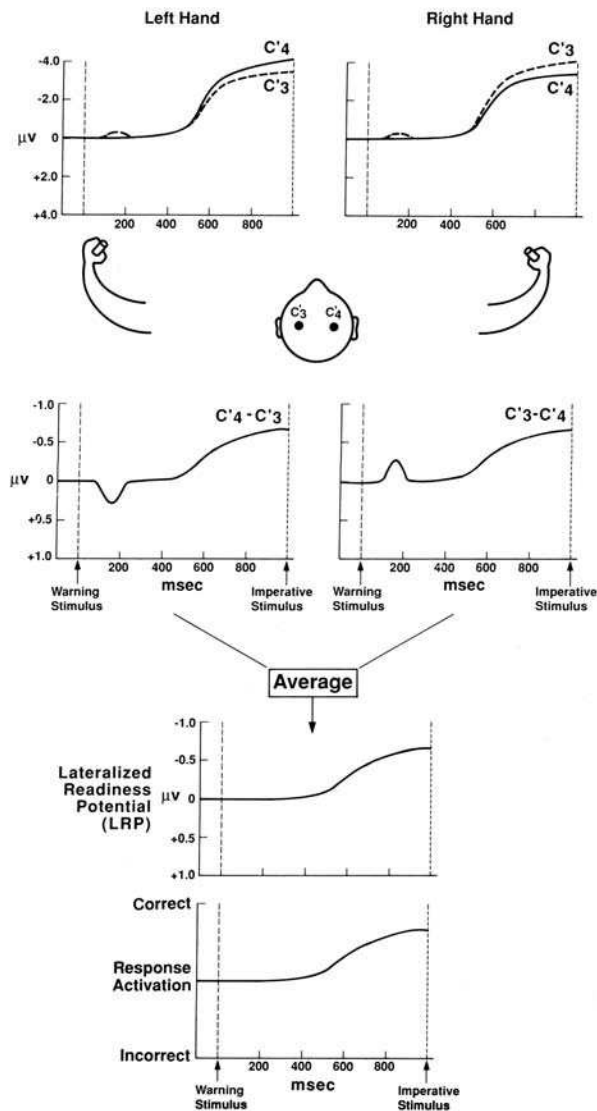


Figure 3.3: Schematic illustration of the derivation of the lateralized readiness potential. The top panel shows idealized scalp-recorded brain potentials from the left (C'3') and right (C'4') electrode sites of a participant performing a two-choice reaction time task (left side: potentials associated with left-hand movements; right side: potentials associated with right-hand movements). The middle panel illustrates the difference potentials for left- and right-hand movements. The asymmetrical activity is computed separately for the left and right motor response by subtracting the activity over the hemisphere ipsilateral to the movement from that over the hemisphere contralateral to the movement. The lateralized readiness potential results from averaging the difference potentials for left- and right-hand movements, as depicted in the lower panel. Response activation to the correct side is depicted upwards, to the incorrect side downwards. (source: Rugg, & Coles, 1995, p.98)

right motor response by subtracting the activity over the hemisphere ipsilateral to the movement from that over the hemisphere contralateral to the movement. Second, the asymmetry across the left-hand and the right-hand movement is averaged¹. The formula for the resulting LRP is as follows:

$$LRP = \frac{Mean(C4' - C3')_{left-hand-movement} + Mean(C3' - C4')_{right-hand-movement}}{2} \quad (3.1)$$

This procedure leads to an elimination of all those asymmetries that remain constant when the side of movement changes. Consequently, asymmetrical brain activity, which is not related to motor function, will be removed.

The LRP has become an important tool in the study of the neural basis of human cognitive-motor processing. It is supposed to reflect the relative activation of left and right motor responses. The LRP can be used to investigate the selection and preparation of response activation processes and can give an index of the relative strength of response priming. Thus, it indicates whether and when a motor response is selected. Particularly, LRPs provide information about partial response activation, such as partial response tendencies.

3.2 Psychophysiological Method: Heart Rate

Psychophysiological measures, such as cardiac activity, can considerably extend behavioral and electrophysiological data. Cognitive processes are always accompanied by reactions of the autonomic nervous system. Consequently, an integrative approach is required, which provides a separation of cognitive subprocesses by psychophysiological measures. The recording of the *heart rate* (HR) is one of the most fine-grained methods to assess changes of the autonomic nervous system (ANS) associated with cognitive, motivational and emotional processes. Possible relationships between cardiovascular responses recorded by the electrocardiogram

¹The first step described by Coles (1989) is equivalent to the double subtraction method reported by De Jong and colleagues (1988). Consequently, the LRP amplitude values obtained with the double subtraction method (De Jong et al., 1988) are exactly twice as large as the values obtained with the subtraction-averaging procedure described by Coles (1989).

and electrophysiological responses recorded by the EEG can be examined in combined experiments using a simultaneous recording procedure.

3.2.1 The Electrocardiogram

The study of electrical changes occurring during the contraction of the heart was initiated by Willem Einthoven of Holland in 1904. Einthoven developed an instrument sensitive enough to record the small, rapidly varying electric currents produced by the contraction of the heart. This early recording device and modern ones take advantage of the fact that a portion of the electrical impulse that passes through the heart during contraction is projected to the surface of the body because of the good conductance of body fluids. Placing electrodes on the skin on either side of the heart, electrical potentials generated by the contraction of the heart can be recorded, termed *electrocardiogram* (ECG) (for an overview see, Brownley, Hurwitz, & Schneiderman, 2000; Andreassi, 1995; Antoni, 1995).

The Cardiac Cycle

The ECG is composed of characteristic deflections referred to as P, Q, R, S, and T waves that are denominated *cardiac cycle*. Figure 3.4 illustrates the different anatomical sources of electrical impulses produced on the ECG. The heart excitation is realized by specialized fibers, including: the sinoatrial (S-A) node, the atrioventricular (A-V) node, the A-V bundle and the left and right bundles of conducting fibers. The S-A node, a small strip of muscle located in the upper part of the right atrium, initiates the impulse that triggers the contraction of the entire heart. The cells of the S-A node are also referred to as pacemaker cells because of their ability to originate an electrical impulse with a rate of 120 beats per minute [bpm] at normal body temperature. The vagus nerve, however, inhibits the pacemaker cells and reduces the rate to approximately 70-80 bpm. The electrical impulse passes through the atria to the A-V node resulting in a depolarisation of the atrial muscle. This is reflected by the *P-wave*. Mechanical contraction of the atria presses the blood into the ventricles till a complete ventricular filling. The electrical impulse then passes through the common bundle of His into

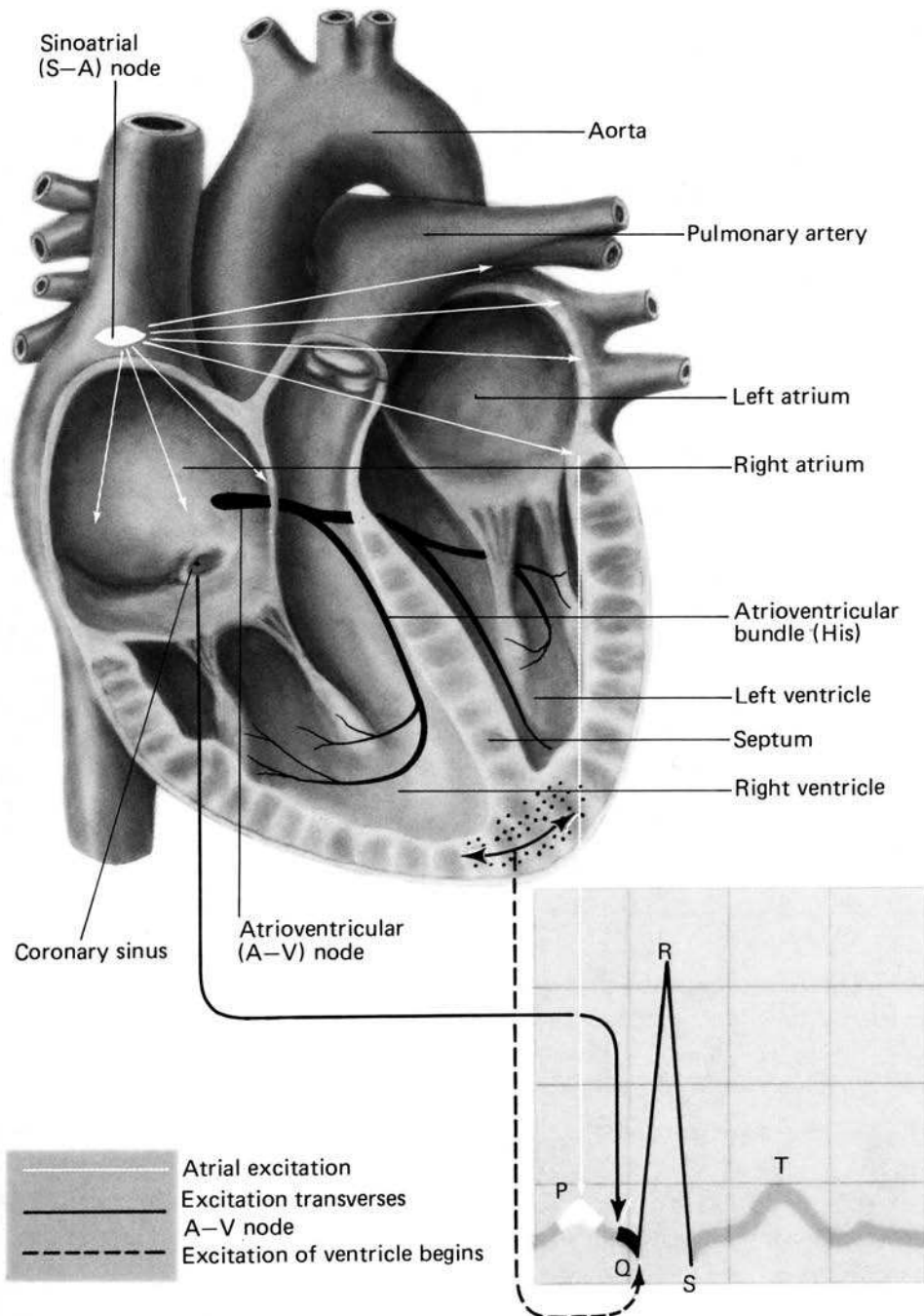


Figure 3.4: Cutaway drawing of the heart that illustrates the anatomical sources of electrical impulses recorded by the electrocardiogram. (source: Andreassi, 1995, p.219)

the ramifications of the Purkinje network and immediately afterwards through the ventricular system resulting in blood being pushed into the lung capillaries and the rest of the body. The depolarization of the ventricles is visible in the ECG as the *QRS-complex*. The *ST-segment* characterizes the activated state of the ventricles. Then the ventricles repolarize reflected by the *T-wave*.

The constituent stages of heart excitation lead to differences of electric currents between excited and unexcited parts of heart fibers. The single heart fiber behaves like an electric dipole represented by a dipole vector, which points from the excited (minus) to the unexcited (plus) part of the fibre. Resting or evenly excited fibers produce no dipole vector. At each time of heart excitation, the dipole vectors of all heart fibers sum up to an integral vector. This integral vector changes its size and direction during the consecutive stages of heart excitation reflected by the characteristic components of the cardiac cycle (for a schematic illustration of the constituent stages of heart excitation and the temporally assigned components of the cardiac cycle, see, Antoni, 1995, p.488). Size and direction of the ECG deflections depend on the size of the integral vector and its projection to the surface of the body.

3.2.2 Measures of Cardiac Activity

Studies examining human performance commonly use HR and heart period (HP) as measures of heart activity. HR can be defined as the number of beats per unit of time and is usually given in beats per minute. It is based on the occurrence of the most prominent component of the ECG, the *R-wave*. The HP is characterized by the time between one R-wave and the next and is usually given in milliseconds. HR and HP are related to each other as follows:

$$HR[bpm] = \frac{60000}{HP[ms]} \quad (3.2)$$

3.2.3 Modulation of HR Activity

Cardiovascular activity is regulated by various mechanisms of the autonomic and central nervous system. The integration of the regulatory factors provides the

basis for both the homeostatic and the adaptive functions of the cardiovascular system. The modulation of HR is a complex system determined by mechanical (venous return of blood), hemodynamic (baroreceptor feedback), humoral (release of neurotransmitters), autonomic and central nervous system factors. Beyond these factors, HR can be influenced by a variety of psychological variables, such as stress, emotion or motivation (for a detailed discussion of the cardiovascular psychophysiology and the modulating components, see, e.g. Oehman, Hamm, & Hugdahl, 2000; Brownley et al., 2000). In the following, the autonomic and the central regulation of the HR will be described in more detail.

Autonomic Regulation

Autonomic regulation of the HR is realized by the parasympathetic (PNS) and sympathetic (SNS) nervous system. The heart is dually innervated by parasympathetic and sympathetic fibers and simultaneously receives impulses that both increase and decrease activity. The *parasympathic branch* of the ANS projects to the heart through the vagal nerve. The synapses of the vagal nerve are located near heart fibers and influence the contraction frequency of the heart by the excretion of the neurotransmitter acetylcholin. The acetylcholin transmits its message by binding to the muscarinic receptors located on the cardiac smooth muscle. The excitation of parasympathetic fibers leads to a release of acetylcholin at the vagus nerve endings resulting in a slowing of activity at the S-A node and a slowing of the cardiac impulse passing into the ventricles. This influence of the PNS is reflected in a *HR deceleration* (negative chronotropic effect). The SNS has the opposite effect. The *sympathetic branch* of the ANS projects to the S-A node, the cardiac muscle, the arterial smooth muscles, and the venous smooth muscles. The release of the neurotransmitter norepinephrine (= noradrenaline) at the sympathetic nerve endings increases the rate of S-A node discharge and the excitability of heart tissue resulting in a *HR acceleration* and in an increase in the force of contraction of the cardiac musculature (positive chronotropic effect). A cardiac acceleration can be also caused by endocrine cells located in the adrenal medulla. The adrenal medulla is innervated by efferent preganglionic sympathetic fibers

that travel in splanchnic nerves and terminate directly in the adrenal gland. The excitation of these fibers leads to a release of the neurotransmitters epinephrine (= adrenaline) and norepinephrine at the ratio of about 80 % : 20 % in humans. The increase of adrenergic substances in the bloodstream produces a HR acceleration. Particularly, physical and emotional stress raise the release of epinephrine and norepinephrine by the sympathetic nerve endings and the adrenal medulla. The HR effector loop acts fast and can induce changes within 2.5 s to 3 s. Concluding, HR changes depend on PNS and SNS activity, so an increase in HR can be due to a decrease in PNS activity, an increase in SNS activity, or both.

Central Regulation

Central regulation involves structures within the spinal cord, brainstem and fore-brain. *Brainstem structures* that are assumed to play a crucial role in the cardiovascular regulation are the brainstem nuclei such as the dorsal nucleus of the vagus, the nucleus ambiguus, and the nucleus tractus solitarius, which control the sympathetic and parasympathetic axes of the ANS and are involved in the regulation of the baroreceptor reflex arc. The ventrolateral medulla mediates tonic and phasic changes in blood pressure and HR.

Cortical and subcortical structures located in the *forebrain* are also engaged in the control of the cardiovascular system. *Subcortical structures* such as the nuclei within the hypothalamus regulate blood volume and modulate autonomic reflexes by the release of the neurotransmitter vasopressin. The amygdala and other limbic structures play an important role in linking stimuli to appropriate emotional responses. The limbic cortex also interacts with the hypothalamus and the periaqueductal gray of the midbrain, which are involved in the cardiorespiratory regulation of defense and vigilance reactions. Regarding *cortical structures*, there is evidence that the FMC, including the ACC and the insular cortex (IC), especially the inferior insula, are engaged in the control of the cardiovascular system (for a review see, Verberne, & Owens, 1998). Both brain regions show anatomical projections in several cortical and subcortical structures involved in cardiovascular control such as the hypothalamus, the ventrolateral medulla or the nucleus tractus

solitarius. In contrast to the FMC, there is an absence of corticospinal projections for the IC and fewer direct connections with brainstem nuclei. Schematic presentations of the afferent connections of the IC and the ACC to control structures directly engaged in HR regulation are illustrated in Figure 3.5.

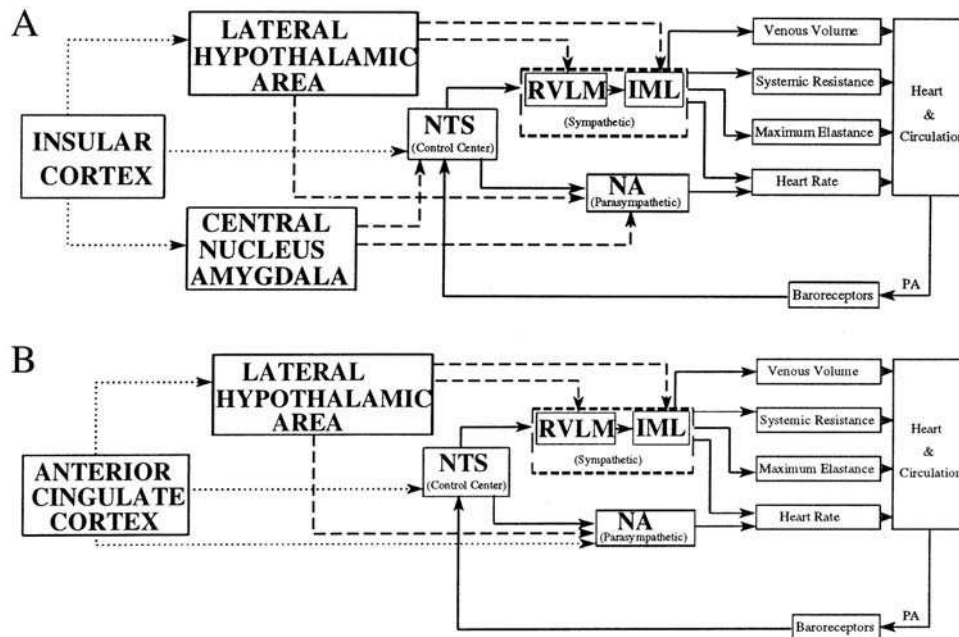


Figure 3.5: Schematic illustration of the direct (dotted) and indirect (dashed) afferent connections of the insular cortex (A) and the anterior cingulate cortex (B) to important structures engaged in the regulation of the cardiovascular system. NTS: nucleus tractus solitarius, RVLM: rostral ventrolateral medulla, IML: intermediolateral cell column, NA: nucleus ambiguus, PA: arterial pressure. (source: van der Veen, 1997, pp. 9, 10)

The ACC is assumed to be involved in HR modulation. Animal studies showed changes of HR caused by electrical and chemical stimulation within both ventral and dorsal regions of the ACC (Crippa, Peres-Polon, Kuboyama, & Correa, 1999; Verberne, & Owens, 1998; Fisk, & Wyss, 1997; TerHorst, Hautvast, De-Jongste, & Korf, 1996; Hardy, & Holmes, 1988; Verberne, Lewis, Worland, Beart, Jarrott, Christie, & Louis, 1987; Burns, & Wyss, 1985). When the ACC is stimulated, a HR deceleration can be observed. Studies in rabbits revealed evidence that

the ACC plays an important role in mediating cardiovascular changes during associative learning tasks (Powell, Buchanan, & Gibbs, 1990). Powell and colleagues (1990) further showed that the ACC is primarily responsible for the decelerative phase of the response, which is attenuated when the ACC is lesioned. HR changes were also found upon electrical stimulation of the IC in rats (e.g., Butcher, & Cechetto, 1995; Oppenheimer, & Cechetto, 1990; Hardy, & Mack, 1990; Hardy, & Holmes, 1988). Similar autonomic responses to ACC (Pool, & Ransohoff, 1949) and IC (Oppenheimer, Gelb, Girvin, & Hachinski, 1992) stimulation are reported in humans. Neuroimaging studies support the view that the ACC and the IC are important determinants in the regulation of cardiac autonomic activity (Critchley, Mathias, Josephs, O'Doherty, Zanini, Dewar, Cipolotti, Shallice, & Dolan, 2003; Critchley, Corfield, Chandler, Mathias, & Dolan, 2000; Williamson, Nobrega, McColl, Mathews, Winchester, Friberg, & Mitchell, 1997). Additional evidence comes from a study by Critchley and colleagues (2003), who investigated autonomic responses in patients with lesions in the dorsal ACC. All three patients showed blunted cardiovascular responses to effortful cognitive task performance compared to a healthy control group suggesting a disruption of autonomic cardiovascular control. There are few electrophysiological studies examining cortical correlates of cardiac regulation. Kubota and colleagues (2001) simultaneously recorded EEG and ECG and found a close relationship between cardiac autonomic function and theta activity, supposedly generated in the ACC (e.g., Pool, & Ransohoff, 1949).

Data Acquisition and Processing

The ECG can be recorded by two or more electrodes attached to the skin fairly far apart. Different electrocardiographic leads can be used: in the unipolar leads, the active electrode is connected to an indifferent electrode at zero electrical potential (e.g., Wilson's chest leads), while in the bipolar leads, two active electrodes are connected (e.g., Einthoven's triangle). The derived ECG signal is converted from an analog signal into a digital signal (AD conversion) at a sampling rate of 250 Hz at minimum and band-pass filtered off-line. The resulting discontinuous

discrete signal is then transformed into a continuous signal by linear interpolation (cf., Koers, Mulder, & van der Veen, 1999; Velden, 1999; Mulder, & Mulder, 1981). Analogously to the ERPs, event-related HR changes can be derived from the continuous HR signal. The arithmetical averaging technique described above can be used to eliminate the randomly varying background signal and to isolate event-related HR activity (cf., page 39).

3.3 Functional Magnetic Resonance Imaging

Imaging techniques are an excellent method to investigate the functional organization of the human brain. Over the past decade, *functional magnetic resonance imaging* (fMRI) has developed into a powerful technique, which provides detailed information about both anatomy and function. This technique allows to identify cortical regions that are activated in relation to different aspects of cognitive processing, such as perceptual or linguistic processing. The aim of fMRI studies is to achieve an understanding of the cortical and subcortical networks that underlie different cognitive processes, and to specify the contribution of each cerebral area to the involved functional network (for a detailed overview about fMRI see, Bandettini, & Moonen, 1999; Debatin, & McKinnon, 1998; Papanicolaou, 1998; Frackowiak, Friston, Frith, Dolan, & Mazziotta, 1997).

3.3.1 Magnetic Resonance Imaging

The MR phenomenon

Magnetic resonance imaging (MRI) is based on the phenomenon of *nuclear magnetic resonance* (NMR). Atomic nuclei are composed of various numbers of protons and neutrons, which carry intrinsic magnetic moments and possess the physical property to rotate around their axis, the so called *spin*. The intrinsic spin of the protons and neutrons causes an electrical circular flow, which creates a magnetic field at right angles to the direction of its motion. If there are even numbers of protons and neutrons in a nucleus, these magnetic moments sum to zero, because the nucleons tend to pair. Thus, nuclear magnetism results from unpaired protons

or neutrons. The human body is composed of tissues that primarily contain water and fat, both of which contain hydrogen. The hydrogen nucleus consists of a single unpaired proton H^+ and possesses a positive electrical charge. Because the H^+ protons are the most abundant magnetic nuclei in the human body, they are primarily measured in most MRI experiments (for an overview about MRI see, Buxton, 2002; Brown, & Semelka, 1999; Markisz, & Whalen, 1998; Smith, & Lange, 1997).

If the protons are exposed to an external constant magnetic field B_0 , as used in an MRI scanner, they are magnetized. The protons align either in the parallel (low energy state) or in the antiparallel (high energy state) direction to the external magnetic field. Slightly more protons align with B_0 in the low energy state and fewer in the high energy state. All protons, besides spinning around their axes, also revolve in a conical manner around an imaginary axis defined by the direction of B_0 , a process termed *precession*. The precessing frequency ω is given by *Larmor's equation*:

$$\omega = \gamma B_0 \quad (3.3)$$

The quantity B_0 is the strength of the external magnetic field; γ is the gyromagnetic ratio of protons. The gyromagnetic ratio of the protons describes the coupling of the spin and the magnetic dipole moment and is characteristic for different materials. The precession frequency depends on the strength of the B_0 field. The stronger the external magnetic field the greater the precessing frequency.

Relaxation

The magnetic strength of each proton in a particular direction (magnetization vector) can be decomposed into two components: the *longitudinal* component, parallel to the B_0 field, and the *transverse* component, at right angles to the longitudinal magnetization. The strength of the net magnetization along the direction of the B_0 field is determined by the number of parallel minus the number of antiparallel protons. If the magnetization is parallel to the B_0 field, no signal is measurable. In order to receive a measurable signal, a brief radio-frequency (RF) pulse has to be emitted. The frequency of the RF pulse must have the same frequency as

the precessing frequency, so that an exchange of energy between the protons and the RF pulse can take place. The uptake of RF energy by the protons is called *resonance*.

The RF pulse has two basic effects on the protons changing their net magnetization. First, protons in the parallel, low energy state jump to the high energy state and begin to spin and precess in the antiparallel direction. This results in a decline of longitudinal magnetization. Second, protons are forced to precess in phase, thus increasing transverse magnetization. When the RF pulse stops, the organized set of protons begins to return to its previous state resulting in a loss of absorbed RF energy (recovery of the longitudinal magnetization) and in a de-phasing of protons (loss of transverse magnetization). Past the excitation, the signal decays freely. This process is called *free induction decay* (FDI). The FDI is determined by the relaxation parameters T_1 , T_2 , T_2^* . The parameter T_1 describes the longitudinal relaxation time. This process is also called spin-lattice relaxation, because the excited protons (spins) transfer their energy to their surrounding (lattice). The parameters T_2 and T_2^* characterize the transverse relaxation time. The parameter T_2 describes the loss of coherence in phase of the protons due to an exchange of energy between protons (spin-spin relaxation). Constant magnetic field inhomogeneities caused by the scanner or the human body result in an additional de-phasing of the protons that is described by the parameter T_2^* .

Image Contrast

In an MR image, different brain tissues can be distinguished by color-coded differences of the relaxation parameters ranging on a scale from black to white. The contrast of an MR image depends on three parameters: proton density, longitudinal (T_1) and transverse (T_2) relaxation times. Depending on the specified parameter within an MR sequence, the recorded images differ in their tissue-to-tissue contrast. Brain images, whose contrast is primarily determined by T_1 , are termed *T_1 -weighted images*, whereas images, whose contrast is primarily determined by T_2 , are termed *T_2 -weighted images*. In T_1 -weighted images, tissues with short T_1 -times are visible in light grey, because the longitudinal relaxation recovers

rapidly resulting in a strong signal release. In contrast, tissues with long T1-times are depicted in dark grey due to longer relaxation recovery times, which lead to a smaller signal release. In T2-weighted images, the contrast of an MR image appears the opposite way around. Tissues with short T2-times are visible in dark grey, whereas tissues with long T2-times are depicted in light grey. For instance, white matter is brightest and cerebrospinal fluid is darkest in T1-weighted images, and this pattern is reversed in T2-weighted images.

Space Encoding

The aim of MRI is to extract information about the spatial distribution of the MR signal. Thus, the source of each component of the signal must be confined to a particular location in the x-,y-, and z-direction of space. If all protons experience the same magnetic field strength, they will all produce a signal at an identical frequency. Thus, all protons will be excited by a given RF pulse resulting in a net signal that reflects the sum of all the signals generated in the tissue volume without any spatial information. In order to generate a useful MR image, several steps have to be applied, which are described in the following.

Spatial localization is based on the property of NMR: the resonant frequency is directly proportional to the magnetic field at the location of a nucleus. In MRI, the resonant frequency is manipulated through control of the local magnetic field by applying *magnetic field gradients*. In an MR scanner, there are three gradient coils in addition to the RF coils and the coils of the magnet itself. Each gradient coil produces a magnetic field that varies linearly along a particular axis. Thus, the three gradient coils produce field gradients along three orthogonal directions (x,y,z), so that a field gradient along any arbitrary direction can be produced.

Space encoding is done in three ways corresponding to the three spatial directions: slice selection, frequency encoding, and phase encoding. To select a single thin slice (typically of 1-10 mm thickness), a gradient field along the *slice selection* axis (z-axis) is turned on while the RF pulse is applied. This results in a variation of the resonant frequency along the z-axis and a tailored RF pulse that contains only a narrow range of frequencies. Thus, resonance occurs only in

this narrow spatial band of the volume. The location of the slice can be varied by changing the frequency of the RF pulse. The spatial thickness of the excited slice depends on the ratio of the frequency width of the RF pulse to the strength of the field gradient. The slice width typically is adjusted by changing the gradient strength. The net signal, however, still reflects the sum of all signals generated across the slice. The localization in the x-y plane is achieved by frequency and phase encoding. For *frequency encoding*, a negative field gradient pulse along the x-axis is turned on after the excitation RF pulse. Following this pulse, a positive x-gradient is switched on so that a gradient echo occurs halfway through the second gradient pulse. Consequently, the precession frequency of the magnetization varies linearly along the x-axis. The net signal is thus transformed into a sum of signals covering a range of frequencies. The signals corresponding to each frequency can be separated. Any signal measured as a series of amplitudes over time can be converted to a series of amplitudes corresponding to different frequencies by calculating the Fourier transform (FT). For *phase encoding*, during the interval between the RF pulse and the data acquisition, a gradient field along the y-axis is applied for a short time interval to localize the y-position of the separated signal. Thus, the transverse magnetization at different y-positions precesses at different rates, so the phase difference between the signal at two positions increases linearly with time. After the gradient is turned off, all spins again precess at the same rate, but show different y-dependent phase differences. As a result, each precessing magnetization is marked with a phase offset proportional to its y-position.

3.3.2 Functional Magnetic Resonance Imaging

Physiological Basis of fMRI

Functional magnetic resonance imaging (fMRI) is based on neurovascular coupling (Roland, 1993). The chain of events leading to the measured signal is illustrated in Figure 3.6. The stimulus first induces local changes in neural activity. The neural activity then triggers increased energy metabolism, such as the consumption of oxygen and glucose resulting in an increase in regional cerebral blood flow (rCBF), regional cerebral blood volume (rCBV), and regional cerebral

metabolic rate of oxygen consumption ($rCMRO_2$). The supply of oxygen attached to the hemoglobin exceeds its consumption such that the concentration of oxygenated hemoglobin increases, while the amount of desoxygenated hemoglobin decreases leading to a change in blood magnetization. In sum, fMRI measures blood flow changes due to a neural event through changes in blood oxygenation.

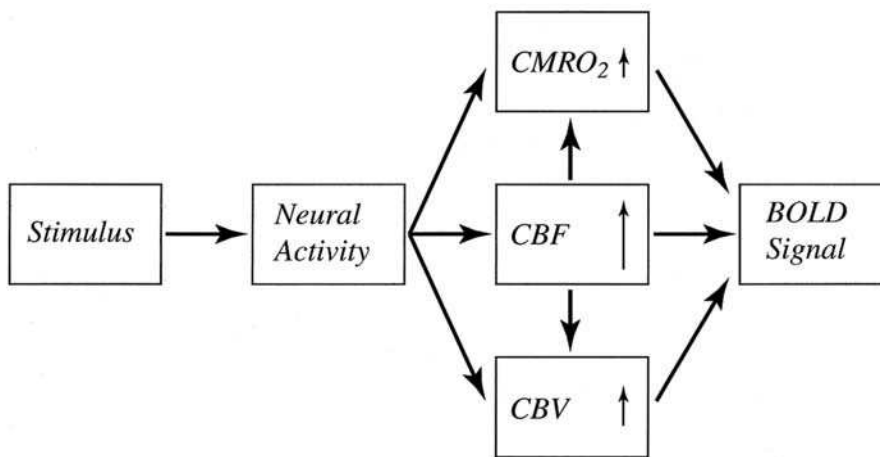


Figure 3.6: The chain of events leading to the BOLD signal. Arrows indicate an increase of these factors. A long arrow represents a large increase, a short arrow a small increase. $CMRO_2$: cerebral metabolic rate of oxygen; CBF: cerebral blood flow; CBV: cerebral blood volume; BOLD: blood-oxygen-level-dependent. (source: Buxton, 2002, p. 419)

Desoxyhemoglobin has a significant paramagnetic moment, whereas oxyhemoglobin is diamagnetic with a very small magnetic moment. The decrease of desoxyhemoglobin reduces the paramagnetic property of the blood volume. As a result, local inhomogeneities caused by the paramagnetic desoxyhemoglobin are reduced and thereby $T2^*$ is increased for the stimulated tissue relative to the unstimulated tissue. Consequently, the stimulated tissue appears higher in signal on $T2^*$ weighted images. This MR signal change is referred to as the blood oxygenation level dependent effect or *BOLD effect* (Ogawa, & Lee, 1990).

The BOLD signal is determined by several parameters. It starts approximately 2 s after neural activity and reaches its maximum after 4 s to 6 s. Within 5 s to 12s after neural activity, the BOLD signal decreases to 10% of its initial value. After

10 s to 12 s, the BOLD signal decays to its initial value and often undershoots this value. The time course and the amplitude of the BOLD signal can vary between brain regions, persons and experimental sessions (Aguirre, Zarahn, & D'Esposito, 1998). The relationship between the BOLD signal and neural activity is still poorly understood. A recent study in monkeys showed that an increased BOLD signal directly reflects an increase in neural activity, i.e., the neural response to a stimulus (Logothetis, Pauls, Augath, Trinath, & Oeltermann, 2001). By simultaneous acquisition of fMRI and intracortical electrophysiological data, Logothetis and colleagues (2001) demonstrated that the BOLD signal reflects rather synaptic activity, i.e., the local input of a neural population in a given area (local field potential), than spiking activity, i.e., the output of a population of neurons in a given area (multi-unit activity).

3.3.3 Experimental Design in fMRI

Two experimental designs are often used in fMRI studies: blocked design and event-related design (Frackowiak et al., 1997). In the *blocked design*, experimental conditions are presented in separate blocks with one condition per block. Each block consists of several trials and usually lasts for 40 s to 60 s. The great number of brief repetitions of trials within a block results in high statistical power. Thus, blocked designs represent very efficient fMRI designs (Friston, Zarahn, Josephs, Henson, & Dale, 1999). Blocked design, however, does not allow to separate the hemodynamic response for each single trial ruling out the possibility to dissociate correct and erroneous responses within one block. A further disadvantage is a constricted randomization of conditions leading to an anticipated sequence of trials.

The *event-related design* is based on the presentation of single trials. The advantages of this design are an unrestricted randomization of all trials, which allows to exclude effects due to anticipation and habituation, and a separation of the hemodynamic response for each trial. Because a distinction of correct and erroneous responses within each trial is crucial for the present fMRI study, an event-related design was used. The hemodynamic delay of the BOLD response

requires long inter-stimulus-intervals (ISIs) that range between 12 s and 20 s. The use of long ISIs results in fewer trial repetitions and a loss in statistical power. Dale and Buckner (1997) varied stimulus presentation rates that ranged between 1 stimulus per 20 s and 1 stimulus per 2 s. The results showed distinct, anatomically segregated responses to different stimulus types for slow as well as rapid stimulus presentations provided that stimuli are carefully randomized.

3.3.4 Analysis of fMRI Data

fMRI records the BOLD signal over time at discrete spatial locations within an imaging plane placed within the brain. This procedure results in a time sequence of digital two-dimensional (2D) images of the brain, which are acquired every second within each defined three-dimensional (3D) volume element that is termed *voxel*. One measured signal value per 2D image is assigned to each voxel. Thus, an fMRI data set consists of a defined amount of voxels, where each voxel represents a time series of its signal value over the experiment.

fMRI studies mainly aim to investigate the relationship between the time series of a voxel and specific experimental conditions to open up new insights into the implementation of cognitive brain functions. The data analysis consists of several steps of preprocessing, co-registration, statistical evaluation and visualization of fMRI data, which will be explained in the following. The present fMRI data is analyzed with the software-package LIPSIA (Lohmann, Müller, Bosch, Mentzel, Hessler, Chen, Zysset, & von Cramon, 2001).

Preprocessing

Several preprocessing steps are required to improve the SNR and to remove artifacts due to motion, slice acquisition, and low frequency drifts. Artifacts due to susceptibility gradients² or blood pulsation in large vessels can be hardly corrected. Therefore, brain regions affected by those artifacts should be excluded from further analysis.

²Susceptibility artifacts primarily occur in tissue bordering air-filled cavities due to different magnetic properties, e.g., in the orbitofrontal cortex.

In the present fMRI experiment, data are corrected for motion artifacts using a matching metric based on linear correlation for geometrical alignment. In this procedure, 2D images are geometrically rotated and shifted until a satisfactory match with a reference scan is achieved. The correction method can only be applied separately for each slice in the axial plane (Friston, Price, Fletcher, Moore, Frackowiak, & Dolan, 1996). The slices acquired in one fMRI scan are measured sequentially resulting in a systematic delay in the acquisition time between each slice. This offset in slice acquisition may affect statistical analysis and needs to be compensated for. A sinc-interpolation algorithm based on the Nyquist-Shannon theorem is applied for slice-time correction (Stark, & Bradley, 1992). Low-frequency drifts due to physiological or technical reasons affect the average signal intensity. Therefore, low-frequency signals are suppressed by applying a 1/120 Hz high-pass filter. Spatial smoothing should be used for multi-subject studies to achieve a sufficient regional overlap of activation foci. In the present fMRI experiment, spatial smoothing of the signal is done by means of a Gaussian filter with a kernel size of 5.65 mm full width at half maximum (FWHM)³. The increased autocorrelation caused by the filtering is taken into account during statistical analysis adjusting the degrees of freedom (Worsley, & Friston, 1995).

Spatial Transformation

In order to enable statistical group comparisons, the images of all participants have to be equal in size and in position in space. The co-registration of the anatomical and functional data is done in three steps: first, the anatomical slices (MDEFT) are rotated and scaled such that they are geometrically aligned with the functional slices (EPI-T1)⁴. This linear registration is used to compute a 3 x 3 transformation matrix, containing three rotational and three translational parameters that register the anatomical slices with the 3D high resolution reference T1-data set. The 3D

³The kernel size of the Gaussian filter is computed: $FWHM = \sqrt{8 * \ln 2} * \sigma * pixelsize$, where sigma indicates the standard deviation of the Gaussian function.

⁴An MDEFT (modified driven equilibrium Fourier transform) sequence is a common method to acquire anatomical images. The BOLD response is usually acquired with an EPI (echo planar imaging) sequence, an ultrafast MRI imaging technique.

reference data set is acquired for each participant in a separate session. Second, each individual transformation matrix is scaled to a standard stereotactic coordinate system (e.g., Talairach stereotactic space, Talairach, & Tournoux, 1988) by applying linear scaling. In the final step, these normalized transformation matrices are applied to the individual functional raw data. Slice gaps are scaled using a trilinear interpolation, generating 3D output data with a spatial resolution of 3 x 3 x 3 mm (27 mm³) per voxel.

Statistical evaluation

The aim of the statistical evaluation is to define brain regions that are significantly correlated with a cognitive function, which is operationalized by the experimental design. This can be obtained by the generation of a *statistical parametric map* (SPM) showing the statistical significance of each voxel for a specified experimental condition. The statistical evaluation of the fMRI data is based on a least-square estimation using the *general linear model* (GLM) for autocorrelated observations (random effects model; Friston, Holmes, Poline, Grasby, Williams, Frackowiak, & Turner, 1995a; Friston, Holmes, Worsley, Poline, Frith, & Frackowiak, 1995b; Worsley, & Friston, 1995; Friston, 1994). The model equation is:

$$Y = X\beta + \epsilon \quad (3.4)$$

This linear combination is called *fitted response*. The model equation, including the observed fMRI data Y , the design matrix X , and the error term ϵ , is convolved with a Gaussian kernel of dispersion of 4 s FWHM. The model includes an estimate of temporal autocorrelation that is used to estimate the effective degrees of freedom (Worsley, & Friston, 1995).

According to event-related designs as used in the present fMRI experiment, the design matrix X is generated from a synthetic hemodynamic response function (Friston, Fletcher, Josephs, Holmes, Rugg, & Turner, 1998; Josephs, Turner, & Friston, 1997) and its first, second, and third derivative, the so called *basis functions*. The derivatives of the synthetic hemodynamic response function are assumed to model different properties of its function: the first derivative should

be more sensitive to the amplitude, while the second derivative should be more sensitive to the time course and the third derivative should be more sensitive to the time dispersion. The model parameters β are weighting coefficients for the linear combination of the basis functions and are influenced by the number of employed basis functions. The model parameters are unknown and have to be estimated based on a least-square estimation. In the present fMRI experiment, three basis functions are used to model the hemodynamic response function. Thus, three weighting coefficients are estimated for each voxel.

In the following, *contrast images*, i.e., estimates of the raw-score differences between specified conditions, are generated for each session and participant. For multi-session analysis, the estimated model parameters for the specified conditions are tested by using a t-statistic (cf., Bortz, & Döring, 1995). The resulting t-values are transformed into z-scores resulting in an individual SPM(z) (Lohmann et al., 2001). The z-scores indicate whether the specified conditions significantly differ from each other on a voxel-wise basis. To look for significant differences between groups, the contrast images of each group are tested by using a two-sample t-test. In order to minimize the probability of false positives (type I error), exclusively voxels with a z-score greater than 3.09 ($p \leq 0.001$, uncorrected) and with a satisfactory volume size are considered as activated voxels (Forman, Cohen, Fitzgerald, Eddy, Mintun, & Noll, 1995).

Visualization

In order to visualize the activated regions within the brain, the SPM(z) is superimposed on an anatomical high resolution image. In the present fMRI experiment, the same anatomical high resolution image is used to depict brain images. This anatomical image is an individual brain showing a quite prototypical alignment of gyri and sulci (see Figure 3.7). The significances of the SPM(z) are color-coded for each voxel. Only significantly activated voxels are visible in the image. For the purpose of visualization, the spatial distribution of the SPM is advanced to 1 mm^3 by using an interpolation method (Lohmann, 1998).



Figure 3.7: *Left, medial, and top view of the anatomical image which is used as a reference image to depict brain images revealed in the present fMRI experiment.*

3.4 Concluding Remarks

The described methods are non-invasive procedures that can be repeatedly conducted. Nevertheless, written informed consent according to the declaration of Helsinki is obtained from each participant and their rights are protected. Several precautions have to be considered when conducting fMRI experiments to ensure high safety standards. Because participants are brought into a very high magnetic field (e.g., 3 Tesla [T]), those with pace makers or other metalloid objects inside the bodies have to be excluded categorically from fMRI studies. Therefore, participants must be informed about the exclusion criteria and the possible risks about their attendance of an fMRI study. In general, each fMRI experiment has to be approved by the local ethic committee of the respective university.

Chapter 4

Experiment 1a (ERP)

4.1 Introduction

The aim of the present ERP study is to investigate the electrophysiological correlates of *error correction* and its temporal characteristics by means of behavioral data, ERPs, and LRPs. First, the issue is addressed whether error correction is reflected by a modulation of the amplitude and/or the latency of error-related ERP components. To achieve this aim, participants were randomly divided into two groups. One group was instructed to correct each committed error by immediately pressing the correct key. A second group was unaware of error corrections being recorded. A similar design was used in the study by Rodriguez-Fornells and colleagues (2002) with an important difference. While in their study error correction was forbidden in the non-instructed group, here immediate corrective behavior was merely not instructed. This design offers two important advantages: first, additional processes of control due to the prohibition of error correction can be ruled out, and second, a supplementary comparison between incidental corrections expected in the non-instructed group and intentional corrections expected in the instructed group can be conducted to get a more detailed view of the correction process.

Second, the present experiment further examines whether *correction speed* affects error-related ERP components. Based on the current models of performance

Table 4.1: *Predictions for ERN latency and amplitudes for slow and fast error corrections based on current models of performance monitoring.*

	<i>fast correction</i>	<i>slow correction</i>
Mismatch Hypothesis: comparison upon completion of correct response representations		
<i>ERN Latency</i>	early, at correction	late, at correction
<i>ERN Amplitude</i>	large	large
Alternative version of Mismatch Hypothesis: comparison upon receipt of efference copy		
<i>ERN Latency</i>	early	early
<i>ERN Amplitude</i>	large	small
Response Conflict Hypothesis: maximal post-response conflict		
<i>ERN Latency</i>	early	delayed
<i>ERN Amplitude</i>	large	small

Note: ERN: error-related negativity.

monitoring (cf., chapter 2.3), the following predictions can be made for amplitude and latency of the ERN (for an overview, see Table 4.1). The *Mismatch Hypothesis* put forward by Falkenstein and colleagues (1990) assumes that the ERN is elicited at the moment of the completion of the response selection process. Thus, the comparison between response representations can take place solely after the selection of the corrective response. This reasoning leads to the prediction that the ERN should be elicited time-locked to the corrective response. Following this idea, a substantial delay of the ERN on slowly relative to quickly corrected errors can be predicted. Concerning the ERN amplitude, no difference between slow and fast error corrections should be hypothesized. Due to the fact that corrected errors are assumed to be easy to detect, they should elicit a large mismatch reflected in a large ERN amplitude. The *alternative version of the Mismatch Hypothesis* (Coles

et al., 2001) predicts that the ERN peaks when the efference copy is received. Since there is no reason to assume that the speed of the efference copy is causally connected to the corrective behavior, the latency of the ERN should be constant across fast and slow error corrections. The amplitude of the ERN should be reduced for slowly relative to quickly corrected errors as a result of a smaller mismatch caused by a delayed second response representation. The *Response Conflict Hypothesis* assumes that the ERN peaks at the time of maximal post-response conflict. Slow error corrections should be based on a delayed second response tendency leading to a delayed and decreased maximum of post-response conflict. During fast error corrections, the second correct response tendency follows very closely the erroneous one and the corrective response is committed quickly after the error. Thus, a longer latency and smaller amplitude of the ERN for slowly relative to quickly corrected errors should be expected.

4.2 Method

4.2.1 Participants

Forty-four individuals participated in the experiment. They were randomly divided into two groups: one group was instructed to correct errors immediately by pressing the correct button after committing an erroneous response (correction instructed, CI); a second group was unaware that error corrections were recorded (correction non-instructed, CN). It is important to note that all volunteers were naive to the experiment and did not participate in any previous experiment involving immediate error correction. To guarantee a homogeneous corrective behavior within each group, exclusion criteria for the two samples were chosen. Participants in the CI group were excluded from analysis, when they showed a correction rate below 50%, while in the CN group participants with a correction rate above 50% were excluded. Data from two volunteers met these exclusion criteria. In addition, two participants were excluded from analysis because of an error rate below 10% resulting in an insufficient number of error trials to allow meaningful statistical analysis. The sample of forty volunteers (CI group: N=20, 9 female;

CN group: N=20, 12 female) was right-handed and had normal or corrected-to-normal vision. They ranged in age from 20 to 31 years ($M = 24$). Volunteers were paid for participating in the experiment.

4.2.2 Experimental Procedure

The present experiment consisted of five experimental blocks, 10 minutes each. Participants had the possibility to relax for a short time between the blocks. A modified version of the Eriksen flanker task known to yield high error rates was used in the present ERP experiment (Ullsperger, & von Cramon, 2001). The time course of the task is illustrated in Figure 4.1. At the beginning of each trial, a fixation mark was presented for 500 ms at the center of the screen, after which four flanker arrows occurred for 110 ms. The arrows were 0.46° tall and 1.08° wide and appeared 0.52° above and 1.04° below the screen center. The target arrow was presented for 30 ms in the center of the flanker arrows with a delay of 80 ms from the flanker's onset. If the target arrow points in the same direction as the flanker arrows, we refer to it as a compatible trial. If the target arrow points in the opposite direction, we refer to it as an incompatible trial. Compatible and incompatible trials appeared in randomized order. Participants were instructed to respond with maximal speed and accuracy to the target arrow with the hand indicated by its direction. Additionally, members of the CI group were instructed to correct their errors by immediately pressing the correct key after committing an error. Each response was followed by a symbolic feedback about response speed, which was presented for 600 ms at the screen center and informed the participants, whether their answer was fast enough or should be speeded up. After the feedback a fixation cross occurred for 500 ms such that the ISI amounted to 2580 ms.

An adaptive algorithm was introduced, which dynamically adjusts the response time pressure based on the participant's performance. The algorithm aims at an optimization of error rate (goal: 20 % incompatible errors) and late response rates (as low as possible). This procedure helps to reduce drop-outs for low number of error trials. The mean response deadlines were comparable between the CN group ($M = 434$ ms, $SEM = 13$) and the CI group ($M = 444$ ms, $SEM = 9$; $t(38) =$

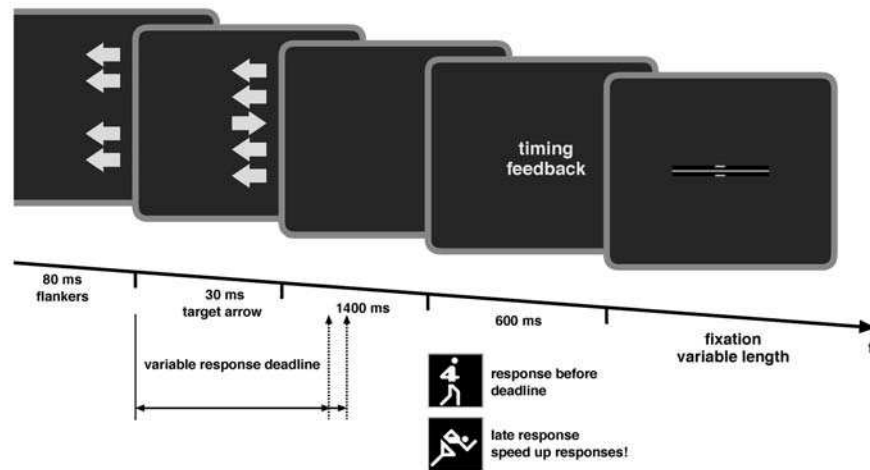


Figure 4.1: *Time course of the modified version of the Eriksen flanker task showing an incompatible trial.*

-0.56, $p = .58$). In addition, a probability bias towards the incompatible trials was applied to further optimize the number of error trials: 45% of trials (540 trials) were compatible, the other 55% of the trials (660 trials) incompatible.

4.2.3 Data Recording

The volunteers sat comfortably in a dimly lit, electrically and acoustically shielded chamber in front of a computer screen. The EEG was recorded with Ag/AgCl electrodes from 51 electrode sites (the extended 10-20 system) referenced to left mastoid and offline re-referenced to linked mastoids. Electrode impedance was kept below 5 kilohm [$k\Omega$]. The EOGV was recorded from electrodes placed above and below the right eye. To monitor horizontal eye movements, the EOGH was collected from electrodes placed on the outer canthus of the left and right eye. EEG and EOG were AD converted with 22-bit resolution at a sampling rate of 250 Hz. Artifacts caused by facial movements as well as drifts were rejected off-line.

4.2.4 Data Analysis

The signals were averaged time-locked to the first response. This was done separately for incompatible correct trials and incompatible erroneous trials, in which the response was delivered before reaching the response deadline (-100 to 600 ms in response-locked ERP averages, -500 to 500 ms in response-locked LRP averages). The average voltage in the 100 ms preceding the onset of the flanker arrows served as baseline. The single trial EEG signals were corrected for horizontal and vertical EOG artifacts by means of an eye movement correction procedure (Pfeifer, 1993) based on a linear regression method described by Gratton, Coles and Donchin (1983).

In the response-locked averages, peak-to-peak measurements were calculated to determine baseline-independent amplitudes of negative deflections by subtracting the amplitude of the preceding positive peak from the subsequent negative peak of the components of interest (cf., Falkenstein et al., 2000). Based on the literature, the time search windows of the ERN and the Pe were chosen a-priori. For the ERN, two early time windows were defined from -80 to 0 ms for the positive peak preceding the ERN and from 0 to 120 ms for the following negative peak, the ERN. Because the Pe is a more sustained positive deflection, peak search was not possible in many participants' data. Therefore, the mean amplitude in the late time window from 300 to 500 ms was used for statistical analysis. To investigate the observed new ERP component, the correction-related negativity (CoRN), two middle time windows centered around the deflection of interest were chosen post-hoc: first, a time window from 100 to 180 ms for the positive peak preceding the CoRN and second, a time window from 120 to 300 ms for the consecutive negative peak, the CoRN. Because peak search was not possible for uncorrected errors in the middle time window, the mean amplitude in the time window from 150 to 250 ms was used to compare corrected and uncorrected errors within the CN group. The negative peaks found for the ERN and CoRN also served for obtaining latencies. In the presented illustrations of ERP waveforms, negative amplitude values are plotted upwards, positive amplitude values downwards.

In order to avoid a loss of statistical power that occurs when repeated-measures ANOVAs are employed to quantify multichannel and multitime window data (Gevins, Smith, Le, Leong, Bennett, Martin, McEvoy, Du, & Whitfield, 1996; Oken, & Chiappa, 1986), electrode sites were pooled to form 6 topographical regions. The following regions of interest (ROIs) were defined: left anterior (F5, FC3, FC5, C3), midline anterior (F3, Fz, F4, FCz), right anterior (F6, FC4, FC6, C4), left posterior (CP3, P5, P3, PO7), midline posterior (Pz, PO3, POz, PO4) and right posterior (CP4, P4, P6, PO8). Figure 4.2 depicts the position of the defined ROIs.

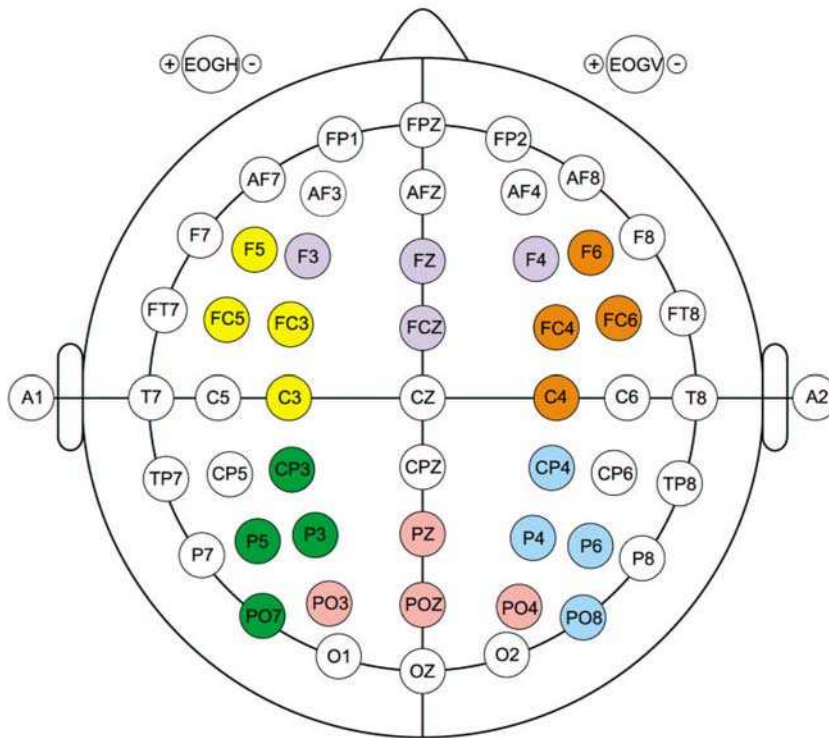


Figure 4.2: Recorded electrode sites following the 10-20 system. Electrode sites pooled into regions of interest (ROIs) are color-coded (yellow: left anterior; purple: midline anterior; orange: right anterior; green: left posterior; pink: midline posterior; blue: right posterior.)

The LRP was assessed by using the ERP waveforms recorded at C3 and C4, in which the amplitude of the readiness potential is maximum (Kutas & Donchin, 1980). The double subtraction method described in chapter 3.1.4 was used to compute the LRP waveforms (cf., De Jong et al., 1988). The mean amplitude of the response-locked LRP was calculated in three time windows (early time window: 10-40 ms; middle time window: 100-200 ms; late time window: 250-400 ms) centered around the lateralizations of interest, which were chosen post-hoc. In the depicted LRP results, response activation to the correct side is plotted upwards, to the incorrect side downwards.

Only for illustration purposes, a low-pass filter with a cutoff frequency of 15 Hz was applied.

Statistical Analysis

For behavioral statistics, repeated-measures ANOVAs with the within-subject factors *Response Type* (two levels: correct and erroneous responses), *Previous Response Type* (two levels: preceding correct and preceding erroneous responses), *Correction Type* (two levels: corrected and uncorrected errors), *Correction Speed* (two levels: fast and slow corrections), *Compatibility* (two levels: compatible and incompatible trials), *Response Time Quartile* (four levels: Q1, Q2, Q3, Q4), and the between-subject factor *Group* (two levels: CI and CN group) were conducted. Interactions were analyzed by computing subsequent lower-order ANOVAs and *t*-tests (cf., Bortz & Döring, 1995). All effects with more than one degree of freedom in the numerator were adjusted for violations of sphericity according to the formula of Greenhouse and Geisser (1959). Percentage values of the response rate data were tested additionally after arcsine normalization¹. All reported statistical effects also reached significance by applying the converted data to the ANOVA. Compatible erroneous trials were excluded from statistical analyses, because of an insufficient number of trials ($\leq 1\%$) to calculate meaningful statistics.

¹The conversion was performed as follows: $X = \arcsin(\sqrt{Y/100})$, where X indicates the normalized value and Y indicates the percentage value.

Response times were defined as the time between target onset and the beginning of the button press. Correction time was calculated as the response time difference between the erroneous response and the subsequent corrective response. To disentangle fast and slow error corrections, corrected error trials were divided by the median of the correction time for each participant in the CI group. The mean correction time for fast corrections amounted to 132 ms (SEM = 9) and for slow corrections to 274 ms (SEM = 17). In order to investigate error corrections within and between the two groups, a sub-sample of the CN group that showed a sufficient number of corrected error trials was chosen (N=14; 8 female). To rule out the influence of group differences in error rates and power, a sub-sample of the CI group (N=14; 6 female) was used whose group power was identical and whose performance (mean error rates) matched with the performance of the CN sub-sample.

The ERP statistics were based on repeated-measures ANOVAs with the within-subject factors *Response Type*, *Correction Type*, *Correction Speed*, *Anterior-Posterior Dimension* (two levels: anterior and posterior scalp regions), *Lateral Dimension* (three levels: right, midline and left scalp regions) and the between-subject factor *Group*. Subsequently, lower-order ANOVAs and *t*-tests were computed to analyze resulting interactions (cf., Bortz, & Döring, 1995). All effects with more than one degree of freedom in the numerator were adjusted for violations of sphericity according to the formula of Greenhouse and Geisser (1959). Reported effects revealed in lower-order ANOVAs also reached significance using Bonferoni correction² (Huberty, & Morris, 1989). In order to avoid to report large amounts of statistical results not relevant to the issues under investigation, only main effects or interactions including the factors *Response Type*, *Correction Type*, *Correction Speed* and *Group* are reported. Scalp potential topographic maps were generated using a two-dimensional spherical spline interpolation (Perrin, Pernier, Bertrand, & Echallier, 1989) and a radial projection from Cz, which respects the length of the median arcs. The time course of the LRP was statistically analyzed

²Bonferoni correction was applied as follows: $\alpha = 0.05/n$, where α is the probability of Type I error and n is the number of comparisons.

by using repeated-measures ANOVAs with the within-subject factors *Correction Type* and *Correction Speed* and the between-subject factor *Group* as well as by *t*-tests (cf., Bortz, & Döring, 1995). Compatible erroneous trials and late responses (delivered after the response deadline) were excluded from statistical analyses.

4.3 Behavioral Data

4.3.1 Results

Table 4.2: Mean proportion, and reaction times of correct, erroneous, and late responses for each stimulus type.

		<i>Group</i>							
		<i>CN</i>				<i>CI</i>			
	<i>Stimulus Type</i>	<i>Compatible</i>	<i>Incompatible</i>	<i>Compatible</i>	<i>Incompatible</i>	<i>Compatible</i>	<i>Incompatible</i>	<i>Compatible</i>	<i>Incompatible</i>
<i>RR</i> <i>in %</i>	Correct	93.2	(1.5)	59.6	(1.4)	93.3	(1.4)	61.4	(1.0)
	Error	0.7	(0.2)	17.6	(1.2)	1.0	(0.2)	22.9	(1.9)
	Correct late	4.7	(0.7)	20.9	(2.5)	5.1	(1.4)	15.1	(2.2)
	Error late	0.2	(0.1)	0.5	(0.2)	0.2	(0.03)	0.2	(0.04)
<i>RT</i> <i>in ms</i>	Correct	305	(5)	369	(5)	302	(5)	368	(5)
	Error	*		270	(4)	*		265	(3)
	Correct late	447	(14)	438	(12)	455	(14)	437	(9)
	Error late	*		*		*		*	

Note: *RR*: response rate; *RT*: reaction time; *CN*: correction non-instructed group; *CI*: correction instructed group. Standard error of mean is presented in parentheses. *Too few trials for meaningful analyses.

As depicted in Table 4.2, typical effects of incompatibility were found for both reaction times and error rates. Correct response times, including in-time and late correct responses, were submitted to an ANOVA with the within-factor Compatibility and between-factor Group. The analysis revealed a significant main effect of

Compatibility reflecting longer reaction times for incompatible correct trials than for compatible correct trials ($F(1,38) = 1653.2, p \leq .0001$) (see, Figure 4.3). In addition, error rates were higher for incompatible trials compared to compatible trials ($F(1,38) = 973.9, p \leq .0001$) (see, Figure 4.3). Consistent with previous findings, volunteers were faster on incompatible erroneous trials than on incompatible correct trials ($F(1,38) = 1909.6, p \leq .0001$). All three ANOVAs revealed no interaction with the factor Group.

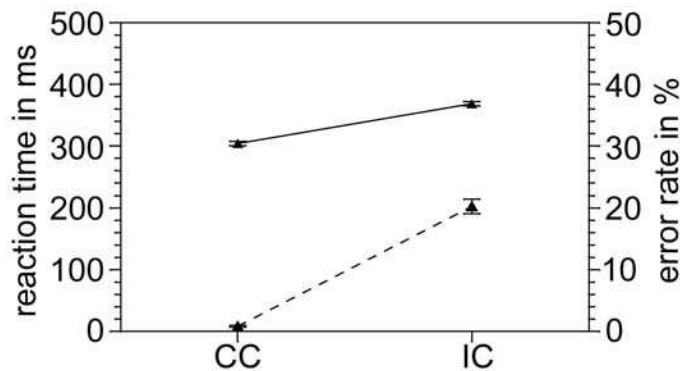


Figure 4.3: Reaction times (solid line) and error rates (dashed line) for compatible correct (CC) and incompatible correct (IC) trials.

Group-specific effects occurred for the percentage of erroneous and late responses. The CN group showed significantly lower error rates ($F(1,38) = 5.4, p \leq .05$) and a higher number of late responses ($F(1,38) = 4.7, p \leq .05$) compared to the CI group (see, Figure 4.4).

To test whether prolonged effects of errors differed between groups, an ANOVA with the factors Previous Response Type and Group was performed revealing a significant interaction of these factors ($F(1,38) = 8.1, p \leq .01$)³. A subordinate within-group analysis showed a typical post-error slowing effect in the CN group: reaction times of correct trials were significantly slowed after errors than after cor-

³Trials preceded by compatible trials were excluded from analysis of post-error adjustments so that the comparison was between trials preceded by incompatible hits and incompatible errors. This procedure rules out confounds with the conflict sequence effect often observed in flanker tasks (Gratton, Coles, & Donchin, 1992)

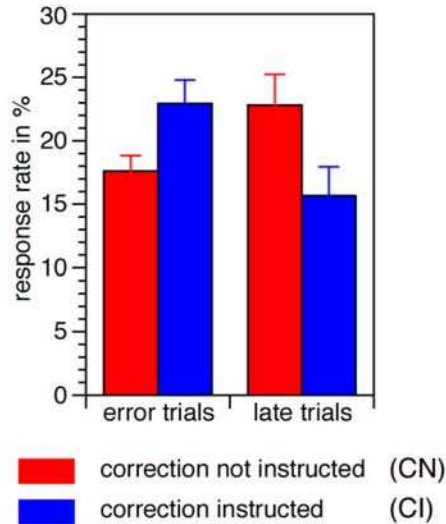


Figure 4.4: Percentage of erroneous and late responses for the correction instructed (CI) group and the correction non-instructed (CN) group.

rect responses ($F(1,19) = 8.9, p \leq .01$) (see, Figure 4.5 left). This effect was not present in the CI group ($F(1,19) = 0.4, p = .51$). A significant Previous Response Type \times Group interaction was also found for error rates ($F(1,38) = 11.1, p \leq .01$). The CN group committed more errors after erroneous responses ($M = 18\%$, $SEM = 2$) than after correct responses ($M = 13\%$, $SEM = 1$) in contrast to the CI group (see, Figure 4.5 right).

Corrective Behavior

Participants in the CI group corrected their errors significantly more often ($M = 96\%$, $SEM = 1$) than participants in the CN group ($M = 18\%$, $SEM = 3$; $t(38) = 7.3, p \leq .0001$). The mean correction time was 109 ms ($SEM = 8$) for the CN group and 200 ms ($SEM = 13$) for the CI group and differed significantly between the two groups ($t(38) = -6.0, p \leq .0001$).

Corrective behavior varied depending on the reaction times of erroneous responses. Figure 4.6 illustrates the percentage of corrected errors sorted into the reaction time quartiles of erroneous responses. An ANOVA with the factors Quar-

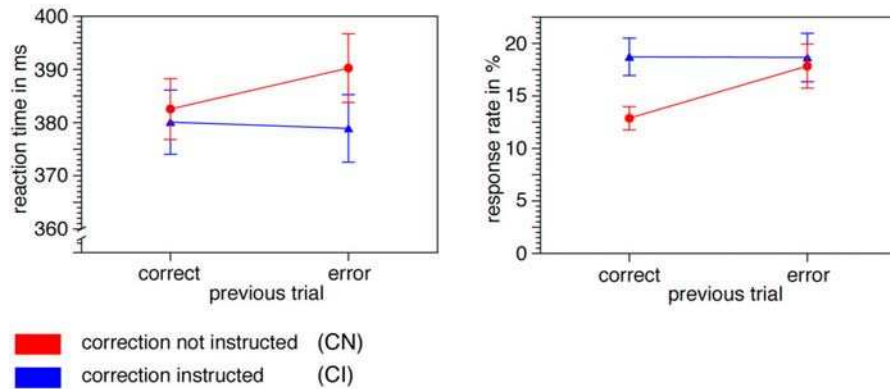


Figure 4.5: *Left: Reaction time of incompatible correct responses following incompatible correct and erroneous trials for the correction non-instructed (CN) group and the correction instructed (CI) group. Right: Percentage of erroneous responses following incompatible correct and erroneous trials for both groups.*

tile and Group revealed a main effect of the factor Group ($F(1,26) = 430.7, p \leq .0001$) exhibiting a higher correction rate in the CI group. Secondly, there was a significant interaction between the factors Quartile and Group ($F(3,78) = 29.7, p \leq .0001$). This result suggests a different distribution of corrective behavior across reaction time quartiles for the two groups. A subsequent within-group comparison showed an equivalent number of corrected errors within each quartile in the CI group ($F(3,39) = 1.4, p = .27$), while the percentage of corrected errors significantly differed among the quartiles in the CN group ($F(3,39) = 37.5, p \leq .0001$). As can be seen in Figure 4.6, the slower the reaction time for erroneous responses the larger is the percentage of corrected errors in the CN group. The correction time for each error response time quartile in the CI group is depicted in Figure 4.6. The ANOVA revealed a main effect of Quartile ($F(3,39) = 13.70, p \leq .0001$): correction times decreased when error response time increased.

Figure 4.7 illustrates the distribution of the mean number of corrective responses across correction times in bins of 50 ms. As reported above, there were more corrections in the CI group than in the CN group across all correction time bins ($F(14,364) = 7.3, p \leq .0001$). Incidental corrections in the CN group fell

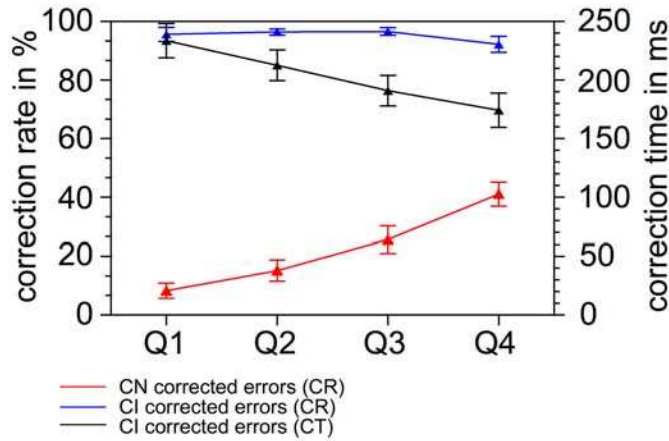


Figure 4.6: *Quartile analysis of error response times for the correction instructed (CI) group and the correction non-instructed (CN) group. Correction rates (CR) and correction time (CT) are depicted as a function of error response times. Q1 - Q4 refer to the ascending RT quartile score of erroneous responses calculated separately for the two groups. Q1: fastest RT quartile, Q4: slowest RT quartile.*

mostly into the fastest correction time bins, while error corrections in the CI group were distributed primarily across slower correction time bins.

4.3.2 Discussion

As expected, typical effects of incompatibility were found suggesting a higher response conflict on incompatible trials than on compatible trials. Erroneous responses seem to be caused by premature responding reflected in shorter reaction times on errors relative to correct responses. The observed data reveal evidence that error correction rate can be manipulated by experimental instruction. Moreover, response strategy seems to be affected by the possibility to correct errors. Participants who were unaware that error corrections were recorded showed a smaller error rate, a higher number of late responses as well as a post-error slowing effect suggesting a more cautious response behavior (Ridderinkhof, 2002). When participants are explicitly told to correct their errors, they view errors as

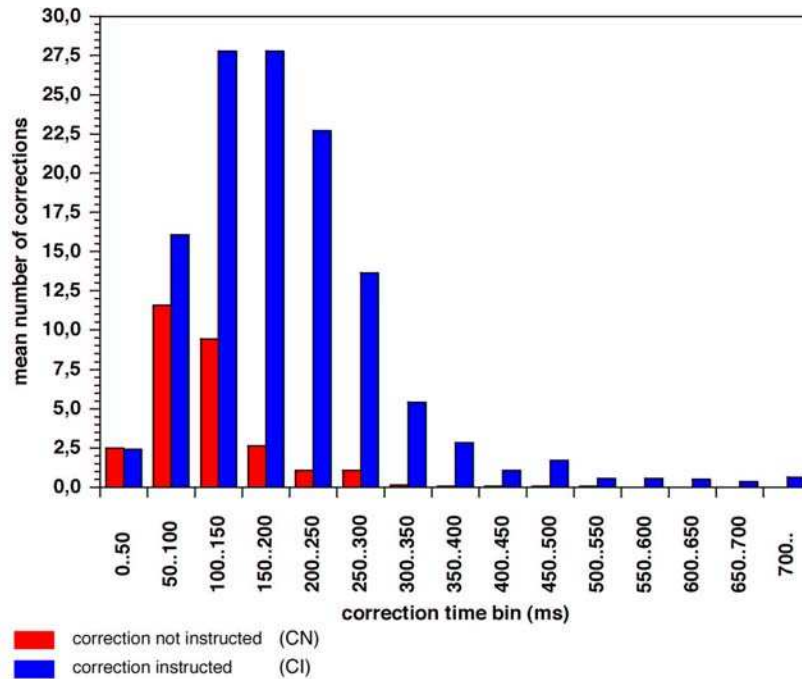


Figure 4.7: *Distribution of error corrections across 50 ms bins of correction times for the correction instructed (CI) group and the correction non-instructed (CN) group. The y-axis shows the mean number of error corrections, the x-axis shows 15 ascending correction time bins.*

expected and more acceptable than participants who do not receive an instruction about error correction. Possibly, participants in the CN group consider errors to be unacceptable thereby attaching more significance to them and therefore respond with more caution. Participants in the CN group make sure that the response is completely appropriate before its execution resulting in lower error rates and increased late response rates. In line with the findings by Rabbitt and Rodgers (1977), responses following erroneous responses on the preceding trial were not only slow, but also inaccurate in the CN group. This finding hints at a confused behavior after errors.

Consistent with previous findings, participants who were instructed to correct errors were able to correct errors very efficiently without being given an external signal that indicated a committed error (Rabbitt, 1966a,b, 1967; Higgins & Angel,

1970). In line with Rabbitt (1967), participants in the CN group also showed immediate error corrections although to a lesser degree. The distributional analysis suggests that the gain in error correction rate observed in the CI group is due to an increase in slow error corrections. This could be caused by a phasic intentional process based on error detection. That process can lead to an active enhancement of stimulus processing and/or to an evolving second response tendency. An alternative explanation is that a change in the response mode of the motor system has resulted either in a general prolongation of stimulus processing or in an enabling of multiple responses.

Rabbitt (2002) reported a study, in which intentional "error signaling responses" were much slower than slow error corrections revealed in the present study: 650-750 ms compared to 240 ms (correction time in the fastest error RT quartile). This finding seems to challenge the account that slow error corrections in the CI group result from a phasic, intentional process based on error detection. It is important to note that the intention to produce an error signaling response in Rabbitt's task requires to leave the current task set, to recode the responses, and to establish a new response tendency. In contrast, intentional corrections in the present study merely require that the existing correct response tendency is enhanced to exceed response threshold. It seems conceivable that this enhancement is less time-consuming than the generation of a new response.

Incidental corrections in the CN group occurred in a narrow time range from 0 to 100 ms after committing an error. The CI group, however, also committed such fast error corrections, but in the minority of corrections. The distributions of incidental corrections in the CN group and fast corrections in the CI group widely overlap in the two shortest correction time bins (0 to 100 ms) and start to differ significantly when extending a correction time of 100 ms. The number of intentional corrections increases with increasing correction time, whereas the number of incidental corrections decreases. The quartile analysis demonstrates that incidental corrections occur mostly for slow error response times. A similar pattern was observed for fast corrections in the CI group appearing predominantly for slower erroneous responses. These findings suggest a similar underlying mechanism for

incidental corrections in the CN group and fast corrections in the CI group, which is independent of the intention to correct errors and has to be distinguished from intentional slow corrections in the CI group.

In the CN group, the majority of errors remained uncorrected. It seems that usually the response to a task can only be executed once, because in most cases errors cannot be corrected by immediately executing the opposite response. The quartile analysis of error response times revealed that error correction rate in the CN group decreases with decreasing error response times. The low correction rate may result from a large portion of trials involving an early erroneous response tendency and a delayed second correct response tendency, which does not reach response threshold within a given time after the first response. It can be speculated that the second correct response tendency either does not further evolve because stimulus processing is finished, or its execution is blocked as soon as an efference copy of the first response has been received. This seems to be altered by the intention to correct errors so that also late corrections become possible.

4.3.3 Derivation of ERP Hypotheses

Based on the behavioral findings, two types of error correction can be hypothesized depending on the instructional context: *incidental error correction* and *intentional error correction*. In accordance with Rabbitt (2002), it can be assumed that incidentally corrected errors are delayed correct responses, which arise from ongoing stimulus processing resulting in a second correct response tendency, which in turn produces the corrective response. Incidental error corrections are expected in the CN group, when two response tendencies reach their maximum nearly simultaneously. Fast error corrections in the CI group should rely on similar processes as incidental corrections in the CN group. On the other hand, slow error corrections in the CI group should be based on an intentional process. Following this view, it can be assumed that ERN amplitude and latency is more similar for incidental and fast error corrections than for fast and slow error corrections or incidental and slow error corrections.

Concerning uncorrected errors in the CN group, current models of performance monitoring would lead to concordant predictions about the modulation of ERN amplitude and latency. Table 4.3 illustrates the completed version of Table 4.1 based on the behavioral results (for a description of the predictions of ERN modulation by fast and slow corrections in the CI group see page 65). The Mismatch Hypothesis (Falkenstein et al., 1990) assumes that the ERN is elicited at the moment of the completion of the response selection process. Thus, the ERN should be significantly more delayed for uncorrected errors than for incidentally corrected errors. A reduction of the ERN amplitude can be expected for uncorrected errors assuming that the error remained uncorrected due to a weaker corrective response representation (cf., Falkenstein et al., 1996). The alternative version of the Mismatch Hypothesis, put forward by Coles et al. (2001), would predict no changes in ERN latency by incidentally corrected and uncorrected errors, because the efference copy should not be causally connected to the corrective behavior. The ERN amplitude should be reduced for uncorrected errors caused by a delayed second response tendency, which leads to a smaller mismatch. Analogous to this argument, the Response Conflict Hypothesis assumes that uncorrected errors in the CN group are based on a delayed second response tendency predicting a delayed and decreased maximum of post-response conflict. Thus, a longer latency and smaller amplitude of the ERN for uncorrected errors can be expected. Note that the latency shift would not be predicted to be as large as with the original Mismatch Hypothesis, because maximal conflict is elicited when performed and corrective response tendencies maximally overlap.

4.4 Electrophysiological Data

4.4.1 ERP Results

Figure 4.8 illustrates the response-locked ERPs for incompatible correct and incompatible erroneous trials for the electrode sites of the ROIs (for an enlarged illustration of the ERP time course at FCz see Figure 4.9). For the CI group, ERPs for corrected errors are depicted, for the CN group, ERPs for uncorrected

Table 4.3: Predictions for ERN latency and amplitudes for uncorrected errors, incidental, fast, and slow error corrections based on current models of performance monitoring.

	CN		CI	
	<i>no corr</i>	incidental corr	fast corr	<i>slow corr</i>
Mismatch Hypothesis: comparison upon completion of correct response representations				
<i>ERN Latency</i>	delayed	early, at corr	early, at corr	late, at corr
<i>ERN Amplitude</i>	small	large	large	large
alternative version of Mismatch Hypothesis: comparison upon receipt of efference copy				
<i>ERN Latency</i>	early	early	early	early
<i>ERN Amplitude</i>	small	large	large	small
Response Conflict Hypothesis: maximal post-response conflict				
<i>ERN Latency</i>	delayed	early	early	delayed
<i>ERN Amplitude</i>	small	large	large	small

Note: Intentional processes are printed in italic, incidental correction processes in bold italic. CI: correction instructed group; CN: correction non-instructed group; corr: correction.

errors. The ERN was identified for erroneous responses peaking around 80 ms after the first button press. The ERN showed a fronto-central scalp distribution with its maximum at FCz. The ERN was followed by a broadly distributed positivity on erroneous trials, the Pe. Exclusively on corrected error trials, an additional negative deflection occurred 200 to 240 ms after the erroneous response. This deflection will be termed *correction-related negativity*, short *CoRN*. The cortical distributions of these error-related ERP components are depicted in Figure 4.9.

In order to investigate group differences in the error-related ERP components, the amplitude values from incompatible erroneous trials were subjected to a three-

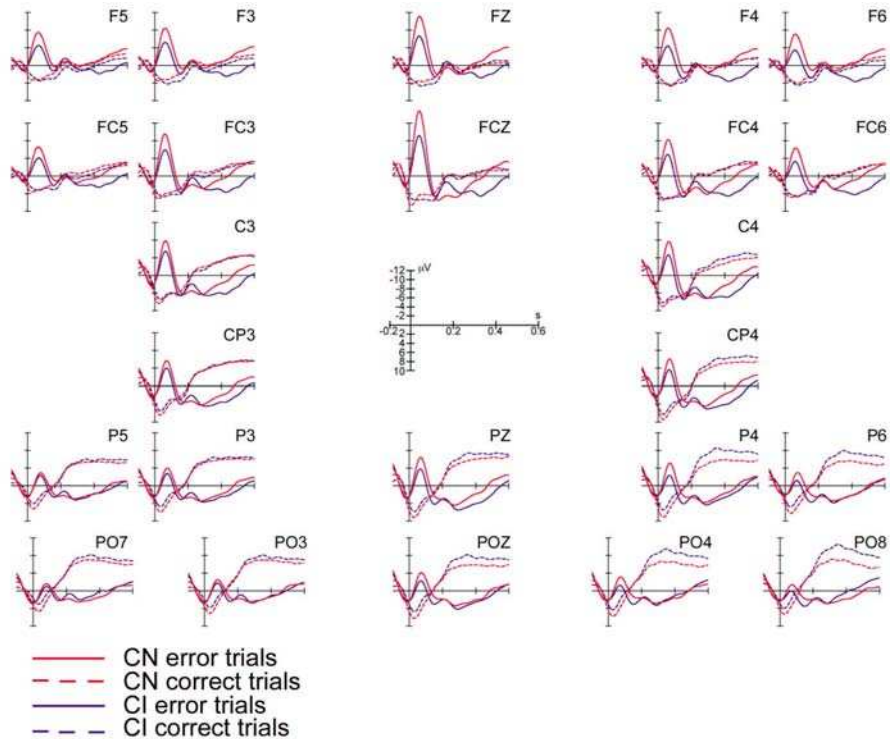


Figure 4.8: Response-locked ERPs for incompatible correct and incompatible erroneous trials for the correction instructed (CI) group and the correction non-instructed (CN) group for the electrode sites of the ROIs. For the CI group, ERPs for corrected errors are depicted, for the CN group, ERPs for uncorrected errors.

way ANOVA with the within-subject factors Lateral Dimension and Anterior-Posterior Dimension and the between-subject factor Group.

Early time window. In the early time window, the statistical analysis revealed a significant main effect for the factor Group showing a less pronounced ERN for the CI group than for the CN group ($F(1,37) = 8.0, p \leq .01$). Secondly, a significant interaction Group \times Anterior-Posterior Dimension was observed ($F(1,37) = 5.0, p \leq .05$). Follow-up analyses revealed a significantly smaller ERN for the CI group in each anterior ROI (left: $t(38) = -2.8, p \leq .01$; middle: $t(38) = -4.0, p \leq .001$; right: $t(38) = -4.0, p \leq .001$).

Middle time window. In the middle time window, a second negative deflection occurred on corrected error trials in the CI group, termed CoRN. Conducting a paired two-sample t-test on incompatible erroneous trials, this effect reached marginal significance at one midline electrode (FCz) ($t(38) = 1.8, p \leq .10$).

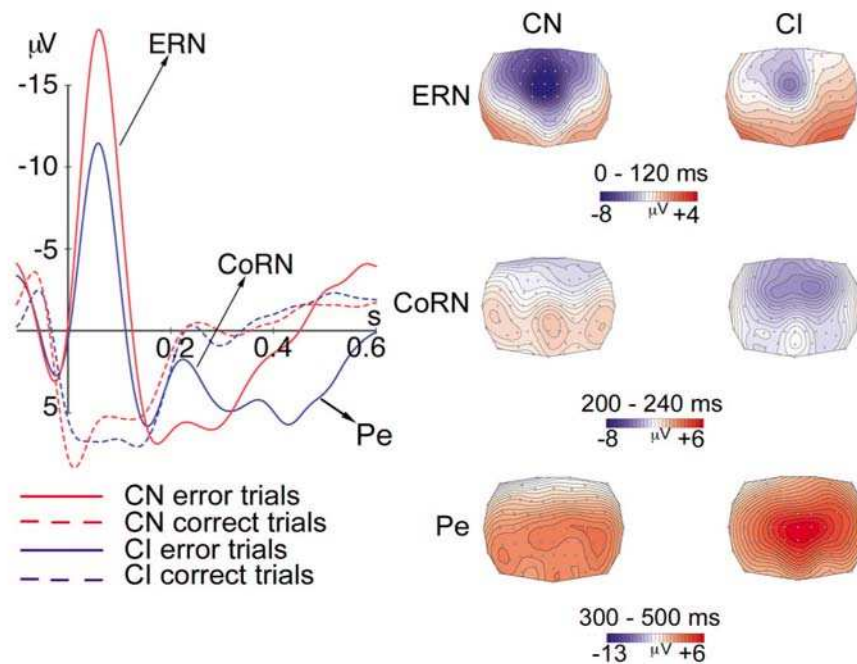


Figure 4.9: *Left: Response-locked ERPs for incompatible correct and incompatible erroneous trials in the correction instructed (CI) group and the correction non-instructed (CN) group at the midline electrode FCz. Right: Isopotential maps of the ERPs for corrected error trials in the correction instructed (CI) group and uncorrected error trials in the correction non-instructed (CN) group in the time windows of the ERN, the CoRN, and the Pe. ERN: error-related negativity, CoRN: correction-related negativity, Pe: error positivity.*

Late time window. The ANOVA in the late time window elicited neither a significant main effect for the factor Group ($F(1,38) = 1.8, p = .19$) nor any significant interactions with this factor.

Incidental Error Correction

In order to investigate the hypothesized types of error correction, incidental and intentional error correction, several sub-group analyses were performed. As mentioned before, participants from the CN group incidentally corrected almost one fifth of their errors although corrective behavior was not instructed. Incidental error corrections were investigated by a within-group analysis comparing uncorrected error trials and incidentally corrected error trials within the CN group. The time course of the response-locked ERP data for incidentally corrected and uncorrected error trials of the CN group is illustrated in Figure 4.10.

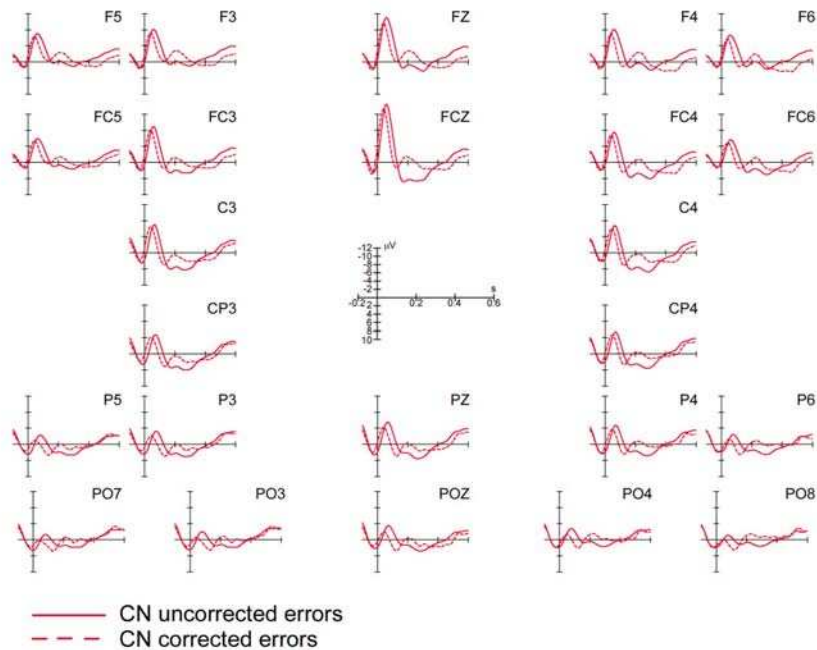


Figure 4.10: *Response-locked ERPs for uncorrected and incidentally corrected error trials in the correction non-instructed (CN) group for the electrode sites of the ROIs.*

Early time window. A three-way ANOVA with the factors Correction Type, Lateral Dimension and Anterior-Posterior Dimension was conducted. The data revealed no significant difference of the ERN amplitude between incidentally corrected and uncorrected errors ($F(1,13) = 0.2, p = .68$). In a second ANOVA with

the factors Correction Type, Lateral Dimension and Anterior-Posterior Dimension, peak latencies of incidentally corrected and uncorrected errors were compared. The analysis revealed a significant main effect of the factor Correction Type showing a significantly later peak for uncorrected errors ($F(1,13) = 30.2, p \leq .0001$).

Middle time window. In the middle time window, the CoRN was elicited on incidentally corrected errors. In the mean amplitude analysis, a significant Correction Type x Lateral Dimension x Anterior-Posterior Dimension triple interaction was observed ($F(2,26) = 4.5, p \leq .05$). Follow-up analyses revealed a larger CoRN for incidentally corrected than for uncorrected error trials in each anterior ROI (left: $F(1,13) = 24.5, p \leq .001$; middle: $F(1,13) = 33.2, p \leq .0001$; right: $F(1,13) = 27.0, p \leq .001$).

Late time window. To test for differences in the Pe amplitude, repeated measures ANOVAs were conducted revealing neither a significant main effect of the factor Correction Type ($F(1,13) = 0.7, p = .43$) nor any interactions with this factor.

Incidental versus Intentional Error Correction

To test whether correction speed modulates error-related ERP components, a within-group ANOVA was conducted comparing fast and slow error corrections within the CI group. Furthermore, a between-group ANOVA was performed to investigate whether incidental corrections in the CN group and fast corrections in the CI group are based on a similar underlying mechanism. The response-locked ERPs for quickly and slowly corrected errors in the CI group as well as incidentally corrected and uncorrected errors in the CN group are depicted in Figure 4.11. An enlarged illustration of the ERP waveforms at one midline electrode is displayed in Figure 4.12.

Early time window. To compare the amplitude and peak latencies of the ERN for slowly and quickly corrected errors within the CI group, a three-way ANOVA with the within-subject factors Correction Speed, Lateral Dimension and Anterior-Posterior Dimension was performed. The analysis revealed no signifi-

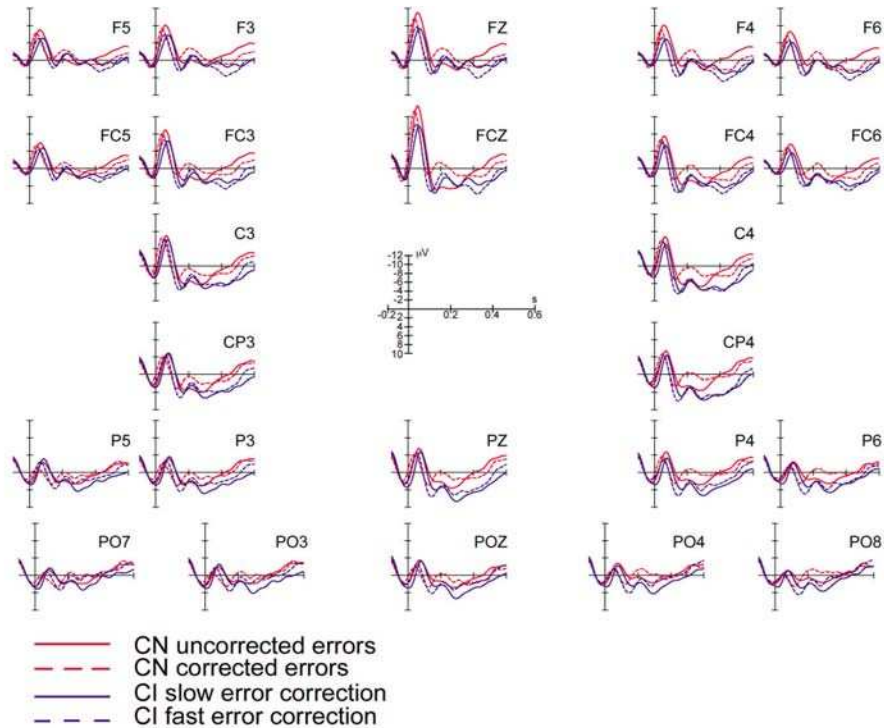


Figure 4.11: *Response-locked ERPs for uncorrected and incidentally corrected errors in the correction non-instructed (CN) group and for slow and fast error corrections in the correction instructed (CI) group for the electrode sites of the ROIs.*

cant difference of the ERN amplitude between slow and fast error corrections ($F(1,13) = 1.1, p = .31$). The latency data for the ERN showed a significant main effect for Correction Speed reflected in a later peak for slow as compared to fast corrections ($F(1,13) = 51.2, p \leq .0001$).

In a second step, amplitudes and peak latencies of the ERN between incidentally corrected errors in the CN group and both slow and fast corrections in the CI group were contrasted by means of two ANOVAs, including the factors Lateral Dimension, Anterior-Posterior Dimension and Group. ERN amplitudes did not differ significantly between incidental corrections in the CN group and fast ($F(1,26) = 1.2, p = .29$) and slow ($F(1,26) = 0.3, p = .59$) corrections in the CI group. Concerning the ERN latency, the between-group analyses revealed sig-

nificant main effects for the factor Group. The ERN for incidentally corrected errors in the CN group peaked significantly earlier than for both quickly (latency difference = 7 ms; $F(1,26) = 5.2, p \leq .05$) and slowly (latency difference = 27 ms; $F(1,26) = 69.9, p \leq .0001$) corrected errors in the CI group. Note, there was a larger latency difference between incidental and slow error corrections than between incidental and fast error corrections.

Middle time window. First, the CoRN amplitudes of incidentally corrected errors in the CN group and quickly corrected errors in the CI group were contrasted. The ANOVA with the factors Anterior-Posterior Dimension, Lateral Dimension and Group exhibited a main effect of the factor Group ($F(2,26) = 6.4, p \leq .05$), but no interaction with the topographical factors Anterior-Posterior Dimension and Lateral Dimension. The data showed a larger CoRN for fast corrections in the CI group than for incidental corrections in the CN group. A similar result was obtained in the comparison of incidentally corrected errors in the CN group with slowly corrected errors in the CI group (main effect of Group, $F(2,26) = 4.7, p \leq .05$). The within-group comparison of the CoRN amplitudes for fast and slow corrections revealed neither a significant main effect ($F(1,13) = .80, p = .40$) nor any interactions with the factor Correction Speed. As depicted in Figure 4.9, both ERP components, the ERN and the CoRN, are fronto-centrally distributed. The CoRN seems to extend more to lateral electrodes than the ERN with a slight lateralization to the right. This was confirmed by an ANOVA, to which normalized amplitude data for the ERN and CoRN in fast error corrections were submitted (Component x Lateral Dimension interaction: $F(2,26) = 8.7, p \leq 0.01$).

To investigate the latency differences of the CoRN, a three-way ANOVA including the factors Correction Speed, Lateral Dimension and Anterior-Posterior Dimension was performed. The comparison between quickly and slowly corrected errors within the CI group revealed a significant Correction Speed x Anterior-Posterior Dimension interaction ($F(1,26) = 7.7, p \leq .05$). The data showed a later peak of the CoRN for slow corrections ($M = 244$ ms, $SEM = 7$) as compared to fast corrections ($M = 218$ ms, $SEM = 8$). This effect was most pronounced at anterior electrode sites ($F(1,26) = 5.0, p \leq .05$). The CoRN latency also differed signifi-

cantly between slow corrections in the CI group and incidental corrections in the CN group ($M = 211$ ms, $SEM = 8$; $F(1,26) = 5.9$, $p \leq .05$) peaking significantly later for slow corrections. This effect was again largest at anterior electrode sites ($F(1,26) = 8.8$, $p \leq .01$). No significant latency shift of the CoRN was found between fast corrections in the CI group and incidental corrections in the CN group ($F(1,26) = 0.3$, $p = .58$).

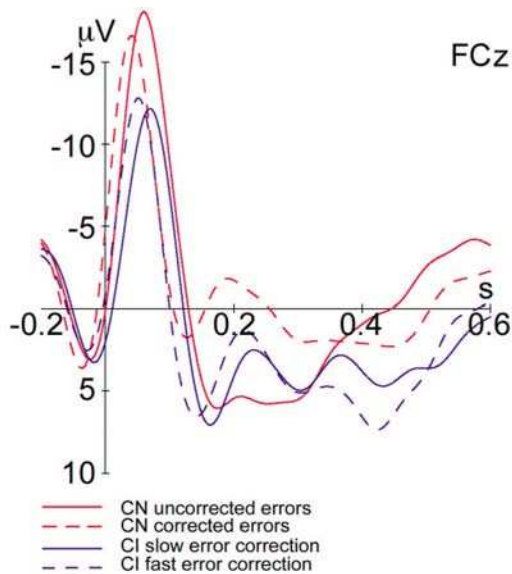


Figure 4.12: *Response-locked ERPs for uncorrected and corrected error trials in the correction non-instructed (CN) group and for slow and fast error correction trials in the correction instructed (CI) group at one midline electrode.*

In order to investigate whether the CoRN is temporally dependent either on the first erroneous response or on the second corrective response, an ERP-image plot was computed (Delorme, & Makeig, 2004). Figure 4.13A illustrates the ERN and the CoRN components scaled to μV levels at channel FCz, aligned with the erroneous button press, and sorted according to the participants' correction times. The ERP-image plot revealed a distinct negative deflection in the time window of the ERN time-locked to the initial error. In the time window of the CoRN, a negativity occurred after the corrective response, which showed a distribution along the correction time.

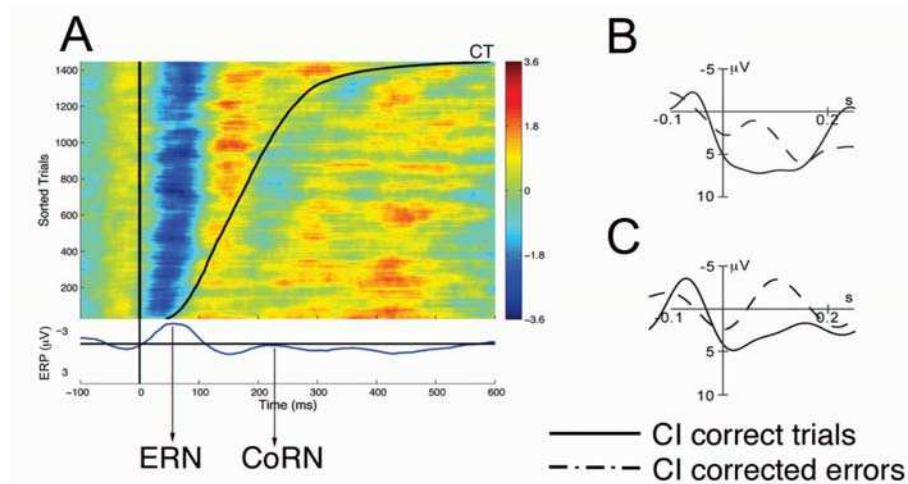


Figure 4.13: *A: Response-locked ERP-image plot for incompatible corrected error trials at channel FCz. Each vertically stacked thin color-coded horizontal bar represents a single trial in the event-related dataset. Trials are sorted according to the participants' correction time (CT), smoothed across 50 neighboring trials in the sorting order. The trace below the ERP image shows the ERP average of the imaged data epochs. As data from all subjects of the correction instructed (CI) group were collapsed, amplitudes of each trial were normalized for each subject. B: Correct-response locked and corrective-response locked ERP averages, respectively, for incompatible correct trials (solid, black line) and incompatible corrected error trials (dashed, black line) for the CI group at channel FCz. C: Same ERPs as depicted in Figure 4.13 B after 3.5 Hz high-pass filtering. ERN: error-related negativity, CoRN: correction-related negativity.*

Late time window. An ANOVA with the factors Lateral Dimension, Anterior-Posterior Dimension and Group was conducted to investigate differences in Pe amplitude between fast and slow corrections in the CI group. The ANOVA revealed a main effect of the factor Correction Speed ($F(1,13) = 33.0, p \leq .001$) and two interactions, a Correction Speed x Anterior-Posterior Dimension interaction ($F(1,13) = 5.2, p \leq .05$) and a Correction Speed x Lateral Dimension interaction ($F(2,26) = 8.1, p \leq .01$). Follow-up contrasts showed a larger positivity for fast

compared to slow error corrections at frontal electrode sites ($F(1,13) = 33.0, p \leq .0001$). This effect was reversed at posterior electrode sites ($F(1,13) = 15.7, p \leq .01$). The Pe amplitude did not differ significantly between incidentally corrected and uncorrected errors in the CN group ($F(1,13) = 0.7, p = .43$).

Differences in the Pe amplitude were observed in the between-group analysis contrasting incidental corrections in the CN group and fast corrections in the CI group. The ANOVA revealed a triple interaction Group \times Anterior-Posterior Dimension \times Lateral Dimension ($F(2,52) = 6.0, p \leq .01$). Follow-up comparisons exhibited a significantly larger Pe for fast corrections in the CI group than for incidental corrections in the CN group at midline frontal electrodes. Comparing incidental corrections in the CN group and slow corrections in the CI group, a significant main effect of the factor Group was found ($F(1,26) = 12.6, p \leq .01$) indicating a larger Pe for slow corrections in the CI group.

4.4.2 LRP Results

Analogous to the ERP analysis, LRPs for fast and slow error corrections within the CI group were calculated. To allow an additional comparison with incidentally corrected errors in the CN group, the same CN and CI sub-group samples as in the ERP analysis were used. Figure 4.14 illustrates the LRPs for incidentally corrected and uncorrected errors in the CN group as well as for fast and slow corrections in the CI group time-locked to the erroneous response. As expected, a clear lateralization to the incorrect side preceded the erroneous response. An interesting pattern in the time course of the LRP was observed for the lateralization to the correct side in the CI group: a deflection in the early time window was immediately followed by a second deflection in the middle time window to the same side.

Early time window. In the early time window, incidental corrections in the CN group ($t(13) = -2.9, p \leq .05$) and fast corrections in the CI group ($t(13) = -3.1, p \leq .01$) showed a lateralization to the correct side, which differed significantly from zero. There was no difference in the size of the amplitudes between incidental and fast corrections ($t(13) = -0.6, p = .56$). Uncorrected errors in the CN group

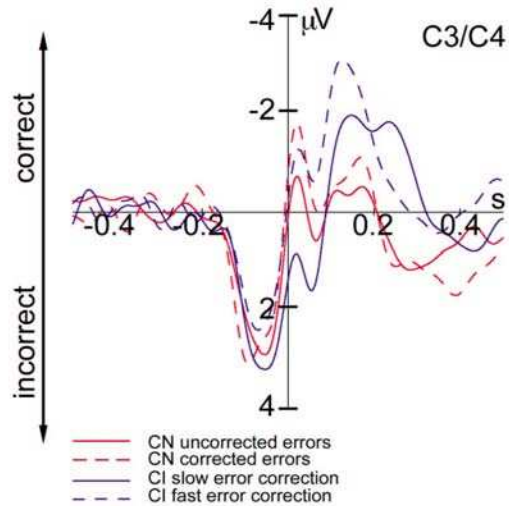


Figure 4.14: Response-locked LRPs for uncorrected and corrected error trials in the correction non-instructed (CN) group and for slow and fast error correction trials in the correction instructed (CI) group calculated from homologous electrodes C3 and C4. Upwards plotted deflections indicate an activation of a motor response to the correct response side; downwards plotted deflections to the incorrect response side.

showed a small lateralization to the correct side, which did not reach statistical significance ($t(13) = -0.6, p = .58$). Slow corrections in the CI group still remained on the incorrect side ($t(13) = 2.1, p \leq .10$).

Middle time window. As illustrated in Figure 4.14, fast ($t(13) = -7.0, p \leq .0001$) and slow ($t(13) = -4.1, p \leq .01$) corrections of the CI group lateralized to the correct side, while incidental corrections in the CN group returned to zero ($t(13) = -1.5, p = .17$). Uncorrected errors in the CN group showed no lateralization to the correct side ($t(13) = -1.1, p = .30$). Within-group ANOVAs revealed no difference in the size of the amplitudes comparing fast and slow corrections in the CI group ($F(13) = 2.9, p = .11$).

Late time window. Surprisingly, in the late time window the LRPs of incidentally corrected errors in the CN group lateralized to the erroneous side ($t(13) = 3.3, p \leq .01$), while the LRPs of fast ($t(13) = 0.5, p = .66$) and slow ($t(13) = -0.9,$

$p = .41$) corrections in the CI group and of uncorrected errors in the CN ($t(13) = -0.2, p = .84$) group did not significantly differ from zero.

4.4.3 Discussion

The ERP experiment was designed to investigate the time course of error correction and whether error correction and/or correction speed modulate error-related ERP components. Based on the different theories of performance monitoring, specific amplitude and latency patterns of the ERN for fast and slow error corrections are predicted. Adapted from the behavioral results, two types of error corrections, incidental and intentional error correction, are suggested, which were tested in the ERP study. The following Discussion chapter will first focus on the LRP data on error correction. Then, the new ERP component associated with immediate error correction, the CoRN, will be elaborated and preliminary suggestions about its functional role will be offered. The temporal characteristics of the ERN depending on error correction will be discussed within the framework of the performance monitoring theories. Finally, the Pe findings will be addressed.

LRPs and Error Correction

In the LRP data, errors were reflected by a pre-response activation to the incorrect side. Consistent with previous findings, corrected errors showed a clear lateralization to the correct side, while uncorrected errors elicited no lateralization (Falkenstein et al., 1994; Rodriguez-Fornells et al., 2002). The LRPs also differed for the two proposed types of error correction. Incidental corrections in the CN group and fast corrections in the CI group exhibited an early lateralization of comparable size to the correct side, which immediately followed the error. Intentional slow corrections were associated with a later lateralization to the correct side, which was more extended in time. In the same time range, fast corrections in the CI group showed a second, even larger lateralization to the correct side, whereas the LRP of incidental corrections in the CN group quickly returned to zero.

The data suggest that incidental corrections in the CN group are reflected by the first short-lasting lateralization to the correct side. The following late, sus-

tained lateralization for slow corrections in the CI group seems to be specific for the intention to correct errors. It seems conceivable that this late lateralization reflects the (pre)motor activity triggered by error detection and the resulting supra-threshold enhancement of the corrective response tendency. In uncorrected errors, however, a small but not significant short-lasting lateralization followed the erroneous response (cf., Figure 4.14). This small corrective response tendency could be too weak to exceed response threshold in order to initiate an incidental correction. The cause of the late lateralization to the incorrect side for incidental corrections in the CN group remains unclear.

In contrast to the observed monotonic shift from the initial error to the corrective response reported by Falkenstein et al. (1994) and Rodriguez-Fornells et al. (2002), the present data revealed a biphasic lateralization for fast corrections in the CI group. One can speculate that the first lateralization to the correct side corresponds to the incidental correction process based on ongoing stimulus processing, which does not require error detection. The subsequent longer-lasting lateralization may correspond to the intentional correction process that leads to the enhancement of the corrective response tendency after error detection. In fast corrections, this active enhancement occurs after the second response has been initiated, in slow corrections it could be the initiating event itself. Thus, the LRP findings hint at a phasic intentional process on slow corrections, which actively enhances stimulus processing and/or the evolving second response tendency, and is triggered by error detection.

Correction-related Negativity

Exclusively for corrected errors, the ERN was followed by a negative waveform associated with the corrective motor response, termed *correction-related negativity* (CoRN). Both ERP waveforms, the ERN and the CoRN, are distributed over fronto-central electrode sites. The topography of the CoRN is slightly broader than the scalp distribution for the ERN. It extends to electrode sites covering pre-

motor cortices⁴. The CoRN peaks in the time window from 200 to 240 ms after the onset of an incorrect response and has a peak-to-peak amplitude of about 5 μ V at FCz.

The CoRN was also visible in previous experiments revealing high correction rates (Dikman, & Allen, 2000; Falkenstein et al., 1996, 1994), but was not reported by the authors. In previous studies by Falkenstein and colleagues (1996, 1994), a small CoRN is visible after visual and auditory stimuli suggesting that it is not affected by stimulus modality. It is unlikely that the CoRN is elicited by the additional motor response reflecting MRPs (Shibasaki et al., 1980; Vaughan et al., 1968) of the correcting key press rather than by a cognitive process. Recently published data by Rodriguez-Fornells and Münte (2004) compared one-hand responses and two-hand responses in a two-choice reaction time task. The data showed no additional negative deflection for the second motor response. In an experiment by Falkenstein and colleagues (1994), participants were asked to press the response key twice. The time delay between the successive key presses approximated the delay of the correction key press. The results demonstrated that MRPs only affect later ERP effects in the time range of the Pe (around 300 ms).

The presence of the CoRN does not seem to be related to the intention to correct errors, since it was observed in incidental corrections in the CN group as well as in fast and slow corrections in the CI group. Its amplitude, however, may be modulated by the intention to correct errors reflected in a larger amplitude for intentional error corrections relative to incidental error corrections. The ERP-image plot indicates that the CoRN is rather time-locked to the second corrective response than to the initial error. This offers the interpretation that the CoRN is just a CRN; an ERN-like wave observed after correct responses in some studies (Vidal et al., 2000; Ford, 1999). If the second corrective response, however, elicits a CRN, this component should also occur after the response on correct trials. As depicted in Figure 4.13B, there was no CRN found following the response on correct

⁴The CoRN also showed a slight lateralization to the right scalp sites. Analysis of error rates and correction rates revealed no differences for right- and left-handed responses, so that the reason for the slight lateralization remains unclear.

trials. This is confirmed by the statistical analysis revealing a significant main effect of the factor Condition (incompatible correct trials vs. incompatible corrected error trials) in the time window from 0 to 120 ms in the correct-response locked and corrective-response locked ERP averages, respectively ($F(1,13) = 13.7, p \leq .01$). In order to rule out the differential influence of the stimulus-related P300 that might have masked the CRN on correct first responses, a high-pass filter with a cut-off frequency of 3.5 Hz was applied. As depicted in Figure 4.13C, no CRN is visible on correct trials, whereas the CoRN remains present for corrective responses ($F(1,13) = 12.8, p \leq .01$).

In sum, it can be concluded that the CoRN is most likely related to error correction. The CoRN is believed to be associated with ongoing stimulus-response mapping based on continued stimulus processing and/or an enhancement of the evolving corrective response tendency. The timing pattern of the CoRN precludes the notion that it could be directly related to response selection.

ERN Latency

As expected, an ERN was elicited after erroneous responses. The observed latency pattern of the ERN fits best with the predictions made by the response conflict model (cf., Table 4.3, page 83). The latency was delayed by about 15 ms to 20 ms for uncorrected and slowly corrected errors as compared to incidental and fast corrections, respectively. The results are in line with the notion that the maximal post-response conflict is postponed, when the second response tendency is delayed (Yeung et al., in press). The notion of a delayed second response tendency on slowly corrected errors is corroborated by the LRP findings showing a later lateralization to the correct side.

The present findings are inconsistent with both variants of the Mismatch Hypothesis. The original version of the Mismatch Hypothesis suggests that the ERN is elicited when both response representations are completed (Falkenstein et al., 1991). This should result in an ERN latency in the time range of the corrective response. Particularly in slow corrections, this should have led to an ERN latency increase of more than 150 ms instead of 15 ms to 20 ms as found in the

present experiment. According to the alternative version of the Mismatch Hypothesis proposing that the comparison eliciting the ERN takes place upon arrival of the efference copy (Coles et al., 2001), no latency differences would have been predicted.

Similar findings about the modulation of the ERN latency by correction speed were reported by Falkenstein et al. (1996). Surprisingly, no latency differences between quickly and slowly corrected errors were observed in the study by Rodriguez-Fornells and colleagues (2002). This difference might be explained by the different medians of the reaction time for fast and slow error corrections. In the study by Rodriguez-Fornells et al. (2002), a difference between the median of fast and slow corrections amounted to 104 ms, whereas in the present experiment there was a difference of 141 ms. Assuming that the latency difference of the ERN depends on correction speed, a decreasing temporal distance between quickly and slowly corrected errors should diminish the ERN latency difference.

ERN Amplitude

The ERN showed a significantly smaller amplitude for corrected errors in the CI group relative to uncorrected errors in the CN group over frontal electrode sites. This result is inconsistent with previous studies reporting no amplitude difference between corrected and uncorrected errors (Falkenstein et al., 1994) or a decreased ERN amplitude for uncorrected compared to corrected errors (Rodriguez-Fornells et al., 2002; Falkenstein et al., 1996; Gehring et al., 1993). The latter finding would be predicted by the Response Conflict Hypothesis (Yeung et al., in press; Botvinick et al., 2001) and the alternative version of the Mismatch Hypothesis (Coles et al., 2001). Both hypotheses assume a smaller ERN for uncorrected errors based on a delayed second response tendency, which results in a decreased maximum of post-response conflict and a smaller mismatch, respectively.

In contrast to the Mismatch Hypothesis and the Response Conflict Hypothesis, the evaluative monitoring account provides a satisfactory explanation for the observed amplitude pattern. Several studies showed that a higher motivational significance of errors is reflected in a larger ERN amplitude (Ullsperger, & Szy-

manowski, 2004; Hajcak et al., 2003; Gehring, & Willoughby, 2002; Hajcak, & Simons, 2002; Dikman, & Allen, 2000; Luu et al., 2000a; Gehring et al., 2000, 1993). Thus, errors should be more significant for the CN group than for the CI group. This assumption was confirmed by the behavioral data revealing differences in response behavior between the two groups (cf., section 4.3, page 74). Due to the fact that the possibility to correct errors was not instructed to participants of the CN group, they believed errors to be unacceptable attaching more significance to them and therefore responded with more caution. It is suggested that the higher motivational error significance in the CN group is reflected in the larger ERN amplitude. Latest findings revealed supportive results demonstrating a significant correlation between ERN amplitude and error significance: the larger the ERN amplitude the higher the error significance (unpublished observations).

Inconsistent with the predictions of the current models of performance monitoring, the ERN amplitudes showed no significant difference in the sub-group comparisons. The absence of an amplitude difference might have been caused by a loss of statistical power. While in the overall group comparison 20 participants were collapsed in each group, only 14 participants per group were included in the sub-group comparisons. Moreover, the sub-groups were matched according to their performance diminishing between-group differences, which have supposedly elicited the amplitude modulation of the ERN in the overall group comparison. It remains unclear why the relationship of ERN amplitude and error correction shows this inconsistent pattern of results comparing the literature and the present study. It can be speculated that the ERN size depends on the amount of post-response conflict in a non-linear manner and shows ceiling effects.

Pe Amplitude

Sub-group comparisons showed a significant difference between incidental and fast corrections as well as fast and slow corrections, mostly due to a larger positivity on fast error corrections at mid-frontal electrode sites. There was, however, no amplitude difference between incidentally corrected and uncorrected errors within the CN group. The functional significance of these findings is rather un-

clear, since the Pe is usually maximal at centro-parietal electrodes (Falkenstein et al., 1996, 1994). On the other hand, some studies also reported a more midline central distribution of the Pe (Ullsperger, & von Cramon, 2001; Falkenstein et al., 2000). Falkenstein et al. (1994) suggested that the Pe in corrected errors could be affected by a MRP of the correcting key press. The fact that no Pe difference was observed between corrected and uncorrected errors within the CN group renders this account unlikely.

The Pe results are inconsistent with the notion that this component is associated with post-error slowing (Nieuwenhuis, Ridderinkhof, Blom, Band, & Kok, 2001), since a smaller Pe for the CN group was found showing post-error slowing compared to the CI group, in which post-error slowing was absent. The findings strengthen the view that the Pe has a large variability across different individuals and different tasks such that the nature of this component still remains questionable (Stemmer et al., 2004; Falkenstein, 2004; Falkenstein et al., 2000).

4.5 Conclusion

Experiment 1A examined the electrophysiological correlates of error correction using behavioral data, ERPs, and LRPs. Moreover, the modulation of error-related ERP components by correction speed was investigated. ERP findings demonstrate a new component associated with error correction, the correction-related negativity (CoRN). The results further hint at two types of error correction depending on the instructional context: incidental and intentional error correction. Behavioral results indicate that response strategy is affected by the possibility to correct errors. Participants in the CN group seem to attach increased significance to errors leading to a more cautious response behavior. This high motivational error significance seems to be reflected in an enhanced ERN amplitude. ERN latency can be modulated by correction speed: the ERN peaked earlier for quickly corrected errors compared to slowly corrected errors as predicted by the Response Conflict Hypothesis. The amplitude of the Pe significantly differed between fast and slow correction, whereas the ERN amplitude did not.

Chapter 5

Experiment 1b (HR)

5.1 Introduction

The second focus of the ERP experiment is to investigate cardiac changes associated with error detection and error correction. Previous studies showed that cardiac deceleration reflects external feedback to response errors (van der Veen et al., 2004; Crone et al., 2003, Somsen et al., 2000) as well as internal error monitoring (Hajcak et al., 2003). Positive feedback and correct responses, respectively, as well as negative feedback and erroneous responses, respectively, elicited a decelerative response. The strength, however, of HR deceleration depended on the valence of the stimuli. Negative feedback and erroneous responses showed an enhanced cardiac slowing relative to positive feedback and correct responses. Based on these findings, a HR deceleration for both, correct and error trials, with a more pronounced deceleration for errors can be predicted.

In order to examine cardiac changes associated with error correction, cardiac deceleration on immediately corrected errors in the CI group and uncorrected errors in the CN group is contrasted. A study by van der Veen et al. (2004) related cardiac deceleration to successful response adjustments on the subsequent trial following response errors. Based on these results, HR deceleration is also associated with immediate error corrections occurring within the error trials.

5.2 Method

In the experiment, the EEG and the ECG were simultaneously recorded while participants performed the modified version of the Eriksen flanker task (for the task description see chapter 4.2.2, page 68).

5.2.1 Participants

The sample is described in chapter 4.2.1 (page 67). Six participants (three out of each group) were excluded from analysis because of heavy noise in the data making an identification of the R-peaks impossible. The sample of thirty-four volunteers (CI group: N=17, 7 female; CN group: N=17, 11 female) was right-handed and had normal or corrected-to-normal vision. They ranged in age from 21 to 29 years ($M = 25$).

5.2.2 Data Recording

The ECG was bipolarly recorded with two Ag/AgCl electrodes placed on the left and right ventral forearm. Analogous to the EEG recording, the ECG signal was AD converted with 22-bit resolution at a sampling rate of 250 Hz. The data were band-pass filtered off-line with 2 to 60 Hz. The position of the R-peaks was detected off-line with an accuracy of 4 ms and corrected for movement artifacts and signal drifts. The HR was calculated based on the interval time between successive R-peaks. The discontinuous HR signal was transformed into a continuous signal by linear interpolation (cf., Koers et al., 1999; Velden, 1999; Mulder, & Mulder, 1981).

5.2.3 Data Analysis

The same logic as described for the ERP data was used to analyze the HR data (cf., chapter 4.2.4, page 70). Response-locked averages were calculated for incompatible correct and incompatible erroneous trials in the time range from -200 to 1300 ms. The average voltage in the 100 ms preceding the onset of the flanker

arrows served as baseline. The mean amplitude was calculated for two defined time windows (early time window: 0-600 ms; late time window: 600-1300 ms).

Statistical Analysis

In order to investigate HR changes associated with error detection and error correction, a two-way repeated-measures ANOVA with the within-subject factor *Response Type* (two levels: correct and erroneous responses) and the between-subject factor *Group* (two levels: CI and CN group) was conducted. Interactions were analyzed by computing subsequent lower-order ANOVAs and *t*-tests (cf., Bortz, & Döring, 1995). All effects with more than one degree of freedom in the numerator were adjusted for violations of sphericity according to the formula of Greenhouse and Geisser (1959). Late responses (delivered after the response deadline) were excluded from statistical analyses.

5.3 Results

Figure 5.1 illustrates the response-locked averages of HR changes for incompatible correct trials and incompatible error trials in both groups. Corrected error trials are depicted in the CI group, uncorrected error trials in the CN group.

Early time window. In the early time window, the two-way ANOVA with the factors Response Type and Group revealed neither a significant main effect of the factor Response Type ($F(1,32) = 0.9, p = .35$) nor a Response Type x Group interaction ($F(1,32) = 2.1, p = .16$).

Late time window. In the late time window, the two-way ANOVA with the factors Response Type and Group showed a significant main effect for the factor Response Type exhibiting a more pronounced HR deceleration for errors compared to correct trials ($F(1,32) = 30.6, p \leq .0001$). Furthermore, a significant Response Type x Group interaction was observed reflecting a larger HR deceleration for uncorrected errors in the CN group than for corrected errors in the CI group ($F(1,32) = 4.2, p \leq .05$).

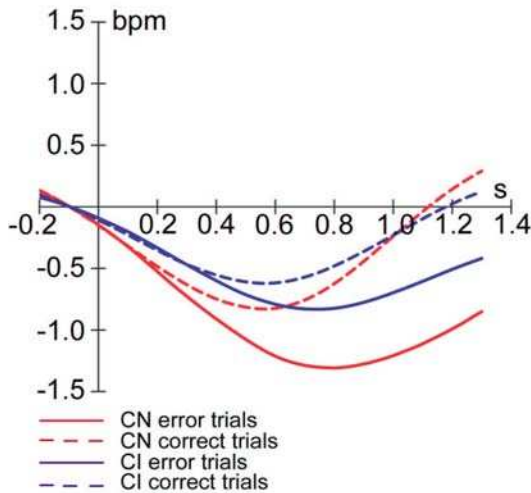


Figure 5.1: *Response-locked event-related HR averages for incompatible correct and incompatible erroneous trials for the correction instructed (CI) group and the correction non-instructed (CN) group. For the CI group, event-related HR averages for corrected errors are depicted, for the CN group, event-related HR averages for uncorrected errors are depicted.*

5.4 Discussion

In line with previous results, errors as well as correct responses elicit a cardiac deceleration being more pronounced for errors. This result suggests that HR deceleration reflects autonomic responses induced by internal performance monitoring. If the performance monitoring process is interrupted, an error might occur resulting from a mismatch between the appropriate and the actually performed response. This detected mismatch seems to be reflected in an enhanced cardiac deceleration (cf., Crone et al., 2003). The result, however, could also be interpreted in terms of valence (positive versus negative outcome), as suggested by van der Veen and colleagues (2004).

As expected, HR deceleration was modulated by error correction showing a larger decelerative response for uncorrected errors in the CN group than for corrected errors in the CI group. Taking the results by van der Veen et al. (2004) into account, cardiac deceleration seems to be related to long-term as well as short-

term behavioral adjustments following response errors. Based on the behavioral findings (cf., chapter 4.3), an alternative interpretation of the HR data is favored. The behavioral results showed that the CN group and the CI group differed with respect to their response strategy. It can be assumed that the CN group believes errors to be unacceptable thereby attaching more significance to them and therefore responds with more caution to prevent response errors. The instructed possibility to correct errors in the CI group seems to decrease the motivational significance of response errors. Crone et al. (2003) related HR deceleration to a violation in the predictions of the outcome. Thus, the higher motivational error significance in the CN group is suggested to lead to a stronger violation of the performance-based expectations on error trials reflected in a larger HR deceleration.

5.5 Conclusion

Experiment 1B investigated cardiac changes related to error detection and error correction. The HR results revealed a cardiac slowing on correct trials as well as on erroneous trials. There was, however, a larger HR deceleration on errors. Furthermore, cardiac slowing on errors differed between the two groups. The CN group showed a more pronounced HR deceleration relative to the CI group. In line with the findings of Experiment 1A, the data suggest that high motivational error significance in the CN group is reflected by an enhanced HR deceleration.

Chapter 6

Experiment 2 (fMRI)

6.1 Introduction

While many fMRI studies have focused on the neural correlates of error detection and response conflict, there are few investigations examining the cortical implementation of the consequences of errors. Dehaene and colleagues (1994) proposed that a system located in the dorsal ACC and/or the pre-SMA is engaged when an error is detected in time for a correction to be attempted. The involvement of the dorsal ACC or more precisely of the RCZ in behavioral adjustments following errors was strengthened by single cell recording studies in monkeys (Shima & Tanji, 1998). FMRI findings in humans showed similar areas on the frontomedian wall related to long-term behavioral adjustments, i.e., post-error slowing (Kerns et al., 2004; Garavan et al., 2002; Carter et al., 2001).

The aim of the present fMRI experiment is to investigate the neural correlates of short-term behavioral adjustments following response errors, namely immediate error correction. In order to achieve comparability to the present ERP experiment, the same task and group classification were used. Considering the cortical function of the RCZ in error processing (Ullsperger, & von Cramon, 2001; Botvinick et al., 2001) and of the pre-SMA in motor planning (Tanji, 1994), these brain areas seem to be suitable for a functional implementation of immediate error correction. The fMRI experiment focuses on the identification of cortical areas

on the frontomedian wall associated with immediate error correction. Taking the neural correlates of error detection into account, the issue of whether both processes, error detection and error correction, rely on a common neuroanatomical substrate is addressed.

Based on the HR results reported in chapter 5.3, this experiment further examines the relation of the inferior insula and cardiac changes caused by error responses. The inferior insula is proposed to be a central determinant in the regulation of cardiac autonomic activity (see chapter 3.2.3). The anatomical projections of the inferior insula to several cortical and subcortical structures directly engaged in HR regulation argue for its suitable role in autonomic cardiovascular control (Verberne, & Owens, 1998). Empirical studies in rats (e.g., Butcher, & Cechetto, 1995) as well as in humans (Oppenheimer et al., 1992) also suggest the involvement of the inferior insula in the cardiac regulation. In the present fMRI experiment, the question is raised whether the revealed error-related HR modulation is reflected on the brain level focussing on the inferior insula.

6.2 Method

6.2.1 Participants

Thirty-one individuals participated in the experiment. The group classification and the exclusion criteria were analogous to the ERP experiment (cf., chapter 4.2.1, page 67). Two participants in the CI group were excluded from analysis because of a correction rate below 50% and one participant in the CN group due to a correction rate above 50%. In addition, one participant was excluded for an insufficient number of error trials ($\leq 10\%$). The sample of twenty-seven healthy volunteers (CI group: $N=14$, 6 female; CN group: $N=13$, 5 female) was right-handed and had normal or corrected-to-normal vision. Their age ranged from 21 to 35 years ($M = 25$). Participants were paid for the experiment.

6.2.2 Experimental Procedure

The speeded modified flanker task applied in the ERP experiment was also used in the fMRI study (for the task description see chapter 4.2.2, page 68). In order to keep the participants' stay within the MR scanner below one hour, the experimental session consisted of one block, which lasted 27 min. This block comprised 162 compatible trials and 162 incompatible trials presented in randomized order. Prior to the experimental session, an anatomical scan was run (see chapter 6.2.3). During this anatomical scan, participants performed two subsequent training sessions (160 trials each), which were used to individually estimate the response deadline applied in the experimental session. When the response deadline was exceeded, a feedback occurred informing the participants to speed up their responding.

6.2.3 fMRI Procedure

Imaging was performed at 3T on a Bruker (Ettlingen, Germany) Medspec 30/100 system equipped with the standard bird-cage head coil (SGRAD MkIII 580/400/S, MAGNEX Scientific Ltd., Abingdon, UK). Twenty slices (thickness 4 mm, spacing 1 mm) were positioned parallel to the bicommissural (AC-PC) plane covering the whole brain. Prior to the functional runs, a set of 2D anatomical images was acquired for each participant using an MDEFT sequence (256 x 256 pixel matrix). Functional images in plane with the anatomical images were acquired using a single-shot gradient EPI sequence (TR = 2; TE = 30 ms; 64 x 64 pixel matrix; flip angle 90°; field of view 192 mm) sensitive to BOLD contrast¹. In order to improve temporal resolution for modeling of the hemodynamic response, an interleaved design was employed (Miezin, Maccotta, Ollinger, Petersen, & Buckner, 2000). In a separate session, high-resolution whole brain images were acquired from each participant to improve the localization of activation foci using a T1-weighted 3D segmented MDEFT sequence covering the whole brain.

¹The parameter TR (time to repeat) specifies the time between two consecutive excitations of the same slice by a sequence of RF pulses. The parameter TE (time to echo) specifies the time period between the exposure of the RF pulse and the acquired MR-signal.

Participants received the instruction before the fMRI experiment started. Then, they were asked to lie on a scanner bed with their left and right index finger positioned on MRI-suitable response buttons. In order to prevent body movements, the head of the participants was carefully fixated and their arms and hands were stabilized by vacuum cushions. Earplugs were used to protect the participants against scanner noise. Participants wore mirror-glasses to look at the visual stimuli, which were projected to a pane of glass positioned at the end of the scanner. The fMRI experiment started with the anatomical scan, which lasted about 20 min and was also used as a training session. Immediately after that, the functional data were acquired, while participants performed the experimental task.

6.2.4 Statistical Analysis

For behavioral statistics, repeated-measures ANOVAs with the within-subject factors *Response Type* (two levels: correct and erroneous responses), *Correction Type* (two levels: corrected and uncorrected errors), *Compatibility* (two levels: compatible and incompatible trials), and the between-subject factor *Group* (two levels: CI and CN group) were conducted. Interactions were analyzed by computing subsequent lower-order ANOVAs and *t*-tests (cf., Bortz, & Döring, 1995). All effects with more than one degree of freedom in the numerator were adjusted for violations of sphericity according to the formula of Greenhouse and Geisser (1959). Response rate data were also tested after arcsine normalization (see page 72). All reported statistical effects also reached significance by applying the converted data to the ANOVA.

The analysis of the fMRI data was conducted using the software package LIPSIA (Lohmann et al., 2001) as described in chapter 3.3.4. Next, the computed contrast images will be explained in more detail.

The following conditions were specified in the GLM: compatible correct trials, incompatible correct trials, incompatible erroneous trials (CI group: corrected errors; CN group: uncorrected errors) and late responses (delivered after response deadline). Compatible erroneous trials were excluded from statistical analysis because of an insufficient trial number ($\leq 4\%$). *Response conflict* was examined by

contrasting compatible correct trials and incompatible correct trials. *Error detection* was investigated by the contrast incompatible erroneous trials versus incompatible correct trials. The resulting SPMs were thresholded at $p \leq .001$ threshold (uncorrected). Local maxima of the z-maps residing in activation areas of size smaller than 360 cubic millimeters (= 8 measured voxels) were not reported to minimize the probability of false positive results (type I error). In order to investigate the brain activity related to immediate *error correction*, a between-group analysis was performed contrasting the brain activity on corrected errors committed in the CI group and the brain activity on uncorrected errors committed in the CN group. The comparison was confined to regions that were significantly activated during errors in at least one of both groups. The between-group analysis consisted of a two-sample *t*-test. Because of the anatomical variability of the observed cortical regions, a less conservative threshold at $p \leq 0.05$ (uncorrected) was used for the resulting SPM of the group comparison.

6.3 Results

6.3.1 Behavioral Data

The behavioral data revealed instruction-based behavior: participants in the CI group corrected their errors significantly more often ($M = 82\%$, $SEM = 4$) than participants in the CN group ($M = 21\%$, $SEM = 6$; $t(25) = 8.7$, $p \leq .0001$). The mean correction time was 104 ms ($SEM = 10$) for the CN group and 161 ms ($SEM = 11$) for the CI group and differed significantly between the two groups ($t(24) = 3.7$, $p \leq .01$).

As depicted in Table 6.1, typical effects of incompatibility were found for both reaction times and error rates. Correct response times were submitted to an ANOVA with the within-factor Compatibility and the between-factor Group. The analysis revealed a significant main effect of Compatibility showing longer reaction times for incompatible correct trials ($M = 416$ ms, $SEM = 4$) than for compatible correct trials ($M = 360$ ms, $SEM = 4$; $F(1,25) = 1035.4$, $p \leq .0001$). Secondly, error rates were higher for incompatible trials ($M = 37\%$, $SEM = 2$)

Table 6.1: Mean proportion, and reaction times of correct, erroneous and late responses for each stimulus type.

		<i>Group</i>							
		<i>CN</i>				<i>CI</i>			
	<i>Stimulus Type</i>	<i>Compatible</i>	<i>Incompatible</i>	<i>Compatible</i>	<i>Incompatible</i>	<i>Compatible</i>	<i>Incompatible</i>	<i>Compatible</i>	<i>Incompatible</i>
<i>RR</i> <i>in %</i>	Correct	92.9 (1.6)	42.5 (5.3)	88.8 (1.5)	42.0 (4.6)				
	Error	1.6 (0.3)	33.6 (2.8)	3.5 (0.8)	39.2 (3.2)				
	Correct late	4.8 (1.2)	22.0 (3.3)	7.1 (1.4)	17.1 (3.2)				
	Error late	0.6 (0.3)	1.9 (1.0)	0.6 (0.3)	1.7 (0.5)				
<i>RT</i> <i>in ms</i>	Correct	362 (6)	421 (7)	359 (5)	414 (5)				
	Error	*	334 (6)	*	334 (6)				
	Correct late	500 (9)	489 (10)	498 (9)	491 (9)				
	Error late	*	*	*	*				

Note: *RR*: response rate; *RT*: reaction time; *CN*: correction non-instructed group; *CI*: correction instructed group. Standard error of mean is presented in parentheses. *Too few trials for meaningful analyses.

compared to compatible trials ($M = 3\%$, $SEM = 1$; $F(1,25) = 290.4$, $p \leq .0001$). Consistent with previous findings, participants were significantly faster on incompatible erroneous trials ($M = 334$ ms, $SEM = 4$) than on incompatible correct trials ($M = 417$ ms, $SEM = 4$; $F(1,25) = 651.8$, $p \leq .0001$). All three ANOVAs revealed no interaction with the factor Group.

6.3.2 FMRI Data

Error Detection

In the fMRI analysis, brain areas related to error detection were examined contrasting incompatible erroneous trials with incompatible correct trials. A list of all significant activations of the Error Detection contrast is presented in Table 6.2.

Table 6.2: *Anatomical specification, Talairach coordinates (x,y,z), and maximal z-scores (Z) of voxels covarying significantly ($p \leq .001$) with Error Detection (incompatible erroneous vs. incompatible correct trials).*

<i>Area</i>	<i>Hemisphere</i>	<i>x</i>	<i>y</i>	<i>z</i>	<i>Z</i>
pre-SMA (BA 6)	L	-2	2	62	4.2
pre-SMA (BA 8)	L	-1	14	53	4.2
pre-SMA (BA 6)	R	7	20	62	3.4
pre-SMA (BA 8)	R	2	29	56	3.8
RCZ (BA 24/32)	R	1	21	38	4.2
anterior inferior insula	L	-46	14	-4	3.4*

*Note: SMA: supplementary motor area; RCZ: rostral cingulate zone; MFG: medial frontal gyrus; BA: Brodmann Area; R: right; L: left. *significant activation observed on a lower spatial threshold (90 cubic millimeters).*

The fMRI data exhibited a clear activation pattern on the frontomedian wall. On errors, the focus of the hemodynamic activity was primarily localized in two areas: the right RCZ and the pre-SMA bilaterally. As illustrated in Figure 6.1, there was a widespread activation in the pre-SMA extending into BA 32. The error-related activation in the RCZ was located on the border BA 24 / BA 32 and showed a more focal distribution.

In the Error Detection contrast, no activation in the inferior insula was observed. When reducing spatial threshold (90 cubic millimeters), however, a significant activation in the anterior inferior insula was revealed on error trials relative to correct trials (see, Figure 6.1).

Error Correction

In a second step, the issue was addressed whether error correction is implemented in similar brain areas as engaged in error detection or relies on a different cortical network. In order to isolate correction-related brain regions, corrected error trials occurring in the CI group and uncorrected error trials occurring in the CN group

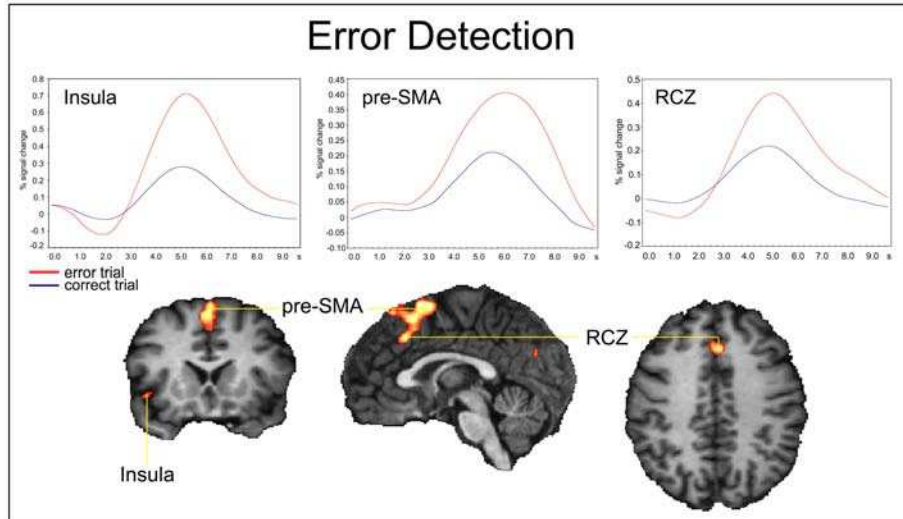


Figure 6.1: Cortical activations of the contrast incompatible erroneous trials vs. incompatible correct trials on coronal ($y=15$), sagittal ($x=1$) and axial ($z=31$) slices of a 3D structural MRI. Trial averaged time courses of the anterior inferior insula, the pre-supplementary motor area (pre-SMA) and the rostral cingulate zone (RCZ) are depicted on the top of the figure.

were contrasted by using a two sample t -test (e.g., Bortz, & Döring, 1995). Table 6.3 lists the significant activation foci related to error correction.

Consistent with the results reported for error detection, the fMRI data revealed activation foci in the right RCZ and in the left pre-SMA associated with immediate error correction. The correction-related activations on the frontomedian wall and the corresponding trial-averaged time courses are illustrated in Figure 6.2.

Additional activations associated with error correction were found in the right caudal part of the SMA (SMA proper) and in the left cuneus. An interesting activation pattern was also observed in the parietal cortex of the right hemisphere. The data revealed a higher hemodynamic response for corrected errors in the parietal operculum, an area located between the central sulcus and the posterior ascending branch of the Sylvian fissure, where an imaginary lateral extension of the postcen-

Table 6.3: *Anatomical specification, Talairach coordinates (x,y,z), and maximal z-scores (Z) of voxels covarying significantly ($p \leq .05$) with Error Correction (corrected erroneous vs. uncorrected erroneous trials).*

<i>Area</i>	<i>Hemisphere</i>	<i>x</i>	<i>y</i>	<i>z</i>	<i>Z</i>
pre-SMA (BA 6)	L	-5	0	62	2.9
SMA proper (BA 6)	R	4	-6	56	2.5
RCZ (BA 24/32)	R	1	21	38	2.1
parietal operculum (BA 40)	R	55	-23	23	4.1
supramarginal gyrus (BA 39)	R	61	-32	38	2.4
postcentral gyrus (BA 1)	R	58	-15	35	2.1
cuneus (BA 18)	L	-5	-87	12	2.2

Note: SMA: supplementary motor area; RCZ: rostral cingulate zone; BA: Brodmann Area; R: right; L: left.

tral sulcus points to the middle of the parietal operculum (see Figure 6.2). Separated activation foci were located in two areas superior to the parietal operculum: one on the crown of the postcentral gyrus, and a second focus in the supramarginal gyrus posterior to the parietal operculum and adjacent to the posterior ascending branch of the Sylvian fissure.

6.4 Discussion

The fMRI experiment focused on the neural correlates of error detection and error correction. Accordingly, it was investigated whether similar brain areas are engaged in these two processes. Based on the observed error-related HR changes in the EEG study, the hypothesis was tested whether the modulation of cardiac activity is reflected by the inferior insula.

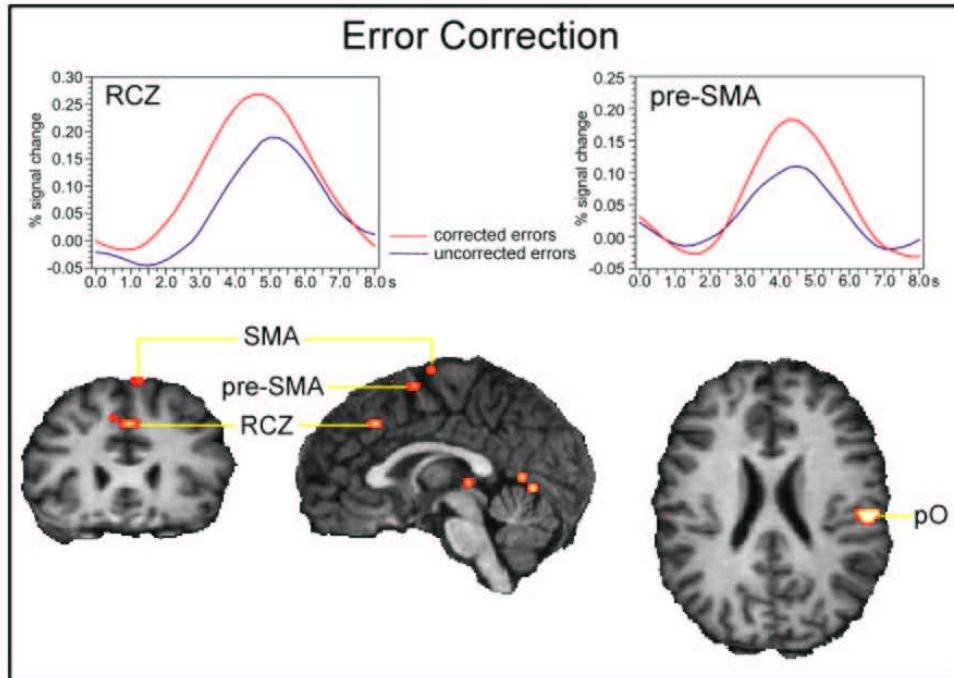


Figure 6.2: Cortical activations of the contrast corrected erroneous trials vs. uncorrected erroneous trials on coronal ($y=22$), sagittal ($x=1$) and axial ($z=23$) slices of a 3D structural MRI. Activations in the cisterna laminae tecti and in the cisterna cerebelli superior were likely caused by pulsation artifacts. Trial averaged time courses of the rostral cingulate zone (RCZ) and the pre-supplementary motor area (pre-SMA) are depicted on the top of the figure. pO: parietal Operculum.

In accordance with the behavioral results revealed in the ERP study, the data showed an increase in error correction rate by experimental instruction. Participants in the CI group corrected more than 80% of their errors, whereas participants in the CN group corrected only 21% (cf., Rabbitt, 1967).

The following Discussion chapter will first concentrate on activated brain areas associated with error detection. The relation of the anterior inferior insula and cardiac changes due to error detection will be discussed afterwards. Finally, the functional implementation of error correction will be elaborated.

6.4.1 Error Detection

Findings that error detection is reflected by a frontomedian cortical network of brain regions with a focus in the RCZ and the superior pre-SMA could be replicated (Garavan et al., 2003, 2002; Ullsperger, & von Cramon, 2001; Kiehl et al., 2000; Carter et al., 1998). This result supports the notion that the RCZ plays a decisive role in error detection. The involvement of the pre-SMA in error detection is still unclear. Ullsperger and von Cramon (in press) speculated that the error-related activation in the pre-SMA might be due to insufficient inhibition of the erroneous response. In line with the response conflict model, Garavan and colleagues (2002) argued that the activation of the pre-SMA may reflect post-response conflict, which is present on error trials (cf., Yeung et al., in press). The activation in the pre-SMA, however, reported in the present study was located posteriorly and superiorly to the activations associated with response conflict.

In contrast to some previous studies (Garavan et al., 2002; Kiehl et al., 2000), no significant activation was found in the lateral prefrontal cortex (LPFC). It seems that error-related activation in the LPFC is a more reliable finding for Go-NoGo tasks (Garavan et al., 2002; Kiehl et al., 2000) than for flanker tasks (see also Ullsperger, & von Cramon, in press; Ullsperger, & von Cramon, 2001). It can be speculated that errors in Go-NoGo tasks result in more robust task-set-related adjustment processes leading to lateral prefrontal activations (cf., Garavan, Hester, & Fassbender, 2004) than flanker tasks do.

Based on the HR findings revealed in the present EEG study (cf., chapter 5.3), it was tested whether the error-related HR modulation is reflected on the inferior insula, a region strongly associated with cardiovascular control. The Error Detection contrast revealed an activation focus in the left anterior inferior insula on errors relative to correct responses. Note, this activation was small but significant. It can be argued that the higher activation in the anterior inferior insula reflects the larger HR deceleration elicited on response errors.

6.4.2 Error Correction

To investigate cortical areas related to immediate error correction, corrected and uncorrected error trials were contrasted. The major finding of this study is the increased activation in the RCZ and the pre-SMA on both corrected and uncorrected errors. The common activated brain regions, however, differed in strength of activation showing a significantly greater hemodynamic response for corrected than for uncorrected errors.

The fMRI data demonstrate that both error detection and error correction activate cortical networks involving the pdFMC. This finding suggests that cortical areas involved in error detection play also a role in the implementation of immediate error correction. According to the Talairach-coordinates, the regional overlap of the maxima in the RCZ was nearly perfect (cf., Table 6.2 and 6.3). A clinical study reported a reduced error correction rate in a patient with an RCZ lesion assuming an involvement of the RCZ in error correction (Swick, & Turken, 2002). Taking previous results into account, the RCZ and the pre-SMA seem not only to be involved in long-term adjustments as post-error slowing but also to be engaged in immediate corrective behavior as evidenced by the present data (cf., Kerns et al., 2004; Garavan et al., 2002; Carter et al., 2001). In contrast, Husain et al. (2003) showed that a selective lesion in the pre-SMA does neither impair error monitoring nor error correction challenging the important role of the pre-SMA in error correction. Taking the neuroanatomy into account, the pre-SMA, however, appears to be particularly suitable for an involvement in the preparation of corrective behavior.

Neurons in the rostral CMA, the monkey homologue of the human RCZ, respond to alternations in the motor behavior (Shima, & Tanji, 1998) after error detection in order to reach the intended goal (Ito et al., 2003). The important role of the RCZ in error correction is strengthened by neuroanatomical findings in monkeys revealing direct projections from the rostral CMA to (pre)motor areas and the SMA to facilitate movement-related processes (Picard, & Strick, 1996; Dum, & Strick, 1991). Dum and Strick (1991) argued that the rostral CMA has the potential to generate and control movements as necessary in corrective behavior.

The present findings fit very nicely with the monkey data. An increased activation in the RCZ was found during error correction in terms of an alternation of motor behavior after error detection.

An alternative view is provided by the Response Conflict Hypothesis (Yeung et al., in press; Botvinick et al., 2001; Carter et al., 1998). FMRI studies suggest that the ACC (Botvinick et al., 2001; Carter et al., 1998) or adjacent areas on the frontomedian wall (Ullsperger, & von Cramon, in press, 2001; Garavan et al., 2003, 2002) monitor response conflict. One could speculate that the increased activation in the RCZ and the pre-SMA during error correction found in the present data reflects an enhanced conflict in the CI group caused by a stronger activation of the second correct response tendency exceeding threshold. Recently published data, however, showed that the RCZ is activated during errors even in the absence of response conflict, e.g., in feedback-based error processing (Holroyd et al., 2004; Ullsperger, & von Cramon, 2003). The question whether the RCZ reflects post-response conflict or the initiation of remedial actions after errors cannot be decided on the basis of current knowledge.

Furthermore, additional activation related to error correction was observed in the SMA proper, a region highly interconnected with the RCZ. Considering the dense projections from the SMA proper also to the primary motor cortex and the spinal cord (Dum, & Strick, 1993, 1991), this area is considered to be directly engaged in generating concrete motor commands, which is in accordance with its involvement in immediate error correction. In contrast, the pre-SMA is stronger connected to prefrontal cortices and more closely related to cognitive than to motor processes (Picard, & Strick, 2001).

In sum, from an anatomical point of view the RCZ and the pre-SMA are optimally qualified to be involved in the preparation of error correction. The higher activation in the SMA proper during error correction is likely to be related to the execution of the corrective response. This argument does not hold for the pre-SMA and the RCZ, as these regions were also active in the Error Detection contrast when performed for the CN group alone, in which purely motor-related activations should be cancelled out.

The Somatosensory Network in Error Correction

The increased activation found for corrected errors in the posterior frontomedian cortex was accompanied by activations in the anterior parietal lobe. These activation foci represent an interconnected cortical network, which processes somatosensory information of tactile stimuli.

The activation in the postcentral gyrus lies in the primary somatosensory cortex (SI) known as a cortical region for finger representation. Imaging studies indicated single and unique centers of mass for each finger (e.g., Francis, Kelly, Bowtell, Dunseath, Folger, & McGlone, 2000). The activation found in the present data was located on the crown of the postcentral gyrus (BA1). This area has been shown to represent the index finger, which was used by the participants to correct the errors in the present study.

The anatomical location of the activation in the parietal operculum coincides with the position of the secondary somatosensory cortex (SII) (Penfield, & Boldrey, 1937). Activity in SII was reported, while volunteers performed motor tasks showing an enhanced response during active movements than during passive movements (Mima, Sadato, Yazawa, Hanakawa, Fukuyama, Yonekura, & Shibasaki, 1999). This motor-related modulation of SII activity suggests mechanisms for enhancing sensory information from a limb as a guide to behavior involving that limb. During successive, targeted finger movements enhanced sensory messages processed in SII are available to direct and control integrated sequential touching (Binkofski, Buccino, Posse, Seitz, Rizzolatti, & Freund, 1999). This area therefore appears to be qualified in the preparation and the initiation of the corrective response subsequent to the erroneous button press. Furthermore, Burton (2002) suggested that SII provides a conduit for information from cutaneous receptors to the motor cortex. Besides central error processing, this proprioceptive feedback mediated by SII can be used to enhance the error signal to initiate the corrective response.

The activation in the supramarginal gyrus represents the third cortical region of the somatosensory network and is best noted when participants receive discrete vibrotactile stimulation to a single fingertip (Burton, 2002). Considering the lack

of visual motor response feedback in the scanner, vibrotactile information can be used to confirm a full button press (i.e., "click-feeling").

6.5 Conclusion

The aim of Experiment 2 was to examine the neural correlates of error correction. The present data demonstrated error-related activations in the right RCZ, the pre-SMA bilaterally, and the left anterior inferior insula. Error correction activated the right RCZ, the left pre-SMA, the right SMA proper and brain regions in the parietal cortex. The findings suggest a common neuroanatomical substrate of error detection and error correction comprising the RCZ and the pre-SMA. The increased activation in the anterior inferior insula on erroneous responses could be related to cardiac changes due to response errors. Activations in the parietal cortex associated with error correction represent an interconnected cortical network, which processes somatosensory information of tactile stimuli.

Chapter 7

General discussion and future perspectives

Successful behavior in daily-life activities as well as in laboratory tasks requires that humans monitor their performance and detect and correct their errors. There is growing knowledge about the electrophysiological and hemodynamic correlates of error detection and response conflict. Yet, neural mechanisms underlying error correction are still hardly understood. The aim of the present work is a comprehensive multi-methodological investigation of the temporospatial characteristics of error correction. For this purpose, two experiments were conducted: Experiment 1A examines the time course of error correction by means of behavioral measures as well as ERPs and LRPs. Experiment 1B focuses on cardiovascular changes associated with error correction. Using fMRI, the neural correlates of error correction are investigated in Experiment 2. The results of the two experiments are discussed in detail in the respective chapters 4 to 6.

The main findings can be summarized as follows: first, error correction is associated with a new ERP component, the correction-related negativity (CoRN). Second, motivational error significance is reflected by an increased ERN amplitude and an increased heart rate deceleration. Third, correction speed modulates ERN latency as predicted by the Response Conflict Hypothesis. Fourth, two types of error correction, incidental and intentional error correction, can be dissociated

on the basis of behavioral, ERP and LRP findings. And fifth, the RCZ and the pre-SMA represent a common neuroanatomical substrate of error detection and error correction. The following chapter will provide an integrative discussion of these results including implications and future perspectives.

In the present experiments, participants were randomly divided into two groups: in one group, participants were instructed to correct errors by immediately pressing the correct key after an erroneous response (CI); in the second group, they were unaware that error corrections were recorded (CN). Participants had to perform a modified version of the Eriksen flanker task (Ullsperger, & von Cramon, 2001). Previous findings are replicated demonstrating that participants in the CI group were able to correct errors very efficiently without being given an external signal that indicated a committed error (Higgins, & Angel, 1970; Rabbitt, 1967, 1966a,b). Participants in the CN group also showed immediate error corrections although to a lesser degree.

Psychophysiological research provides inconsistent results about the relationship between error correction and error-related ERP components. While some studies report a modulation of ERN amplitude by error correction (Falkenstein et al., 1996; Gehring et al., 1993), other studies deny such a relationship (Rodriguez-Fornells et al., 2002; Falkenstein et al., 1994). Furthermore, the Pe has been associated with post-error processing, i.e., adaptation of response strategy after perceived errors (Hajcak et al., 2003; Nieuwenhuis et al., 2001; Leuthold, & Sommer, 1999). Experiment 1A reveals a new ERP component exclusively occurring on corrected error trials termed *correction-related negativity (CoRN)*. In spite of the fact that this deflection has also been visible in previous experiments revealing high correction rates (Dikman, & Allen, 2000; Falkenstein et al., 1996, 1994), it has not been reported by the authors. Studies by Falkenstein and colleagues (1996, 1994) show a CoRN after auditory and visual stimuli indicating that the CoRN is not affected by stimulus modality. Results of Experiment 1A demonstrate that the CoRN is time-locked rather to the corrective than to the erroneous response, whereas the ERN is clearly temporally dependent on the initial error. Thus, the CoRN is more likely to be associated with error correction than the ERN.

The CoRN is characterized by a negative deflection, which peaks between 200 to 240 ms after the onset of the erroneous response. Both, the ERN and the CoRN, exhibit a fronto-central scalp distribution. The topography of the CoRN, however, is slightly broader than the scalp distribution of the ERN covering also premotor cortices. This is supported by the fMRI data of Experiment 2, which reveal a larger activation for corrected than for uncorrected errors in motor-related brain areas comprising the pre-SMA and the SMA proper. One can infer that the CoRN is associated with continued stimulus-response mapping based on ongoing stimulus processing and/or an enhancement of the evolving corrective response tendency.

Based solely on the present findings, it is too early to come up with further explanations about the precise functional role of the CoRN. Continuing research is needed to specify its functional significance in the correction process. A possible modulating factor of CoRN latency could be correction difficulty due to increased difficulties on the stimulus level, e.g., stimulus detectibility, or on the response level, e.g., complexity of response key order. Decreasing stimulus detectibility should lead to a delayed establishment of the second correct response tendency, which results in a delayed error correction reflected in a later peak of the CoRN. On the response level, raised complexity of the response key order requires enhanced response recoding and the establishment of a new response tendency. As a consequence of this time-consuming process, a later peak of the CoRN can be predicted for a highly complex response key order relative to a less complex one. The CoRN amplitude could be modulated by correction significance, e.g., financial penalties for incorrect or non-committed error corrections. Based on the present results of Experiment 1A, CoRN amplitude should increase for highly significant corrections compared to less significant corrections reflecting a higher investment in response monitoring in conditions of high motivational relevance (cf., Pailing, & Segalowitz, 2004).

The behavioral results of Experiment 1A demonstrate that participants who were unaware that error corrections were recorded (CN group) responded with more caution. It seems they attach more significance to their errors, which in

turn leads to a change in response strategy. Consistent with previous findings (e.g., Ullsperger, & Szymanowski, 2004), the increase in ERN amplitude in the CN group is suggested to be caused by a higher *motivational error significance*. This account is strengthened by the HR data of Experiment 1B showing a larger cardiac deceleration on error trials for the CN group than for the CI group. Crone and colleagues (2003) propose a relationship between the strength of HR slowing and the degree of violation in the predictions of the outcome. Thus, one can reason that the higher motivational error significance in the CN group leads to a stronger violation of the performance-based expectations on error trials causing a larger HR deceleration.

Starting from the current models of performance monitoring, different amplitude and latency patterns of the ERN depending on correction speed are hypothesized. Inconsistent with the derived predictions, the results of Experiment 1A show no significant difference of ERN amplitude between slow and fast error corrections. It remains unclear, why the relationship of ERN amplitude and error correction yields this heterogeneous pattern of results in the literature and in the present study. It can be speculated that the ERN size depends on the amount of post-response conflict in a non-linear manner and shows ceiling effects. Refined models of performance monitoring are needed to explain previous findings of error detection and error correction more precisely. Regarding ERN latency, the present results reveal a significantly later peak of the ERN for slow relative to fast corrections. This finding is consistent with the predictions of the Response Conflict Hypothesis, which proposes a delayed second response tendency on slowly corrected errors leading to a delayed maximum of post-response conflict (Yeung et al., in press). The Response Conflict Hypothesis further assumes that the ERN is elicited at the time of maximal post-response conflict. Consequently, slow corrections should elicit a later peak of the ERN than fast corrections as is evidenced by the present data.

Fast corrections in the CI group are similar to incidental corrections in the CN group with respect to behavioral, ERP and LRP findings. The behavioral data demonstrate that the longer the error response time the higher the probability to

incidentally correct errors in the CN group. The highest rate of incidental error corrections can be observed in the slowest error response time quartile. A similar pattern is found for fast corrections in the CI group, which fall mostly into the slowest error response time quartile. Moreover, the majority of incidental corrections in the CN group occur during the fastest correction times (≤ 100 ms) and are similar in speed to fast corrections in the CI group. Results of the ERP and LRP analyses also reveal a comparable time course of the two conditions. These findings suggest a similar underlying mechanism for incidental corrections in the CN group and fast corrections in the CI group independent of the intention to correct errors. The gain in error corrections observed in the CI group is mostly due to an increase in slow error corrections. An additional intentional process can be assumed, which fosters delayed corrective responses. Slow corrections in the CI group differ from fast corrections in the CI group and incidental corrections in the CN group with respect to their corrective behavior, correction speed and time course implying a separate underlying mechanism. Based on the present results, two types of error correction are hypothesized: *incidental error correction* and *intentional error correction*. In accordance with Rabbitt (2002), it is assumed that incidental corrections are delayed correct responses arising from ongoing stimulus processing and resulting in a second correct response tendency, which initiates the corrective response. Thus, incidental correction does not necessarily require error detection. In contrast, intentional corrections seem to be based on a delayed correct response tendency, which leads to a later corrective response. The present data, however, do not allow to assess whether the intention to correct errors yields a change in the response mode or a phasic implementation of intentional corrections after an error has been detected. The notion that error detection is not necessary for incidental correction bears one important implication for clinical studies of error processing. Incidental error correction rate has been used as an additional measure of error detection abilities in patient groups (e.g., Gehring, & Knight, 2000). To assess error detection, it seems to be more appropriate to investigate

intentional error corrections by instructing patients prior to the experiment or by introducing an error-signaling response (cf., Rabbitt, 2002).

This argumentation leads to different types of error correction based on behavioral results as well as ERP and LRP findings. A more straightforward manner to investigate incidental and intentional error correction could be offered by an experimental design, which separates the response keys applied in the task from the correction keys. This way, intentional correction should be signaled by pressing the correction key, whereas incidental correction should occur on the response keys applied in the task, i.e., the response which should have been made. The measurement of response force could provide an alternative approach. Weak response force on the correction key should reflect incidental corrections, whereas a strong response force on the correction key should mirror intentional corrections.

The fMRI data of Experiment 2 provide further evidence for the important role of the frontomedian wall in error-related processes. In line with previous findings, the RCZ and the pre-SMA are engaged in error detection (e.g., Ullsperger, & von Cramon, 2001). The present study cannot shed more light on the question whether the RCZ is involved in post-response conflict (e.g., Carter et al., 1998) or is part of a dissociation, within which error detection is implemented in the RCZ and post-response conflict in the pre-SMA (e.g., Ullsperger, & von Cramon, 2001).

Errors additionally activate the anterior inferior insula, a cortical region highly interconnected with brain structures involved in the regulation of the cardiovascular system (e.g., Verberne, & Owens, 1998). Experiments in animals and humans reveal evidence that the inferior insula is directly engaged in HR regulation (e.g., Oppenheimer et al., 1992). Several studies also demonstrate an involvement of the ACC in HR modulation. Stimulation of the dorsal ACC is accompanied by an increased HR deceleration, which is attenuated when this region is lesioned (e.g., Critchley et al., 2003). Taking the fMRI data into account, the anterior inferior insula seems to be centrally involved in cardiovascular changes caused by errors. Further, the error-related activation in the RCZ is believed to not be solely attributed to cognitive but also to cardiovascular changes due to errors. The HR

results of Experiment 1B showing a greater HR deceleration for errors compared to correct responses support this hypothesis.

Concerning the neural correlates of error correction, the present fMRI findings reveal evidence that similar brain regions engaged in error detection are also involved in the implementation of immediate error correction. This suggests a common neuroanatomical substrate of error detection and error correction comprising the RCZ and the pre-SMA. Taking the fronto-central scalp distribution of the CoRN into account, the RCZ and the pre-SMA can be considered as potential generators of the CoRN.

References

- Aguirre, G., Zarahn, E., & D'Esposito, M. (1998). The variability of human, BOLD hemodynamic responses. *NeuroImage*, *8*(4), 360–9.
- Amunts, K., Malikovic, A., Mohlberg, H., Schormann, T., & Zilles, K. (2000). Brodmann's areas 17 and 18 brought into stereotaxic space—where and how variable? *NeuroImage*, *11*(1), 66–84.
- Amunts, K., & Zilles, K. (2001). Advances in cytoarchitectonic mapping of the human cerebral cortex. *Neuroimaging Clinics North America*, *11*(2), 151–69, vii.
- Andreassi, J. (1995). *Psychophysiology*, Chapter 11, (pp. 218–257). Hillsdale: Erlbaum.
- Angel, R. (1976). Efference copy in the control of movement. *Neurology*, *26*(12), 1164–8.
- Angel, R., & Higgins, J. (1969). Correction of false moves in pursuit tracking. *Journal of Experimental Psychology*, *82*(1), 185–187.
- Antoni, H. (1995). Erregungsphysiologie des Herzens. In R. Schmidt, & G. Thews (Eds.), *Physiologie des Menschen* Chapter 23, (pp. 472–498). Berlin: Springer.
- Badgaiyan, R., & Posner, M. (1998). Mapping the cingulate cortex in response selection and monitoring. *NeuroImage*, *7*(3), 255–60.

- Bandettini, P., & Moonen, C. (1999). *Functional MRI*. Berlin: Springer.
- Barch, D., Braver, T., Sabb, F., & Noll, D. (2000). Anterior cingulate and the monitoring of response conflict: evidence from an fMRI study of overt verb generation. *Journal of Cognitive Neuroscience*, *12*(2), 298–309.
- Bates, J., & Goldman-Rakic, P. (1993). Prefrontal connections of medial motor areas in the rhesus monkey. *Journal of Comparative Neurology*, *336*(2), 211–28.
- Bechara, A., Tranel, D., & Damasio, A. (2002). The somatic marker hypothesis and decision-making. In F. Boller, & J. Grafman (Eds.), *Handbook of Neuropsychology*, Band 7 (pp. 117–143). Amsterdam: Elsevier.
- Bernstein, P., Scheffers, M., & Coles, M. (1995). "Where did I go wrong?" A psychophysiological analysis of error detection. *Journal of Experimental Psychology: Human Perception & Performance*, *21*(6), 1312–22.
- Binkofski, F., Buccino, G., Posse, S., Seitz, R., Rizzolatti, G., & Freund, H. (1999). A fronto-parietal circuit for object manipulation in man: evidence from an fMRI-study. *European Journal of Neuroscience*, *11*(9), 3276–86.
- Bortz, J., & Döring, N. (1995). *Forschungsmethoden und Evaluation*, Chapter 5, (pp. 133–172). Heidelberg: Springer.
- Botvinick, M., Braver, T., Barch, D., Carter, C., & Cohen, J. (2001). Conflict monitoring and cognitive control. *Psychological Review*, *108*(3), 624–52.
- Botvinick, M., Nystrom, L., Fissell, K., Carter, C., & Cohen, J. (1999). Conflict monitoring versus selection-for-action in anterior cingulate cortex. *Nature*, *402*(6758), 179–81.
- Brazdil, M., Roman, R., Falkenstein, M., Daniel, P., Jurak, P., & Rektor, I. (2002). Error processing—evidence from intracerebral ERP recordings. *Experimental Brain Research*, *146*(4), 460–6.

- Brown, M., & Semelka, R. (1999). *MRI, Basic Principles and Application*. New York: Wiley-Liss.
- Brownley, K., Hurwitz, B., & Schneiderman, N. (2000). Cardiovascular psychophysiology. In J.T. Cacioppo, L.G. Tassinary, & G.G. Berntson (Eds.), *Handbook of Psychophysiology* Chapter 9, (pp. 224–264). Cambridge: University Press.
- Burns, S., & Wyss, J. (1985). The involvement of the anterior cingulate cortex in blood pressure control. *Brain Research*, *340*(1), 71–7.
- Burton, H. (2002). Cerebral cortical regions devoted to the somatosensory system: Results from brain imaging studies in humans. In R. J. Nelson (Ed.), *The Somatosensory System* Chapter 2, (pp. 27–72). CRC Press.
- Bush, G., Luu, P., & Posner, M. (2000). Cognitive and emotional influences in anterior cingulate cortex. *Trends in Cognitive Science*, *4*(6), 215–222.
- Bush, G., Vogt, B., Holmes, J., Dale, A., Greve, D., Jenike, M., & Rosen, B. (2002). Dorsal anterior cingulate cortex: a role in reward-based decision making. *Proceedings of the National Academy of Sciences of the United States of America*, *99*(1), 523–8.
- Butcher, K., & Cechetto, D. (1995). Autonomic responses of the insular cortex in hypertensive and normotensive rats. *American Journal of Physiology*, *268*, r214–r222.
- Buxton, R. (2002). *Introduction to functional magnetic resonance imaging*. Cambridge: University Press.
- Cabeza, R., & Nyberg, L. (2000). Neural bases of learning and memory: functional neuroimaging evidence. *Current Opinions in Neurology*, *13*(4), 415–21.
- Carter, C., Braver, T., Barch, D., Botvinick, M., Noll, D., & Cohen, J. (1998). Anterior cingulate cortex, error detection, and the online monitoring of performance. *Science*, *280*(5364), 747–9.

- Carter, C., Macdonald, A., Botvinick, M., Ross, L., Stenger, V., Noll, D., & Cohen, J. (2000). Parsing executive processes: strategic vs. evaluative functions of the anterior cingulate cortex. *Proceedings of the National Academy of Sciences of the United States of America*, *97*(4), 1944–8.
- Carter, C., Macdonald, A., Ross, L., & Stenger, V. (2001). Anterior cingulate cortex activity and impaired self-monitoring of performance in patients with schizophrenia: an event-related fMRI study. *American Journal of Psychiatry*, *158*, 1423–1428.
- Christ, S., Falkenstein, M., Heuer, H., & Hohnsbein, J. (2000). Different error types and error processing in spatial stimulus-response-compatibility tasks: behavioural and electrophysiological data. *Biological Psychology*, *51*(2-3), 129–50.
- Coles, M. (1989). Modern mind-brain reading: psychophysiology, physiology, and cognition. *Psychophysiology*, *26*(3), 251–69.
- Coles, M., Gratton, G., & Fabiani, M. (1990). Event-related potentials. In J.T. Cacioppo, & M. Fabiani (Eds.), *Principles of psychophysiology: Physical, social, and inferential elements* Chapter 3, (pp. 413–455). New York: Cambridge University Press.
- Coles, M., Gratton, G., Kramer, A., & Miller, G. (1986). Principles of signal acquisition and analysis. In M.G.H. Coles, E. Donchin, & S. Porges (Eds.), *Psychophysiology: Systems, Processes, and Applications* (pp. 26–44). New York: Guilford.
- Coles, M., Scheffers, M., & Holroyd, C. (2001). Why is there an ERN/Ne on correct trials? Response representations, stimulus-related components, and the theory of error-processing. *Biological Psychology*, *56*(3), 173–89.
- Cooke, J., & Diggle, V. (1984). Rapid error correction during human arm movements: Evidence for central monitoring. *Journal of Motor Behavior*, *16*(4), 348–363.

- Crippa, G., Peres-Polon, V., Kuboyama, R., & Correa, F. (1999). Cardiovascular response to the injection of acetylcholine into the anterior cingulate region of the medial prefrontal cortex of unanesthetized rats. *Cerebral Cortex*, *9*(4), 362–5.
- Critchley, H., Corfield, D., Chandler, M., Mathias, C., & Dolan, R. (2000). Cerebral correlates of autonomic cardiovascular arousal: a functional neuroimaging investigation in humans. *Journal of Physiology*, *523* (Pt 1), 259–70.
- Critchley, H., Mathias, C., Josephs, O., O’Doherty, J., Zanini, S., Dewar, B., Cipolotti, L., Shallice, T., & Dolan, R. (2003). Human cingulate cortex and autonomic control: converging neuroimaging and clinical evidence. *Brain*, *126* (Pt10), 2139–52.
- Crone, E., van der Veen, F., van der Molen, M., Somsen, R., van Beek, B., & Jennings, J. (2003). Cardiac concomitants of feedback processing. *Biological Psychology*, *64*(1-2), 143–56.
- Dale, A., & Buckner, R. (1997). Selective averaging of rapidly presented individual trials using fMRI. *Human Brain Mapping*, *5*, 329–340.
- De Jong, R., Wierda, M., Mulder, G., & Mulder, L. (1988). Use of partial stimulus information in response processing. *Journal of Experimental Psychology: Human Perception & Performance*, *14*, 682–692.
- Debatin, J., & McKinnon, G. (1998). *Ultrafast MRI*. Berlin: Springer.
- Dehaene, S., Posner, M., & Tucker, D. (1994). Localization of a neural system for error detection and compensation. *Psychological Science*, *5*(5), 303–305.
- Delorme, A., & Makeig, S. (2004). EEGLAB: An open source toolbox for analysis of single-trial EEG dynamics including independent component analysis. *Journal of Neuroscience Methods*, *134*, 9–21.
- Desmurget, M., & Grafton, S. (2000). Forward modeling allows feedback control for fast reaching movements. *Trends in Cognitive Sciences*, *4*(11), 423–431.

- Devinsky, O., Morrell, M., & Vogt, B. (1995). Contributions of anterior cingulate cortex to behaviour. *Brain*, *118* (Pt 1), 279–306.
- Dikman, Z., & Allen, J. (2000). Error monitoring during reward and avoidance learning in high- and low-socialized individuals. *Psychophysiology*, *37*(1), 43–54.
- Dum, R., & Strick, P. (1991). The origin of corticospinal projections from the premotor areas in the frontal lobe. *Journal of Neuroscience*, *11*(3), 667–89.
- Dum, R., & Strick, P. (1993). The origin of corticospinal projections from the premotor areas in the frontal lobe. In B.A. Vogt, & M. Gabriel (Eds.), *Neurobiology of Cingulate Cortex and Limbic Thalamus* (pp. 415–441). Birkhäuser: Boston.
- Durston, S., Davidson, M., Thomas, K., Worden, M., Tottenham, N., Martinez, A., Watts, R., Ulug, A., & Casey, B. (2003). Parametric manipulation of conflict and response competition using rapid mixed-trial event-related fMRI. *NeuroImage*, *20*, 2135–2141.
- Van 't Ent, D., & Apkarian, P. (1999). Motoric response inhibition in finger movement and saccadic eye movement: A comparative study. *Clinical Neurophysiology*, *110*, 1058–1072.
- Eriksen, B., & Eriksen, C. (1974). Effects of noise letters upon the identification of a target letter in a nonsearch task. *Perception & Psychophysics*, *16*(1), 143–149.
- Falkenstein, M. (2004). ERP correlates of erroneous performance. In M. Ullsperger, & M. Falkenstein (Eds.), *Errors, Conflicts, and the Brain. Current Opinions on Performance Monitoring* (pp. 5–14). Leipzig: MPI for Human Cognitive and Brain Sciences.
- Falkenstein, M., Hohnsbein, J., & Hoormann, J. (1994). Effects of choice complexity on different subcomponents of the late positive complex of the event-

- related potential. *Electroencephalography and Clinical Neurophysiology*, 92(2), 148–60.
- Falkenstein, M., Hohnsbein, J., & Hoormann, J. (1996). Differential processing of motor errors. In *Recent advances in event-related brain potential research* (pp. 579–585). C. Ogura, Y. Koga, M. Shimokochi.
- Falkenstein, M., Hohnsbein, J., Hoormann, J., & Blanke, L. (1990). Effects of errors in choice reaction tasks on the ERP under focused and divided attention. In C.H.M. Brunia, A.W.K. Gaillard, & A.Kok (Eds.), *Psychophysiological Brain Research* (pp. 192–195). Tilburg University Press.
- Falkenstein, M., Hohnsbein, J., Hoormann, J., & Blanke, L. (1991). Effects of crossmodal divided attention on late ERP components. II. Error processing in choice reaction tasks. *Electroencephalography and Clinical Neurophysiology*, 78(6), 447–55.
- Falkenstein, M., Hoormann, J., Christ, S., & Hohnsbein, J. (2000). ERP components on reaction errors and their functional significance: a tutorial. *Biological Psychology*, 51(2-3), 87–107.
- Fisk, G., & Wyss, J. (1997). Pressor and depressor sites are intermingled in the cingulate cortex of the rat. *Brain Research*, 754(1-2), 204–12.
- Ford, J. (1999). Schizophrenia: the broken P300 and beyond. *Psychophysiology*, 36, 667–682.
- Forman, S., Cohen, J., Fitzgerald, M., Eddy, W., Mintun, M., & Noll, D. (1995). Improved assessment of significant activation in functional magnetic resonance imaging (fMRI): use of a cluster-size threshold. *Magnetic Resonance Medicine*, 33(5), 636–47.
- Frackowiak, R., Friston, K., Frith, C., Dolan, R., & Mazziotta, J. (1997). *Human brain function*. San Diego: Academic Press.

- Francis, S., Kelly, E., Bowtell, R., Dunseath, W., Folger, S., & McGlone, F. (2000). fMRI of the responses to vibratory stimulation of digit tips. *NeuroImage*, *11*, 188–202.
- Friston, K. (1994). Statistical parametric mapping. In R.W. Thatcher, M. Hallett, T. Zeffiro, E.R. John, & M. Huerta (Eds.), *Functional Neuroimaging* (pp. 79–93). San Diego: Academic Press.
- Friston, K., Fletcher, P., Josephs, O., Holmes, A., Rugg, M., & Turner, R. (1998). Event-related fMRI: characterizing differential responses. *NeuroImage*, *7*(1), 30–40.
- Friston, K., Holmes, A., Poline, J., Grasby, P., Williams, S., Frackowiak, R., & Turner, R. (1995a). Analysis of fMRI time-series revisited. *NeuroImage*, *2*(1), 45–53.
- Friston, K., Holmes, A., Worsley, K., Poline, J., Frith, C., & Frackowiak, R. (1995b). Statistical parametric maps in functional imaging: A general linear approach. *Human Brain Mapping*, *2*, 189–210.
- Friston, K., Price, C., Fletcher, P., Moore, C., Frackowiak, R., & Dolan, R. (1996). The trouble with cognitive subtraction. *NeuroImage*, *4*(2), 97–104.
- Friston, K., Zarahn, E., Josephs, O., Henson, R., & Dale, A. (1999). Stochastic designs in event-related fMRI. *NeuroImage*, *10*(5), 607–19.
- Garavan, H., Hester, R., & Fassbender, C. (2004). The impact of individual differences and prefrontal control on action monitoring revealed through fMRI. In M. Ullsperger, & M. Falkenstein (Eds.), *Errors, Conflict, and the Brain. Current Opinions on Performance Monitoring* (pp. 48–55). Leipzig:MPI for Human Cognitive and Brain Sciences.
- Garavan, H., Ross, T., Kaufman, J., & Stein, E. (2003). A midline dissociation between error-processing and response-conflict monitoring. *NeuroImage*, *20*(2), 1132–9.

- Garavan, H., Ross, T., Murphy, K., Roche, R., & Stein, E. (2002). Dissociable executive functions in the dynamic control of behavior: inhibition, error detection, and correction. *NeuroImage*, *17*(4), 1820–9.
- Gehring, W., & Fencsik, D. (2001). Functions of the medial frontal cortex in the processing of conflict and errors. *Journal of Neuroscience*, *21*(23), 9430–7.
- Gehring, W., Goss, B., Coles, M., & Meyer, D. (1993). A neural system for error detection and compensation. *Psychological Science*, *4*(6), 385–390.
- Gehring, W., Himle, J., & Nisenson, L. (2000). Action-monitoring dysfunction in obsessive-compulsive disorder. *Psychological Science*, *11*(1), 1–6.
- Gehring, W., & Knight, R. (2000). Prefrontal-cingulate interactions in action monitoring. *Nature Neuroscience*, *3*(5), 516–20.
- Gehring, W., & Willoughby, A. (2002). The medial frontal cortex and the rapid processing of monetary gains and losses. *Science*, *295*(5563), 2279–82.
- Gevens, A., Smith, M., Le, J., Leong, H., Bennett, J., Martin, N., McEvoy, L., Du, R., & Whitfield, S. (1996). High resolution evoked potential imaging of the cortical dynamics of human working memory. *Electroencephalography and Clinical Neurophysiology*, *98*(4), 327–48.
- Gough, H. (1957). *Manual for the California Psychological Inventory*. Palo Alto, CA: Consulting Psychologists Press.
- Gratton, G., Coles, M., & Donchin, E. (1983). A new method for off-line removal of ocular artifact. *Electroencephalography and Clinical Neurophysiology*, *55*(4), 468–84.
- Gratton, G., Coles, M., & Donchin, E. (1992). Optimizing the use of information: strategic control of activation of responses. *Journal of Experimental Psychology: General*, *121*(4), 480–506.

- Gratton, G., Coles, M., Sirevaag, E., Eriksen, C., & Donchin, E. (1988). Pre- and poststimulus activation of response channels: a psychophysiological analysis. *Journal of Experimental Psychology: Human Perception & Performance*, *14*(3), 331–44.
- Greenhouse, S., & Geisser, S. (1959). On methods in the analysis of profile data. *Psychometrika*, *25*, 95–112.
- Gusnard, D., Akbudak, E., Shulman, G., & Raichle, M. (2001). Medial prefrontal cortex and self-referential mental activity: relation to a default mode of brain function. *Proceedings of the National Academy of Sciences of the United States of America*, *98*(7), 4259–64.
- Hajcak, G., McDonald, N., & Simons, R. (2003). To err is autonomic: Error-related brain potentials, ANS activity, and post-error compensatory behavior. *Psychophysiology*, *40*.
- Hajcak, G., & Simons, R. (2002). Error-related brain activity in obsessive-compulsive undergraduates. *Psychiatry Research*, *110*(1), 63–72.
- Hardy, S., & Holmes, D. (1988). Prefrontal stimulus-produced hypotension in rat. *Experimental Brain Research*, *73*, 249–255.
- Hardy, S., & Mack, S. (1990). Brainstem mediation of prefrontal stimulus-produced hypotension. *Experimental Brain Research*, *79*, 393–399.
- Higgins, J., & Angel, R. (1970). Correction of tracking errors without sensory feedback. *Journal of Experimental Psychology*, *84*(3), 412–6.
- Hillyard, S., & Kutas, M. (1983). Electrophysiology of cognitive processing. *Annual Review of Psychology*, *34*, 33–61.
- Holroyd, C., & Coles, M. (2002). The neural basis of human error processing: reinforcement learning, dopamine, and the error-related negativity. *Psychological Review*, *109*(4), 679–709.

- Holroyd, C., Dien, J., & Coles, M. (1998). Error-related scalp potentials elicited by hand and foot movements: evidence for an output-independent error-processing system in humans. *Neuroscience Letters*, *242*(2), 65–8.
- Holroyd, C., Nieuwenhuis, S., Yeung, N., & Cohen, J. (2003). Errors in reward prediction are reflected in the event-related brain potential. *NeuroReport*, *14*, 2481–2484.
- Holroyd, C., Nieuwenhuis, S., Yeung, N., Nystrom, L., Mars, R., Coles, M., & Cohen, J. (2004). Dorsal anterior cingulate cortex shows fMRI response to internal and external error signals. *Nature Neuroscience*, *7*, 1–2.
- Huberty, C., & Morris, J. (1989). Multivariate analysis versus multiple univariate analyses. *Psychological Bulletin*, *114*, 145–161.
- Husain, M., Parton, A., Hodgson, T., Mort, D., & Rees, G. (2003). Self-control during response conflict by human supplementary eye field. *Nature Neuroscience*, *6*(2), 117–8.
- Ito, S., Stuphorn, V., Brown, J., & Schall, J. (2003). Performance monitoring by the anterior cingulate cortex during saccade countermanding. *Science*, *302*, 120–122.
- Jasper, H. (1958). The ten-twenty electrode system of the International Federation. *Electroencephalography & Clinical Neurophysiology*, *10*, 371–375.
- Josephs, O., Turner, R., & Friston, K. (1997). Event-related fMRI. *Human Brain Mapping*, *5*, 243–248.
- Kaufers, D., & Lewis, D. (1999). Frontal lobe anatomy and cortical connectivity. In B.L. Miller, & J.L. Cummings (Eds.), *The human frontal lobes* Chapter 2, (pp. 27–44). New York: The Guilford Press.
- Kerns, J., Cohen, J., Macdonald, A., Cho, R., Stenger, V., & Carter, C. (2004). Anterior cingulate conflict monitoring and adjustments in control. *Science*, *303*(5660), 1023–6.

- Kiehl, K., Liddle, P., & Hopfinger, J. (2000). Error processing and the rostral anterior cingulate: an event-related fMRI study. *Psychophysiology*, *37*(2), 216–23.
- Koers, G., Mulder, L., & van der Veen, F. (1999). The computation of evoked heart rate and blood pressure. *Journal of Psychophysiology*, *13*(2), 83–91.
- Kopp, B., & Rist, F. (1999). An event-related brain potential substrate of disturbed response monitoring in paranoid schizophrenic patients. *Journal of Abnormal Psychology*, *108*, 337–346.
- Kopp, B., Rist, F., & Mattler, U. (1996). N200 in the flanker task as a neurobehavioral tool for investigating executive control. *Psychophysiology*, *33*(3), 282–94.
- Kornhuber, H., & Deecke, L. (1965). Hirnpotentialänderungen bei Willkürbewegungen und passiven Bewegungen des Menschen: Bereitschaftspotential und reafferente Potentiale. *Pflügers Archiv für die gesamte Physiologie*, *248*, 1–17.
- Kubota, Y., Sato, W., Toichi, M., Murai, T., Okada, T., Hayashi, A., & Sengoku, A. (2001). Frontal midline theta rhythm is correlated with cardiac autonomic activities during the performance of an attention demanding mediation procedure. *Cognitive Brain Research*, *11*, 281–287.
- Kutas, M., & Donchin, E. (1980). Preparation to respond as manifested by movement-related brain potentials. *Brain Research*, *202*(1), 95–115.
- Leuthold, H., & Sommer, W. (1999). ERP correlates of error processing in spatial S-R compatibility tasks. *Clinical Neurophysiology*, *110*(2), 342–57.
- Logothetis, N., Pauls, J., Augath, M., Trinath, T., & Oeltermann, A. (2001). Neurophysiological investigation of the basis of the fMRI signal. *Nature*, *412*(6843), 150–7.
- Lohmann, G. (1998). *Volumetric Image Analysis*. Leipzig: Teubner.

- Lohmann, G., Müller, K., Bosch, V., Mentzel, H., Hessler, S., Chen, L., Zysset, S., & von Cramon, D. (2001). LIPSIA—a new software system for the evaluation of functional magnetic resonance images of the human brain. *Computerized Medical Imaging and Graphics*, *25*(6), 449–57.
- Luu, P., Collins, P., & Tucker, D. (2000a). Mood, personality, and self-monitoring: negative affect and emotionality in relation to frontal lobe mechanisms of error monitoring. *Journal of Experimental Psychology: General*, *129*(1), 43–60.
- Luu, P., Flaisch, T., & Tucker, D. (2000b). Medial frontal cortex in action monitoring. *Journal of Neuroscience*, *20*(1), 464–9.
- Luu, P., & Tucker, D. (2001). Regulating action: alternating activation of mid-line frontal and motor cortical networks. *Clinical Neurophysiology*, *112*(7), 1295–306.
- Macdonald, A., Cohen, J., Stenger, V., & Carter, C. (2000). Dissociating the role of the dorsolateral prefrontal and anterior cingulate cortex in cognitive control. *Science*, *288*(5472), 1835–8.
- Markisz, J., & Whalen, J. (1998). *Principles of MRI*. Stamford: Appleton & Lange.
- Masaki, H., Tanaka, H., Takasawa, N., & Yamazaki, K. (2001). Error-related brain potentials elicited by vocal errors. *NeuroReport*, *12*, 1–5.
- Mathalon, D., Whitfield, S., & Ford, J. (2003). Anatomy of an error: ERP and fMRI. *Biological Psychology*, *64*, 119–141.
- Mesulam, M. (1996). Patterns in behavioral neuroanatomy: association areas, the limbic system, and hemispheric specialization. In M.M. Mesulam (Ed.), *Principles of behavioral neurology* Chapter 1, (pp. 1–70). Philadelphia: F.A. Davis Company.

- Miezin, F., Maccotta, L., Ollinger, J., Petersen, S., & Buckner, R. (2000). Characterizing the hemodynamic response: effects of presentation rate, sampling procedure, and the possibility of ordering brain activity based on relative timing. *NeuroImage*, *11*, 735–59.
- Milham, M., Banich, M., Webb, A., Barad, V., Cohen, N., Wszalek, T., & Kramer, A. (2001). The relative involvement of anterior cingulate and prefrontal cortex in attentional control depends on nature of conflict. *Cognitive Brain Research*, *12*(3), 467–73.
- Miltner, W., Braun, C., & Coles, M. (1997). Event-related brain potentials following incorrect feedback in a time-estimation task: Evidence for a "generic" neural system for error detection. *Journal of Cognitive Neuroscience*, *9*(6), 788–798.
- Mima, T., Sadato, N., Yazawa, S., Hanakawa, T., Fukuyama, H., Yonekura, Y., & Shibasaki, H. (1999). Brain structures related to active and passive finger movements in man. *Brain*, *122*, 1989–1997.
- Morris, R., Pandya, D., & Petrides, M. (1999). Fiber system linking the mid-dorsolateral frontal cortex with the retrosplenial/presubicular region in the rhesus monkey. *The Journal of Comparative Neurology*, *407*, 183–192.
- Mulder, G., & Mulder, L. (1981). Information processing and cardiovascular control. *Psychophysiology*, *18*(4), 392–402.
- Nieuwenhuis, S., Ridderinkhof, K., Blom, J., Band, G., & Kok, A. (2001). Error-related brain potentials are differentially related to awareness of response errors: evidence from an antisaccade task. *Psychophysiology*, *38*, 752–60.
- Nieuwenhuis, S., Ridderinkhof, K., Talsma, D., Coles, M., Holroyd, C., Kok, A., & van der Molen, M. (2002). A computational account of altered error processing in older age: dopamine and the error-related negativity. *Cognitive, Affective, & Behavioral Neuroscience*, *2*(1), 19–36.

- Nieuwenhuis, S., Yeung, N., & Cohen, J. (2004). Stimulus modality, perceptual overlap, and the go/no-go N2. *Psychophysiology*, *41*(1), 157–60.
- Norman, D. (1981). Categorization of action slips. *Psychological Review*, *88*(1), 1–15.
- Oehman, A., Hamm, A., & Hugdahl, K. (2000). Cognition and the autonomic nervous system. In J.T. Cacioppo, L.G. Tassinary, & G.G. Berntson (Eds.), *Handbook of Psychophysiology* Chapter 20, (pp. 533–575). Cambridge: University Press.
- Ogawa, S., & Lee, T. (1990). Magnetic resonance imaging of blood vessels at high fields: in vivo and in vitro measurements and image simulation. *Magnetic Resonance in Medicine*, *16*, 9–18.
- Oken, B., & Chiappa, K. (1986). Statistical issues concerning computerized analysis of brainwave topography. *Annals of Neurology*, *19*(5), 493–7.
- Ongur, D., & Price, J. (2000). The organization of networks within the orbital and medial prefrontal cortex of rats, monkeys and humans. *Cerebral Cortex*, *10*(3), 206–19.
- Oppenheimer, S., & Cechetto, D. (1990). Cardiac chronotropic organization of the rat insular cortex. *Brain Research*, *533*, 66–72.
- Oppenheimer, S., Gelb, A., Girvin, J., & Hachinski, V. (1992). Cardiovascular effects of human insular cortex stimulation. *Neurology*, *42*, 1727–1732.
- Pailing, P., & Segalowitz, S. (2004). The error-related negativity as a state and trait measure: Motivation, personality, and ERPs in response to errors. *Psychophysiology*, *41*(1), 84–95.
- Pailing, P., Segalowitz, S., Dywan, J., & Davies, P. (2002). Error negativity and response control. *Psychophysiology*, *39*(2), 198–206.
- Papanicolaou, A. (1998). *Fundamentals of functional brain imaging*. Lisse: Swets & Zeitlinger.

- Penfield, W., & Boldrey, E. (1937). Somatic motor and sensory representation in the cerebral cortex of man studied by electrical stimulation. *Brain*, *60*, 389–443.
- Perrin, F., Pernier, J., Bertrand, O., & Echallier, J. (1989). Spherical splines for scalp potential and current density mapping. *Electroencephalography and Clinical Neurophysiology*, *72*(2), 184–7.
- Petrides, M., & Pandya, D. (1999). Dorsolateral prefrontal cortex: comparative cytoarchitectonic analysis in the human and the macaque brain and corticocortical connection patterns. *European Journal of Neuroscience*, *11*(3), 1011–36.
- Pfeifer, E. (1993). IPCM-Iterative PCA correction method. A new method for the correction of ocular artifacts in the ERP-data. *Psychophysiology*, *30*, 51.
- Picard, N., & Strick, P. (1996). Motor areas of the medial wall: a review of their location and functional activation. *Cerebral Cortex*, *6*(3), 342–53.
- Picard, N., & Strick, P. (2001). Imaging the premotor areas. *Current Opinion Neurobiology*, *11*(6), 663–72.
- Pivik, R., Broughton, R., Coppola, R., Davidson, R., Fox, N., & Nuwer, M. (1993). Guidelines for the recording and quantitative analysis of electroencephalographic activity in research contexts. *Psychophysiology*, *30*, 547–558.
- Pool, I. P. I. (2001). *A Scientific Collaboratory for the Development of Advanced Measures of Personality Traits and Other Individual Differences*. <http://ipip.ori.org/ipip/>.
- Pool, J., & Ransohoff, J. (1949). Autonomic effects on stimulating the rostral portion of the cingulate gyri in man. *Journal of Neurophysiology*, *12*, 385–392.

- Powell, D., Buchanan, S., & Gibbs, C. (1990). Role of the prefrontal-thalamic axis in classical conditioning. In H.B.M. Uylings, C.G. van Eden, J.P.C. de Bruin, & M.G.P. Feenstra (Eds.), *The Prefrontal Cortex: Its Structure, Function and Pathology*, Band 85 (pp. 433–466). Amsterdam: Elsevier.
- Rabbitt, P. (1966a). Error correction time without external error signals. *Nature*, *212*(60), 438.
- Rabbitt, P. (1966b). Errors and error correction in choice-response tasks. *Journal of Experimental Psychology*, *71*(2), 264–72.
- Rabbitt, P. (1967). Time to detect errors as a function of factors affecting choice-response time. *Acta Psychologica*, *27*, 131–42.
- Rabbitt, P. (1968). Three kinds of error-signalling responses in a serial choice task. *Quarterly Journal of Experimental Psychology*, *20*(2), 179–88.
- Rabbitt, P. (2002). Consciousness is slower than you think. *Quarterly Journal of Experimental Psychology A*, *55*(4), 1081–92.
- Rabbitt, P., Cumming, G., & Vyas, S. (1978). Some errors of perceptual analysis in visual search can be detected and corrected. *Quarterly Journal of Experimental Psychology*, *30*(2), 319–32.
- Rabbitt, P., & Rodgers, B. (1977). What does a man do after he makes an error? An analysis of response programming. *Quarterly Journal of Experimental Psychology*, *29*, 727–743.
- Rabbitt, P., & Vyas, S. (1970). An elementary preliminary taxonomy for some errors in laboratory choice RT tasks. *Acta Psychologica*, *33*, 56–76.
- Rabbitt, P., & Vyas, S. (1981). Processing a display even after you make a response to it. How perceptual errors can be corrected. *Quarterly Journal of Experimental Psychology*, *33A*, 223–239.
- Reason, J. (1990). *Human error*, Chapter 1, (pp. 1–18). Cambridge: University Press.

- Reason, J. (2000). Human error: models and management. *British Medical Journal*, *320*, 768–770.
- Ridderinkhof, K. (2002). Micro- and macro-adjustments of task set: activation and suppression in conflict tasks. *Psychological Research*, *66*(4), 312–23.
- Rodriguez-Fornells, A., Kurzbuch, A., & Münte, T. (2002). Time course of error detection and correction in humans: neurophysiological evidence. *Journal of Neuroscience*, *22*(22), 9990–6.
- Rodriguez-Fornells, A., & Münte, T. (2004). Is the error-related negativity driven by simultaneously active motor programs? In M. Ullsperger, & M. Falkenstein (Eds.), *Errors, Conflict, and the Brain. Current Opinions on Performance Monitoring*. (pp. 159–163). Leipzig: MPI for Human Cognitive and Brain Sciences.
- Roland, P. (1993). *Brain activation*. New York: Wiley-Liss.
- Rubia, K., Smith, A., Brammer, M., & Taylor, E. (2003). Right inferior prefrontal cortex mediates response inhibition while mesial prefrontal cortex is responsible for error detection. *NeuroImage*, *20*(1), 351–358.
- Rugg, M., & Coles, M. (1995). The ERP and cognitive psychology: conceptual issues. In M.D. Rugg, & M.G.H. Coles (Eds.), *Electrophysiology of Mind* Chapter 2, (pp. 27–39). Oxford: Oxford University Press.
- Scheffers, M., & Coles, M. (2000). Performance monitoring in a confusing world: error-related brain activity, judgments of response accuracy, and types of errors. *Journal of Experimental Psychology: Human Perception & Performance*, *26*(1), 141–51.
- Scheffers, M., Coles, M., Bernstein, P., Gehring, W., & Donchin, E. (1996). Event-related brain potentials and error-related processing: an analysis of incorrect responses to go and no-go stimuli. *Psychophysiology*, *33*(1), 42–53.

- van Schie, H., Rogier, R., Coles, M., & Bekkering, H. (2004). Modulation of activity in the medial frontal and motor cortices during error observation. *Nature Neuroscience*, 7, 549–554.
- Shibasaki, H., Barrett, G., Halliday, E., & Halliday, A. (1980). Components of the movement-related cortical potential and their scalp topography. *Electroencephalography and Clinical Neurophysiology*, 49(3-4), 213–26.
- Shima, K., & Tanji, J. (1998). Role for cingulate motor area cells in voluntary movement selection based on reward. *Science*, 282(5392), 1335–8.
- Smith, R., & Lange, R. (1997). *Understanding Magnetic Resonance Imaging*. Boca Raton: CRC Press.
- Somsen, R., van der Molen, M., Jennings, J., & van Beek, B. (2000). Wisconsin Card Sorting in adolescents: analysis of performance, response times and heart rate. *Acta Psychologica*, 104(2), 227–57.
- Stark, D., & Bradley, W. (1992). *Magnetic Resonance Imaging*. St. Louis: Mosby-Year Book.
- Stemmer, B., Segalowitz, S., Witzke, W., & Schönle, P. (2004). Error detection in patients with lesions to the medial prefrontal cortex: an ERP study. *Neuropsychologia*, 42(1), 118–30.
- Swick, D., & Turken, A. (2002). Dissociation between conflict detection and error monitoring in the human anterior cingulate cortex. *Proceedings of the National Academy of Sciences of the United States of America*, 99(25), 16354–9.
- Talairach, P., & Tournoux, J. (1988). *A Stereotactic Coplanar Atlas of the Human Brain*. Stuttgart: Thieme.
- Tanji, J. (1994). The supplementary motor area in the cerebral cortex. *Neuroscience Research*, 19(3), 251–68.

- Tellegen, A., & Waller, N. (1996). Exploring personality through test construction: Development of the multidimensional personality questionnaire. In S.R. Briggs, & J.M. Cheek (Eds.), *Personality measures: Development and evaluation* (pp. 133–161). Greenwich, CT: JAI Press.
- TerHorst, G., Hautvast, R., DeJongste, M., & Korf, J. (1996). Neuroanatomy of cardiac activity-regulating circuitry: a transneuronal retrograde viral labelling study in rat. *European Journal of Neuroscience*, *8*, 2029–2041.
- Ullsperger, M., & von Cramon, D. (2001). Subprocesses of performance monitoring: a dissociation of error processing and response competition revealed by event-related fMRI and ERPs. *NeuroImage*, *14*(6), 1387–401.
- Ullsperger, M., & von Cramon, D. (2003). Error monitoring using external feedback: specific roles of the habenular complex, the reward system, and the cingulate motor area revealed by functional magnetic resonance imaging. *Journal of Neuroscience*, *23*(10), 4308–14.
- Ullsperger, M., & von Cramon, D. (in press). Neuroimaging of performance monitoring: error detection and beyond. *Cortex*.
- Ullsperger, M., & Szymanowski, F. (2004). ERP correlates of error relevance. In M. Ullsperger, & M. Falkenstein (Eds.), *Errors, Conflict, and the Brain. Current Opinions on Performance Monitoring*. (pp. 171–177). Leipzig: MPI for Human Cognitive and Brain Sciences.
- Vaughan, H., Costa, L., & Ritter, W. (1968). Topography of the human motor potential. *Electroencephalography and Clinical Neurophysiology*, *25*, 1–10.
- van Veen, V., & Carter, C. (2002). The timing of action-monitoring processes in the anterior cingulate cortex. *Journal of Cognitive Neuroscience*, *14*(4), 593–602.
- van Veen, V., Cohen, J., Botvinick, M., Stenger, V., & Carter, C. (2001). Anterior cingulate cortex, conflict monitoring, and levels of processing. *NeuroImage*, *14*(6), 1302–8.

- van der Veen, F. (1997). Heart-Brain Communication. *Doktoral Thesis, Rijks University Groningen*.
- van der Veen, F., van der Molen, M., Crone, E., & Jennings, J. (2000). Immediate effects of negative and positive feedback on HR and subsequent performance. *International Journal of Psychophysiology, 35*, 75.
- van der Veen, F., van der Molen, M., Crone, E., & Jennings, J. (2004). Phasic heart rate responses to performance feedback in a time production task: effects of information versus valence. *Biological Psychology, 65*, 147–161.
- Velden, M. (1999). New aspects when depicting heart rate and blood pressure over time: Comment on Koers et al.. *Journal of Psychophysiology, 13*(2), 92–94.
- Verberne, A., Lewis, S., Worland, P., Beart, P., Jarrott, B., Christie, M., & Louis, W. (1987). Medial prefrontal cortical lesions modulate baroreflex sensitivity in the rat. *Brain Research, 426*(2), 243–9.
- Verberne, A., & Owens, N. (1998). Cortical modulation of the cardiovascular system. *Progress in Neurobiology, 54*(2), 149–68.
- Vidal, F., Hasbroucq, T., Grapperon, J., & Bonnet, M. (2000). Is the 'error negativity' specific to errors? *Biological Psychology, 51*(2-3), 109–28.
- Vogt, B., Nimchinsky, E., Vogt, L., & Hof, P. (1995). Human cingulate cortex: surface features, flat maps, and cytoarchitecture. *Journal of Comparative Neurology, 359*(3), 490–506.
- Volz, K., Schubotz, R., & von Cramon, D. (2003). Predicting events of varying probability: uncertainty investigated by fMRI. *NeuroImage, 19*, 271–280.
- Vorobiev, V., Govoni, P., Rizzolatti, G., Matelli, M., & Luppino, G. (1998). Parcellation of human mesial area 6: Cytoarchitectonic evidence for three separate areas. *European Journal of Neuroscience, 10*, 2199–2203.

- Watson, D., Clark, L., & Tellegen, A. (1988). Development and validation of brief measures of positive and negative affect: the PANAS scales. *Journal of Personality and Social Psychology*, *54*, 1063–1070.
- Williamson, J., Nobrega, A., McColl, R., Mathews, D., Winchester, P., Friberg, L., & Mitchell, J. (1997). Activation of the insular cortex during dynamic exercise in humans. *Journal of Physiology*, *503* (Pt 2), 277–83.
- Wood, C. (1987). Generators of event-related potentials. In A.M. Halliday, S.R. Butler, & R. Paul (Eds.), *A Textbook of Clinical Neurophysiology* (pp. 535–567). New York: Wiley.
- Worsley, K., & Friston, K. (1995). Analysis of fMRI time-series revisited—again. *NeuroImage*, *2*(3), 173–81.
- Yeung, N., Botvinick, M., & Cohen, J. (in press). The neural basis of error detection: conflict monitoring and the error-related negativity. *Psychological Review*.

List of Figures

2.1	Information Processing Model	7
2.2	The Error-related Negativity (ERN)	9
2.3	The Mismatch-Model	13
2.4	The Holroyd Model	15
2.5	The Response Conflict Model	18
2.6	Brodmann areas of the frontomedian wall	25
2.7	Subdivision of the anterior cingulate cortex	27
2.8	Metaanalysis of frontomedian activations related to error processing	31
3.1	International EEG 10-20 system for electrode placement	38
3.2	Generation of event-related potentials	40
3.3	Derivation of the lateralized readiness potential	43
3.4	Anatomical basis of the cardiac cycle	46
3.5	Connections of the insular cortex and the anterior cingulate cortex to structures engaged in the regulation of the cardiovascular system	50
3.6	The chain of events leading to the BOLD signal	57
3.7	Left, medium, and top view of the anatomical reference image . .	63
4.1	Experimental task	69
4.2	Recorded electrode sites	71
4.3	Incompatibility effects	75
4.4	Behavioral group effects	76
4.5	Prolonged effects of errors	77

4.6	Quartile analysis of error response times	78
4.7	Distribution of error corrections across correction times	79
4.8	Response-locked ERPs for incompatible correct and incompatible erroneous trials	84
4.9	Spatial distribution of the ERN, the CoRN, and the Pe	85
4.10	Response-locked ERPs for uncorrected and incidentally corrected error trials in the CN group	86
4.11	Response-locked ERPs for uncorrected and incidentally corrected error trials in the CN group and for slow and fast correction trials in the CI group	88
4.12	Response-locked ERPs for uncorrected and incidentally corrected error trials in the CN group and for slow and fast error correction trials in the CI group at FCz	90
4.13	Response-locked ERP-image plot and ERPs for correct-response locked and corrective-response locked ERP averages for incompatible correct trials and incompatible corrected error trials	91
4.14	Response-locked LRPs for uncorrected and corrected error trials in the CN group and for slow and fast error correction trials in the CI group	93
5.1	Response-locked HR for incompatible correct and incompatible erroneous trials	104
6.1	Cortical activation of the contrast incompatible erroneous trials vs. incompatible correct trials	114
6.2	Cortical activation of the contrast incompatible corrected error trials vs. incompatible uncorrected error trials	116

List of Tables

3.1	Most prominent frequency ranges of oscillatory activity	37
4.1	Predictions for ERN latency and amplitude for slow and fast error corrections based on current models of performance monitoring	66
4.2	Mean proportion and reaction times of correct, erroneous, and late responses for each stimulus type	74
4.3	Predictions for ERN latency and amplitudes for uncorrected errors, incidental, fast, and slow corrections based on current models of performance monitoring	83
6.1	Mean proportion and reaction times of correct, erroneous, and late responses for each stimulus type	112
6.2	Anatomical specification, and Talairach coordinates of voxels co-varying significantly with Error Detection	113
6.3	Anatomical specification, and Talairach coordinates of voxels co-varying significantly with Error Correction	115

Abbreviations

2D	two dimensional
3D	three dimensional
AC	Anterior Commissure
ACC	Anterior Cingulate Cortex
AD	Analog-Digital
adFMC	anterodorsal Frontomedian Cortex
ANOVA	Analysis Of Variance
ANS	Autonomic Nervous System
A-V	Atrio-Ventricular
BA	Brodmann Area
BOLD	Blood-Oxygen-Level-Dependent
bpm	beats per minute
CI	Correction Instructed
cm	centimeter
CMA	Cingulate Motor Area
CN	Correction Non-Instructed
CoRN	Correction-Related Negativity
CPI	Gough's Socialization Scale
CRN	Correct-Related Negativity
DC	Direct Current
ECG	Electrocardiogram
EEG	Electroencephalogram
EMG	Electromyogram
EOG	Electrooculogram
EOGH	horizontal Electrooculogram
EOGV	vertical Electrooculogram

EPI	Echo-Planar-Imaging
EPSP	Excitatory Post-Synaptic Potential
ERN	Error-Related Negativity
ERP	Event-Related Potential
FDI	Free Induction Decay
FMC	Frontomedian Cortex
fMRI	functional Magnetic Resonance Imaging
FT	Fourier Transform
FWHM	Full Width at Half Maximum
GLM	General Linear Model
HP	Heart Period
HR	Heart Rate
Hz	Hertz
IC	Insular Cortex
IPIP	International Personality Item Pool
IPSP	Inhibitory Post-Synaptic Potential
ISI	Inter-Stimulus-Interval
kΩ	kiloohm
LPFC	Lateral Prefrontal Cortex
LRP	Lateralized Readiness Potential
m	meter
M	Mean
mm	millimeter
mm³	cubic millimeter
MDEFT	Modified Driven Equilibrium Fourier Transform
MFN	Medial Frontal Negativity
MPQ	Multidimensional Personality Questionnaire
MRI	Magnetic Resonance Imaging
ms	millisecond
NA	Negative Affect

Ne	Error Negativity
NEM	Negative Emotionality
NMR	Nuclear Magnetic Resonance
OFC	Orbitofrontal Cortex
OCD	Obsessive-Compulsive Disorder
PA	Positive Affect
PANAS	Positive Affect Negative Affect Scale
PC	Posterior Commissure
pdFMC	posterodorsal Frontomedian Cortex
Pe	Error Positivity
PES	Post-Error Slowing
PET	Positron Emission Tomography
pFMC	posterior Frontomedian Cortex
PNS	Parasympathic Nervous System
pre-SMA	pre-Supplementary Motor Area
rCBF	regional Cerebral Blood Flow
rCBV	regional Cerebral Blood Volume
rCMRO₂	regional Cerebral Metabolic Rate of Oxygen
RCZ	Rostral Cingulate Zone
RCZa	anterior Rostral Cingulate Zone
RCZp	posterior Rostral Cingulate Zone
RF	Radio-Frequency
ROI	Region Of Interest
RP	Readiness Potential
s	second
SI	primary Somatosensory Cortex
SII	secondary Somatosensory Cortex
S-A	Sino-Atrial
SEM	Standard Error of Mean
SMA	Supplementary Motor Area

SMAc	caudal Supplementary Motor Area
SMAr	rostral Supplementary Motor Area
SNR	Signal-to-Noise Ratio
SNS	Sympathetic Nervous System
SPM	Statistical Parametric Map
T	Tesla
TE	Time to Echo
TR	Time to Repeat
VCA	perpendicular line through the AC
vFMC	ventral Frontomedian Cortex
μV	microvolt

Curriculum Vitae

Name	Katja Fiehler
Date of birth	14.11.1977
Place of birth	Dresden
2002-2004	Doctoral candidate at the Max Planck Institute for Human Cognitive and Brain Sciences, Leipzig, Department of Neurology (Prof. Dr. D. Yves von Cramon)
1996-2001	Course of studies in Psychology at the Technical University Dresden
2001	Diploma in Psychology at the Technical University Dresden
2001	Diploma thesis at the Max Planck Institut for Human Cognitive and Brain Sciences, Leipzig, Department of Neuropsychology (Prof. Dr. Angela D. Friederici)
1998	Intermediate diploma in Psychology
1992-1996	Städtisches Gymnasium Freital-Zauckerode
1984-1992	Glückauf-Oberschule, Freital

Selbstständigkeitserklärung

Hiermit erkläre ich, dass die vorliegende Arbeit ohne unzulässige Hilfe und ohne Benutzung anderer als der angegebenen Hilfsmittel angefertigt wurde und dass die aus fremden Quellen direkt oder indirekt übernommenen Gedanken in der Arbeit als solche kenntlich gemacht worden sind.

Katja Fiehler

Leipzig, den 03.08.2004

Bibliographic details of the dissertation

Fiehler, Katja

TEMPOROSPATIAL CHARACTERISTICS OF ERROR CORRECTION

Universität Leipzig, Dissertation

168 pages, 206 bibliographical references, 32 figures, 7 tables

Report

Successful behavior in daily-life activities as well as in laboratory tasks requires that humans monitor their performance and detect and correct their errors. There is growing knowledge about the electrophysiological and hemodynamic correlates of error detection and response conflict. Yet, neural mechanisms underlying error correction are still hardly understood.

The aim of the present work is a comprehensive multi-methodological investigation of the temporal and spatial characteristics of error correction. For this purpose, two experiments were conducted: the first experiment examines the time course of error correction by means of behavioral measures as well as event-related potentials (ERPs) and lateralized readiness potentials (LRPs). This experiment further focuses on cardiovascular changes associated with error correction. Using fMRI, the neural correlates of error correction are investigated in the second experiment. In the present studies, participants were randomly divided into two groups: in one group, participants were instructed to correct errors by immediately pressing the correct key after an erroneous response (CI); in the second group, they were unaware that error corrections were recorded (CN). Participants had to perform a modified version of the Eriksen flanker task.

The ERP results reveal a new ERP component associated with error correction, the correction-related negativity (CoRN). The CoRN peaks between 200 and 240 ms after the onset of the erroneous response and shows a fronto-central scalp distribution. It can be assumed that the CoRN is associated with ongoing stimulus-response mapping based on continued stimulus processing and/or an enhancement of the evolving corrective response tendency. The ERP findings further show that motivational error significance is reflected by an increased ERN amplitude and

an increased heart rate deceleration. In accordance with the Response Conflict Hypothesis, ERN latency is modulated by correction speed exhibiting a later peak of the ERN for slow compared to fast error corrections. Moreover, two types of error correction, incidental and intentional error correction, can be dissociated on the basis of behavioral, ERP and LRP results. The fMRI findings suggest that error detection and error correction share a common neuroanatomical substrate comprising the rostral cingulate zone (RCZ) and the pre-supplementary motor area (pre-SMA). Taking the fronto-central scalp distribution of the CoRN into account, the RCZ and the pre-SMA can be considered as potential generators of the CoRN.

MPI Series in Human Cognitive and Brain Sciences:

- 1 Anja Hahne
Charakteristika syntaktischer und semantischer Prozesse bei der auditiven Sprachverarbeitung: Evidenz aus ereigniskorrelierten Potentialstudien
- 2 Ricarda Schubotz
Erinnern kurzer Zeitdauern: Behaviorale und neurophysiologische Korrelate einer Arbeitsgedächtnisfunktion
- 3 Volker Bosch
Das Halten von Information im Arbeitsgedächtnis: Dissoziationen langsamer corticaler Potentiale
- 4 Jorge Jovicich
An investigation of the use of Gradient- and Spin-Echo (GRASE) imaging for functional MRI of the human brain
- 5 Rosemary C. Dymond
Spatial Specificity and Temporal Accuracy in Functional Magnetic Resonance Investigations
- 6 Stefan Zysset
Eine experimentalpsychologische Studie zu Gedächtnisabrufprozessen unter Verwendung der funktionellen Magnetresonanztomographie
- 7 Ulrich Hartmann
Ein mechanisches Finite-Elemente-Modell des menschlichen Kopfes
- 8 Bertram Opitz
Funktionelle Neuroanatomie der Verarbeitung einfacher und komplexer akustischer Reize: Integration haemodynamischer und elektrophysiologischer Maße
- 9 Gisela Müller-Plath
Formale Modellierung visueller Suchstrategien mit Anwendungen bei der Lokalisation von Hirnfunktionen und in der Diagnostik von Aufmerksamkeitsstörungen
- 10 Thomas Jacobsen
Characteristics of processing morphological structural and inherent case in language comprehension

- 11 Stefan Kölsch
Brain and Music
A contribution to the investigation of central auditory processing with a new electrophysiological approach
- 12 Stefan Frisch
Verb-Argument-Struktur, Kasus und thematische Interpretation beim Sprachverstehen
- 13 Markus Ullsperger
The role of retrieval inhibition in directed forgetting – an event-related brain potential analysis
- 14 Martin Koch
Measurement of the Self-Diffusion Tensor of Water in the Human Brain
- 15 Axel Hutt
Methoden zur Untersuchung der Dynamik raumzeitlicher Signale
- 16 Frithjof Kruggel
Detektion und Quantifizierung von Hirnaktivität mit der funktionellen Magnetresonanztomographie
- 17 Anja Dove
Lokalisierung an internen Kontrollprozessen beteiligter Hirngebiete mithilfe des Aufgabenwechselfaradigmas und der ereigniskorrelierten funktionellen Magnetresonanztomographie
- 18 Karsten Steinhauer
Hirnphysiologische Korrelate prosodischer Satzverarbeitung bei gesprochener und geschriebener Sprache
- 19 Silke Urban
Verbinformationen im Satzverstehen
- 20 Katja Werheid
Implizites Sequenzlernen bei Morbus Parkinson
- 21 Doreen Nessler
Is it Memory or Illusion? Electrophysiological Characteristics of True and False Recognition
- 22 Christoph Herrmann
Die Bedeutung von 40-Hz-Oszillationen für kognitive Prozesse

- 23 Christian Fiebach
*Working Memory and Syntax during Sentence Processing.
A neurocognitive investigation with event-related brain potentials and
functional magnetic resonance imaging*
- 24 Grit Hein
*Lokalisation von Doppelaufgabendefiziten bei gesunden älteren Personen
und neurologischen Patienten*
- 25 Monica de Filippis
*Die visuelle Verarbeitung unbeachteter Wörter:
Ein elektrophysiologischer Ansatz*
- 26 Ulrich Müller
*Die katecholaminerge Modulation präfrontaler kognitiver Funktionen
beim Menschen*
- 27 Kristina Uhl
Kontrollfunktion des Arbeitsgedächtnisses über interferierende Information
- 28 Ina Bornkessel
*The Argument Dependency Model: A Neurocognitive Approach to Incremental
Interpretation*
- 29 Sonja Lattner
*Neurophysiologische Untersuchungen zur auditorischen Verarbeitung
von Stimminformationen*
- 30 Christin Grünewald
*Die Rolle motorischer Schemata bei der Objektrepräsentation:
Untersuchungen mit funktioneller Magnetresonanztomographie*
- 31 Annett Schirmer
*Emotional Speech Perception: Electrophysiological Insights into the
Processing of Emotional Prosody and Word Valence in Men and Women*
- 32 André J. Szameitat
*Die Funktionalität des lateral-präfrontalen Cortex für die Verarbeitung
von Doppelaufgaben*
- 33 Susanne Wagner
*Verbales Arbeitsgedächtnis und die Verarbeitung ambiger Wörter in Wort-
und Satzkontexten*

- 34 Sophie Manthey
Hirn und Handlung: Untersuchung der Handlungsrepräsentation im ventralen prämotorischen Cortex mit Hilfe der funktionellen Magnet-Resonanztomographie
- 35 Stefan Heim
Towards a Common Neural Network Model of Language Production and Comprehension: fMRI Evidence for the Processing of Phonological and Syntactic Information in Single Words
- 36 Claudia Friedrich
Prosody and spoken word recognition: Behavioral and ERP correlates
- 37 Ulrike Lex
Sprachlateralisierung bei Rechts- und Linkshändern mit funktioneller Magnetresonanztomographie
- 38 Thomas Arnold
Computergestützte Befundung klinischer Elektroenzephalogramme
- 39 Carsten H. Wolters
Influence of Tissue Conductivity Inhomogeneity and Anisotropy on EEG/MEG based Source Localization in the Human Brain
- 40 Ansgar Hantsch
Fisch oder Karpfen? Lexikale Aktivierung von Benennungsalternativen bei der Objektbenennung
- 41 Peggy Bungert
*Zentralnervöse Verarbeitung akustischer Informationen
Signalidentifikation, Signallateralisation und zeitgebundene Informationsverarbeitung bei Patienten mit erworbenen Hirnschädigungen*
- 42 Daniel Senkowski
Neuronal correlates of selective attention: An investigation of electrophysiological brain responses in the EEG and MEG
- 43 Gert Wollny
Analysis of Changes in Temporal Series of Medical Images
- 44 Angelika Wolf
Sprachverstehen mit Cochlea-Implantat: EKP-Studien mit postlingual ertaubten erwachsenen CI-Trägern

- 45 Kirsten G. Volz
Brain correlates of uncertain decisions: Types and degrees of uncertainty
- 46 Hagen Huttner
Magnetresonanztomographische Untersuchungen über die anatomische Variabilität des Frontallappens des menschlichen Großhirns
- 47 Dirk Köster
Morphology and Spoken Word Comprehension: Electrophysiological Investigations of Internal Compound Structure
- 48 Claudia A. Hruska
Einflüsse kontextueller und prosodischer Informationen in der auditorischen Satzverarbeitung: Untersuchungen mit ereigniskorrelierten Hirnpotentialen
- 49 Hannes Ruge
Eine Analyse des raum-zeitlichen Musters neuronaler Aktivierung im Aufgabenwechselfparadigma zur Untersuchung handlungssteuernder Prozesse
- 50 Ricarda I. Schubotz
Human premotor cortex: Beyond motor performance
- 51 Clemens von Zerssen
*Bewusstes Erinnern und falsches Wiedererkennen:
Eine funktionelle MRT Studie neuroanatomischer Gedächtniskorrelate*
- 52 Christiane Weber
*Rhythm is gonna het you.
Electrophysiological markers of rhythmic processing in infants with and without risk for Specific Language Impairment (SLI)*
- 53 Marc Schönwiesner
Functional Mapping of Basic Acoustic Parameters in the Human Central Auditory System